The antidiabetic and antioxidant properties of *Athrixia phylicoides* aqueous extract – an *in vitro* and *ex vivo* assessment

by
Nireshni Chellan

Thesis presented in partial fulfilment of the requirements for the degree Master of Science in Medical Science at the University of Stellenbosch

Supervisor: Dr Christo John Frederick Muller
Co-supervisor: Prof Benedict Page and Dr Dalene De Beer
Faculty of Health Sciences
Department of Biomedical Sciences

March 2011

DECLARATION

By submitting this thesis/dissertation electronically, I declare that the entirety of the work contained therein is my own, original work, that I am the sole author thereof (save to the extent explicitly otherwise stated), that reproduction and publication thereof by Stellenbosch University will not infringe any third party rights and that I have not previously in its entirety or in part submitted it for obtaining any qualification.

March 2011

ABSTRACT

Introduction: *Athrixia phylicoides* is an aromatic, indigenous shrub with high antioxidant content and numerous indigenous medicinal properties inferred by ingestion of an herbal brew of the plant. Commercialization of “bush tea” (derived from *A. phylicoides*) holds economic and developmental potential for indigenous communities provided the safety and efficacy of the herbal tea is established. Recently *A. phylicoides* has been shown by McGaw *et al*. (2007) to have similar antioxidant activity to Rooibos tea, and a unique, new flavonol (i.e. a polyphenolic antioxidant plant metabolite) 5-hydroxy-6,7,8,3′,4′,5′-hexamethoxyflavon-3-ol, unique to *A. phylicoides*, was isolated by Mashimbye *et al*. in 2006. With changes in the socio-economic climate and a new trend in merging Western lifestyle with traditional practices, new interest has been shown in herbal/natural remedies.

Study Aim: The aim of this study was to firstly, determine the *in vitro* effect of *A. phylicoides* aqueous extract on glucose metabolism in cell lines that mimic the three key organs implicated in glucose homeostasis. Secondly, the study aimed to determine the potential *ex vivo* antioxidant and anti-inflammatory effect of the extract in pancreatic β-cells and peripheral mononuclear cells respectively.

Methods: Leaves and fine twigs of *A. phylicoides* were processed into an aqueous extract. C2C12, Chang and 3T3-L1 cells were cultured under standard conditions and acutely exposed to increasing concentrations of extract and water vehicle, as well as 1 μM insulin and metformin as positive controls. Glucose uptake from 8 mM glucose culture media was determined using a fluorimetric oxidase method. Radioactive ^{14}C-glucose oxidation to $^{14}CO_2$ and determination of glycogen content of cells were used to assess the fate of intracellular glucose. RT-PCR was used to assess the extract effect on insulin-signalling gene expression. The antioxidative effect of *A. phylicoides* extract in pancreatic β-cells isolated from Wistar rats was determined by measuring nitric oxide (NO) production in response to hyperglycemic conditions. NO was labelled with diaminofluorocein diacetate and fluorescence was measured using flow cytometry. Insulin secretion of pancreatic β-

cells was measured using radio-immuno assay. The anti-oxidative effect of the extract in lipopolysaccharide-stimulated peripheral mononuclear cells isolated from Wistar rats was determined by measuring the production of TNF-α using an ELISA kit.

Results: C2C12 myocytes showed maximal increased glucose uptake at the 0.05 µg/µl extract concentration (228.3% ± 66.2, $p<0.001$). In Chang cells, *A. phylicoides* extract maximally increased the amount of glucose taken up at the 0.05 µg/µl concentration (134.5% ± 2.5, $p<0.05$). In 3T3-L1 cells, the extract maximally increased the amount of glucose taken up at the 0.025 µg/µl concentration (143.5% ± 10.3, $p<0.001$). An extract-induced increase in insulin receptor and glucose transporter four expression was seen in C2C12 myocytes. The oxidation of ^{14}C-glucose to $^{14}CO_2$ by C2C12 myocytes was maximally increased following acute exposure to the extract at 0.1 µg/µl (2919.3 fmol/1x10^6 cells ± 428, $p<0.01$). The oxidation of ^{14}C-glucose to $^{14}CO_2$ by Chang cells was maximally increased following acute exposure to extract at 0.1 µg/µl (4476.7 fmol/1x10^6 cells ± 1620, $p<0.05$); as seen in the C2C12 cells. *A. phylicoides* extract increased glycogen storage at all three concentrations tested in Chang cells, but maximally at the 0.025 µg/µl concentration (13.6 µg/1x10^6 cells ± 0.7, $p<0.05$). *A. phylicoides* extract did not have any measurable effect on the oxidative status of β-cells or the anti-inflammatory status of peripheral mononuclear cells. The extract did show an increase in first phase insulin secretion of β-cells in hyperglycemic conditions, although it was not significant.

Conclusion: *Athrixia phylicoide*s aqueous extract stimulates *in vitro* glucose uptake and metabolism in an insulin-mimetic manner, suggesting that this extract could potentially be beneficial to type two diabetics as an adjunct therapy.

ABSTRAK

Inleiding: *Athrixia phylicoides* is ‘n aromatiese, inheemse struik met ‘n hoë antioksidant inhoud. Vele tradisionele medisinale eienskappe is gekoppel aan die ingestie van ‘n kruie brousel van die plant, wat ook bekend as “bostee” is. Kommersialisering van “bostee” hou ekonomiese en ontwikkelings potensiaal in vir inheemse gemeenskappe mits die veiligheid en effektiwiteit van die kruietee bevestig kan word. McGaw *et al*. (2007) het onlangs bevind dat *A. phylicoides* se antioksidant aktiwiteit vergelykbaar is met die van rooibostee. ‘n Unieke nuwe flavonol (‘n polifenoliese antioksidant plant metaboliet) 5-hydroksie-6,7,8,3′,4′,5′-hexamethoksieflavon-3-ol, eie aan *A. phylicoides*, is deur Mashimbye *et al*. in 2006 geïsoleer. Met veranderings in die sosio-ekonomiese klimaat en ‘n nuwe tendens om die westerse lewenstyl met trandisionele gebruike aantevul word nuwe belangstelling in kruie/natuurlike rate ondervind.

Studie Doelwitte: Die doelwitte van hierdie studie was eerstens om die *in vitro* effek van *A. phylicoides waterekstrak* op die glukosemetabolisme van drie sellyne wat die sleutel organe naboots wat glukosehomeostase beheer, te bepaal. Tweedens, is die potensiële *ex vivo* antioksidant en anti-inflammatoriese effek van die ekstrak op pankreatiese β-selle en perifere mononuklêere-selle onderskeidelik ondersoek.

Metodes: n Waterige ekstrak is van die blare en fyn takkies van *A. phylicoides* berei. C2C12, Chang and 3T3-L1 selle is gekultuur onder standard kondisies en akuut blootgestel aan stygende ekstrakkonsentrasies, Water het as kontrole gedien, met 1 μM insulien en metformien as positiewe kontroles.. Glukose opname vanuit 8 mM glukose kultuurmedia is bepaal deur ‘n fluorimetriese oksidase metode. Radioaktiewe ^{14}C-glukose-oksidasie na $^{14}CO_2$ en die bepaling van die glukogeen inhoud van selle is gebruik om die lot van intrasellulêre glukose te bepaal. RT-PKR is gebruik om die effek van die ekstrak op die insulien-seinpad geen-uitdrukking te ondersoek. Die antioksidant effek van *A. phylicoides* ekstrak in pankreatiese β-selle geïsoleer van Wistar rotte, is bepaal deur

stikstofoksied (NO) produksie na aanleiding van hiperglukemiese kondisies. NO is met diaminofluorosien diasetaat gemerk en die fluoresensie gemeet deur vloeisitometrie. Insulien afskeiding deur die pankreatiese β-selle is deur radio-immuno metode bepaal. Die anti-oksidatiewe effek van die ekstrak op lipopolisakkaried-gestimuleerde perifere mononuklêere-selle afkomstig van Wistar rotte is bepaal deur die meting van TNF-α produksie met ‘n ELISA kit.

Resultate: C2C12 miosiete het ‘n maksimale toename in glukoseopname by ‘n 0.05 µg/µl ekstrakkonsentrasie (228.3% ± 66.2, $p<0.001$) gehad. Dieselfde ekstrakkonsentrasie het maksimale toename in glukoseopname in Chang selle (134.5% ± 2.5, $p<0.05$ getoon. In 3T3-L1 selle is maksimale toename in die glukoseopname by ‘n konsentrasie van 0.025 µg/µl (143.5% ± 10.3, $p<0.001$) bereik. ‘n Ekstrak-geÏnduseerde verhoging in die insulienreseptor en glukosetransporter vier ekspressie is in C2C12 miosiete waargeneem. Die oksidasie van ^{14}C-glukose na $^{14}CO_2$ deur C2C12 miosiete is maksimaal verhoog deur akute blootstelling aan die ekstrak by ‘n konsentrasie van 0.1 µg/µl (2919.3 fmol/1x10^6 cells ± 428, $p<0.01$). Die oksidasie van ^{14}C-glukose na $^{14}CO_2$ deur Chang selle was maksimaal verhoog deur akute blootstelling aan die ekstrak by ‘n konsentrasie van 0.1 µg/µl (4476.7 fmol/1x10^6 cells ± 1620, $p<0.05$) soos gevind in die C2C12 selle. Die ekstrak het glukogeenstoring verhoog teen al drie die konsentrasies waarteen getoets is in Chang selle, maar ‘n maksimale effek is gevind by ‘n konsentrasie van 0.025 (13.6 µg/1x10^6 cells ± 0.7, $p<0.05$). *A. phylicoides* ekstrak het nie ‘n meetbare effek op die oksidatiewe status van β-selle of die anti-inflammatoriese status van perifere mononuklêere-selle gehad nie. Die ekstrak het wel ‘n verhoging in die eerstefase insuliensekresie van β-selle in hyperglukemiese kondisies gehad, alhoewel die verhoging nie statisties betekenisvol was nie.

Afleiding: *Athrixia phylicoide*s waterekstrak stimuleer *in vitro* glukoseopname en metabolisme in ‘n insulin-mimetiese manier, wat beteken dat die ekstrak potensiëel voordele vir tiepe twee diabete kan inhou as aanvullingsterapie.

ACKNOWLEDGEMENTS

The completion of this Masters in Medical Science would not have been possible without the assistance, support, collaboration and contributions of the following people and/or institutes:

- Dr C.J.F. Muller for supervision and scientific impetus.
- Co-supervisors, Prof B.J. Page and Dr D. de Beer.
- The Agricultural Research Council, the Diabetes Discovery Platform and the Medical Research Council for funding.
- The Diabetes Discovery Platform, Primate Unit and Stellenbosch University Flow Cytometry Unit for use of their facilities.
- Dr D. de Beer for providing the aqueous plant extract.
- For scientific and academic contributions -

  Ms S. Ghoor, Ms C. Roux, Dr C. Pheiffer, Dr J. Michie, Dr J. Louw, Dr R. Johnson and Prof E. Joubert.
- Those members of family, as well as friends, that offered support and encouragement throughout this endeavor.
- My parents for providing a firm platform from which to develop; with special thanks to my mom for teaching me to work hard, with diligence and integrity.
- Jesus Christ; for it was not by might, nor by power, but by His Spirit alone (Zechariah 4:6b) that I could achieve anything.

I would like to dedicate the work herewith to my E.V. and Aunty Cissy.

TABLE OF CONTENTS

CHAPTER THREE: RESULTS **67**

LIST OF FIGURES

LIST OF TABLES

LIST OF ABBREVIATIONS

ActB -	Beta actin
ADP -	Adenosine diphosphate
AGE -	Advanced glycation end-product
Akt -	Protein kinase B
ALA -	Alpha-lipoic acid
ANOVA -	Analysis of variance
ARC401 -	*Athrixia phylicoides* aqueous extract
ATP -	Adenosine triphosphate
BSA -	Bovine serum albumin
cDNA -	Complimentary DNA
$C_6H_{12}O_6$ -	Glucose
CH_3COCOO^- -	Pyruvate
DAF -	Diaminofluoroscein diacetate
DAF-2T -	Diaminofluoroscein diacetate-triazol
ddH_2O -	Double distilled water
DMEM -	Dulbecco's modified Eagle's medium
DMSO -	Dimethylsulfoxide
DNA -	Deoxyribonucleic acid
dNTP -	Deoxynucleoside triphosphates
DPBS -	Dulbecco's phosphate buffered saline
ECRA -	Ethical Committee for Research on Animals
EDTA -	Ethylenediaminetetraacetic acid
EMEM -	Eagle's modified essential medium
FCS -	Fetal calf serum
FFA -	Free fatty acids
FL1 -	Emmission wavelength detector one
GAPDH -	Glyceraldehyde 3-phosphate

GLUT1/2/4 -	Glucose transporter one/two/four
HBSS -	Hank’s buffered saline solution
HGP -	Hepatic glucose production
HS -	Horse serum
IBMX -	3-Isobutyl-1-methylxanthine
IL-1β -	Interleuken one beta
IL-6 -	Interleuken six
iNOS -	Inducible nitric oxide
INSR -	Insulin receptor
IRS1/2 -	Insulin receptor substrate one/two
KRBH -	Krebb’s Ringer Buffer with HEPES
LPS -	Lipopolysaccharides isolated from *Escherichia coli*.
Metformin -	1,1-Dimethylbiguanide hydrochloride
MTT -	3-(4,5-dimethylthiazol-2-yl)-2,5-diphenyltetrazolium bromide
NADH -	Nicotinamide adenine dinucleotide
NADPH -	Nicotinamide adenine dinucleotide phosphate
ncNOS -	Neuronal constitutive nitric oxide synthase
NF-κB -	Nuclear factor kappaB
NO -	Nitric oxide
NOS -	Nitric oxide synthase
P75NTR -	p75 neutrophin receptor
PBMC -	Peripheral mononuclear cells
PCR -	Polymerase chain reaction
PDX-1 -	Pancreatic homeobox one
PI3K -	Phosphoinositide-3-kinase
PPARγ -	Peroxisome proliferator activated receptor gamma
RIA -	Radio-immuno assay
RNA -	Ribonucleic acid

RNS -	Reactive nitrogen species
ROS -	Reactive oxygen species
SNARE -	Soluble N-ethylmaleimide-sensitive factor attachment protein receptor
SDS -	Sodium dodecyl sulfate
Sort1 -	Sortillin receptor one
T2D -	Type two diabetes
TMB -	3,3’,5,5’-tetramethylbenzadine
TNF-α -	Tumor necrosis factor alpha
TZD -	Thiazolidinedione
UCP2 -	Uncoupling protein two
XO -	Xanthine oxidase
α-cell -	Alpha cell
β-cell -	Beta cell
δ-cell -	Delta cell

INTRODUCTION

Athrixia phylicoides is an aromatic, indigenous shrub with high antioxidant content and numerous indigenous medicinal properties inferred by ingestion of an herbal brew of the plant. Recently *A. phylicoides* has been shown by McGaw *et al*. (2007) to have similar antioxidant activity to Rooibos tea, and a unique, new flavonol (i.e. a polyphenolic antioxidant plant metabolite) 5-hydroxy-6,7,8,3′,4′,5′-hexamethoxyflavon-3-ol, unique to *A. phylicoides*, was isolated by Mashimbye *et al*. in 2006. With changes in the socio-economic climate and a new trend in merging Western lifestyle with traditional practices, new interest has been shown in herbal/natural remedies. Uncovering the scientific basis of the remedial effects of natural products has been imperative in providing the pharmaceutical industry with “lead” compounds which can be synthesized into new clinical therapies (Haslam, 1996).

The socio-economic burden of type two diabetes (T2D) is rapidly increasing, with predictions of worldwide prevalence increasing from 2.8% in 2000 to 4.4% in 2030 (Wild *et al.*, 2004). T2D is characterized by insulin resistance (Reaven, 1988) and β-cell failure (Porte, 1991), a culmination of which leads to abnormalities in glucose and lipid metabolism and hyperglycaemia. Reactive oxygen species, which may be hyperglycaemia-induced, have been implicated in inducing multiple forms of insulin resistance as well as exacerbating known diabetic complications (e.g. cardiovascular disease) (Johansen *et al.*, 2005; Houstis *et al.*, 2006). In 1980, Logani and Davies suggested that supplementation with non-toxic antioxidants may have a chemoprotective role in T2D. If *Athrixia phylicoides* aqueous extract demonstrates hypoglycaemic and antioxidant properties, commercialization of the extract holds great economic and developmental potential for the indigenous communities as well as to the health of the general populace (Rampedi and Olivier, 2005). The aim of this study was to firstly,

determine the *in vitro* effect of *A. phylicoides* aqueous extract on glucose metabolism in cell lines that mimic the three key organs implicated in glucose homeostasis. Secondly, the study aimed to determine the potential *ex vivo* antioxidant and anti-inflammatory effect of the extract in pancreatic β-cells and peripheral mononuclear cells respectively.

CHAPTER 1

LITERATURE REVIEW

1. Overview of Athrixia phylicoides

1.1. Physical characteristics and indigenous distribution

Athrixia phylicoides is an aromatic, indigenous shrub of approximately one meter in height, commonly found in the mountainous and grassland areas of the eastern parts of South Africa. Distribution includes Mpumalanga, Limpopo, KwaZulu-Natal, Swaziland and northern parts of the Eastern Cape (figure 1) (Fox *et al*., 1982; and Van Wyk and Gericke, 2000).

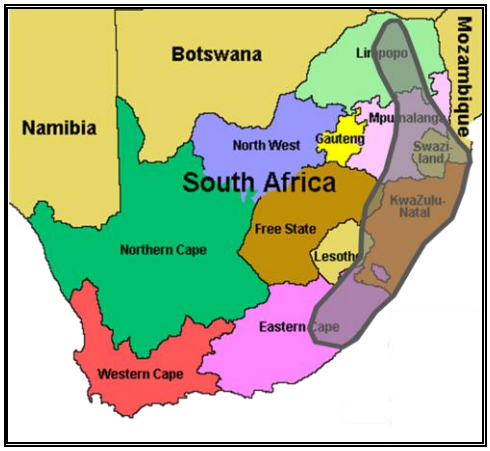

Figure 1. Natural geographical distribution of *A. phylicoides* (grey shaded area) in Southern Africa (adapted from Rampedi and Olivier, 2005).

The dense foliage of this member of the Asteraceae family (tribe Gnaphalieae) is comprised of fine, linear leaves (dark green and shiny above, and grey/white below) that are approximately 30 x 10 mm in size (figure 2) (Van Wyk and Gericke, 2000).

a.  b. 

Figure 2. *Athrixia phylicoides* shrub (a) and flowers (b) (Pooley, 1998)

Known to flower throughout the year, these plants thrive in a variety of habitats, including grassland, forest, bushveld, rocky and sloping environments. Flowers are characteristically mauve with distinct yellow disc florets (figure 2b) (Fox *et al*., 1982; Leistner *et al.,* 2000; Van Wyk and Gericke, 2000; and Rampedi and Olivier*,* 2005).

1.2. Indigenous uses

A. phylicoides is indigenously referred to as Bush or Zulu tea (English); Boesmanstee (Afrikaans); Icholocholo, Itshelo, or Umthsanelo (Zulu). A permutation of the shrub's aerial foliage and stems is dried and used to produce an herbal tea by certain indigenous African people. It is also chewed by the Sotho and Xhosa for sore throats and coughs (Watt and Breyer-Brandwijk, 1932; and van Wyk and Gericke, 2000). The Venda people have been reported to use a brew of *A. phylicoides* as an aphrodisiac (Hutchings *et al.,* 1996; van Wyk and Gericke, 2000). The Zulu people use an herbal tea infusion of this shrub for blood "purification" and to treat sores and boils (Rampedi and Olivier*,* 2005; and Hutchings *et al.,* 1996). In the study by Rampedi and Olivier (2005), South African rural respondents used the *A. phylicoides* tea to treat hypertension, heart disease and diabetes. Medicinal and therapeutic value of this plant has yet to be verified scientifically. This indigenous tea is mainly produced and used in rural areas, with only informal traders supplying the increasing demand in urban areas (Rampedi and Olivier, 2005). Scientific characterisation of health benefits of this tea and commercialisation thereof holds economic, developmental and therapeutic potential for local communities.

1.3. Toxicity screening

Pyrrolizidine alkaloids (PA) are a well-recognized and relatively common group of plant toxins that occur in up to 3% flowering plant species, including the Asteraceae family, and have numerous adverse health implications (Smith and Culvenor, 1981). McGaw *et al.*

(2007) used spectrophotometric and gas chromatography-mass spectrometry analysis to show that the *A. phylicoides* aqueous extract does not contain PA. Cytotoxicity screening, using kidney cell lines and brine shrimp toxicity assays, showed that while the ethanol extract was relatively toxic**,** the aqueous extract was not (McGaw *et al*., 2007). In addition to *in vitro* screening, *in vivo* toxicity screening of plant products is important to account for potential toxicity of derived plant metabolites. An *in vivo* sub-chronic toxicity study of *A. phylicoides* aqueous extract using Wistar rats showed no signs of hepato- or biochemical toxicity, nor were there adverse anthropological or metabolic effects (Chellan *et al*., 2008).

1.4. Phenolic composition

In 1985 Beart *et al.* considered polyphenolic constituents in tea plants purely a chemical defense against birds, insects and animals. Plant-derived flavonoids have subsequently been reported as having numerous medicinal properties, such as anti-inflammatory, anti-mutagenic and anti-bacterial (Hirasawa *et al.*, 2002). Schewe and Sies (2005) and Nijveldt *et al.* (2001) describe flavonoids as being potent antioxidants that are capable of scavenging hydroxyl radicals, superoxide anions as well as lipid peroxyl radicals.

Recently, *A. phylicoides* has been shown by McGaw *et al*. (2007) to have similar antioxidant activity to Rooibos tea, and may well have commercial benefits in addition to its horticultural potential. It has long been known that the health benefits attributed to certain herbal teas are due to the tea's antioxidant properties, such as those inferred by the phenolic composition of rooibos tea (Niwa and Miyachie 1986). Numerous health benefits attributed to the antioxidant properties of polyphenols, particularly flavonoids (Niwa and Miyachie, 1986), include protection against cellular oxidative damage, due to the ability of antioxidants from the plant to scavenge free radicals. An epidemiological study by Arts and Hollman (2005) illustrated the relationship between the intake of flavonoids and a

reduction on the risk of degenerative diseases such as type II diabetes.

Numerous medicinal plants have demonstrated pharmacological actions in lowering blood glucose and/or stimulating insulin secretion; this has been attributed to their rich content of bioactive chemicals such as terpenoids, flavonoids and phenolics (Jung *et al*., 2006). A unique, new flavonol (i.e. a polyphenolic antioxidant plant metabolite) 5-hydroxy-6,7,8,3′,4′,5′-hexamethoxyflavon-3-ol (figure 3) was isolated from *A. phylicoides* (Mashimbye *et al*., 2006). Haslam (1996) reported that the anti-oxidative properties of both green (unfermented) tea and red wine are based on their high yield of polyphenols that are based on the flavon-3-ol carbon oxygen skeleton.

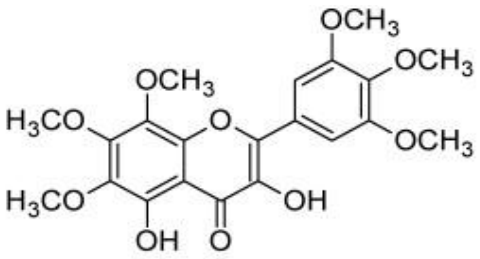

Figure 3. 5-hydroxy-6,7,8,3′,4′,5′-hexamethoxyflavon-3-ol (Mashimbye *et al*., 2006)

2. Glucose metabolism

The cellular process of glycolysis is responsible for the conversion of glucose ($C_6H_{12}O_6$) into pyruvate ($CH_3COCOO^- + H^+$). Glucose that has entered the cell undergoes a series of insulin-induced enzymatic reactions, which include glucose phosphorylation, glycogen synthesis and glucose oxidation (DeFronzo, 2004). The free energy released from this process is used to fuel cells by forming high energy adenosine triphosphate (ATP) and reduced nicotinamide adenine dinucleotide (NADH) (Ganong, 1989). Once in the cell, glucose is phosphorylated by hexokinase to form glucose-6-phosphate. An additional glucose phosphorylating enzyme, glucokinase, is found in the liver and is increased by insulin stimulation. The glucose-6-phosphate is either stored (polymerized into glycogen or converted to fat) or catabolised in the glycolytic pathway (figure 4) to produce energy (Ganong, 1989; and Mathews *et al.*, 2000).

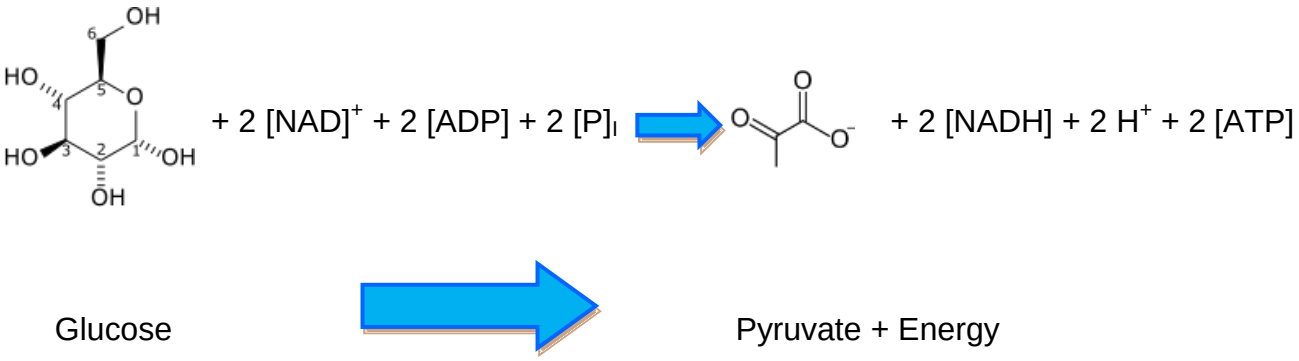

Figure 4. Glycolytic reduction of glucose to pyruvate and energy (ATP and NADH)

2.1. Glucose metabolism in skeletal muscle, fat and liver

Mathews *et al.* (2000) describe the brain as the largest consumer of glucose, whereas glucose homeostasis is maintained by three key organs/tissues; i.e. skeletal muscle, liver and fat/adipose. The brain uses approximately 50% of total glucose taken up in an insulin independent manner (DeFronzo, 2004). The liver and gastrointestinal tissues (responsible

for approximately 25% glucose usage) also use glucose in an insulin independent manner. Glucose uptake in skeletal muscle and adipose tissues is insulin-stimulated, with approximately 80-85% of glucose uptake in peripheral tissues occurring in the muscle (DeFronzo, 2004).

In skeletal muscle glucose is primarily oxidized for energy and secondarily stores glucose as glycogen. Glucose taken up is converted to lactate by glycolysis or stored as glycogen (Cartailler, 2001; and DeFronzo, 2004). At low glucose concentrations and in starvation states, skeletal muscle mobilizes fatty acids by β-oxidation and/or ketogenesis; glycogen stores are also mobilized by glycogenolysis. In the starved state proteins are also broken down (proteolysis) to amino acids (Ganong, 1989; and DeFronzo, 2004).

The liver acts as a glucose sensing device, as determined by glucose transporters of the subclass two (GLUT2) found in hepatocytes. In addition, the liver is responsible for glucose production (hepatic glucose production, HGP) (DeFronzo, 2004; and Chakraborty, 2006). The liver responds to an increase in circulating glucose by converting glucose to storage polymers (glycogen and triacylglycerols). At low glucose concentrations, the liver provides energy substrate by mobilising fatty acids by β-oxidation and glycogen by glycogenolysis. During a period of starvation, the liver also converts amino acids to glucose by gluconeogenesis (Ganong, 1989; Cartailler, 2001; DeFronzo, 2004; and Chakraborty, 2006).

Adipose tissues primarily convert glucose to triglycerides for storage. Stored triacylglyerides are mobilized in states of low glucose and/or starvation (Cartailler, 2001). Although adipose tissue is responsible for only 4-5% of glucose disposal in peripheral tissues, it still plays a key role in glucose homeostasis as well as the development of

defects in glucose metabolism. Adipose tissues secrete adipocytokines and regulate the release of free fatty acids (FFA) from stored triglycerides; both adipocytokines and FFA influence insulin sensitivity in muscle and liver (Ganong, 1989; and DeFronzo, 2004).

2.2. Key Hormones regulating glucose homeostasis

Insulin is a hormonal protein synthesized by pancreatic beta-cells (β-cells) in the islets of Langerhans (Mathews *et al.*, 2000). Biochemical actions of insulin include increasing muscle and fat cell permeability to glucose by facilitating the translocation of glucose transporter four (GLUT4) to the cell membrane. Insulin also increases the processes of glycolysis (glucose catabolism), glycogenesis (glycogen synthesis), triacylglycerol synthesis and protein, DNA and RNA synthesis (Mathews *et al*., 2000). In the liver, insulin decreases gluconeogenesis and glycogenolysis (figure 5).

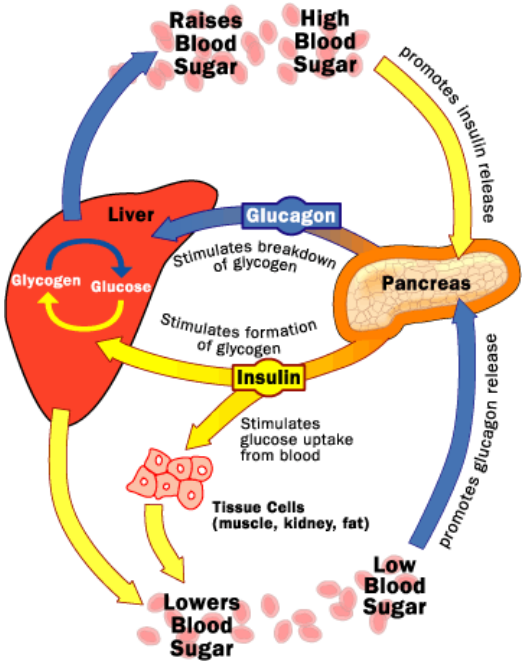

Figure 5. Regulation of glucose homestasis by pancreatic hormones insulin and glucagon. Insulin promotes glucose uptake, catabolism and storage, whereas glucagon promotes mobilization of stored glucose, primarily from the liver and adipose tissues (Freudenrich, 2001).

One of the mechanisms by which insulin decreases HGP is by inhibiting glucagon secretion in the pancreas, this results is decreased gluconeogenesis (DeFronzo, 2004). Schulman (2000) and Sesti (2006) describe the ability of insulin to increase the rate of glucose uptake in skeletal muscle and adipose tissue, this is preceded by insulin-stimulated translocation of GLUT4. Insulin also regulates glycogen synthase in the muscle, controlling the rate of glycogen synthesis (Dent *et al*., 1990 and DeFronzo, 2004). In adipose tissue, insulin increases lipid synthesis and decreases FFA release (Shulman, 2000; and Sesti, 2006). Insulin-induced decrease in lipolysis decreases the amount of circulating FFA (DeFronzo, 2004). Insulin is considered a growth hormone because of its ability to promote biosynthesis (e.g. proteins, DNA etc.). Insulin resistance is characterized by decreased glucose transport (Sesti, 2006), whereby normal circulating insulin concentrations fail to stimulate glucose uptake (Chakraborty, 2006).

Glucagon is also synthesized by pancreatic cells in the islets of Langerhans, known as alpha-cells (α-cells). Glucagon is secreted in response to low circulating glucose concentrations, with its primary target being the liver. In the liver, glucagon promotes glycogenolysis (breakdown of glycogen) and inhibits glycogenesis (synthesis and storage of glycogen polymers) (figure 5). Glucagon also promotes the mobilization of triacylglycerol in adipose tissue (Mathews *et al*., 2000).

Epinephrine, secreted by the adrenal medulla, regulates glucose homeostasis by activating glycogenolysis and inhibiting glycogenesis in response to low circulating glucose levels (Mathews *et al*., 2000).

2.1. Insulin signalling

Insulin is an anabolic hormone involved in the regulation of glucose homeostasis. Synthesis and secretion of insulin is further discussed in section **2.2.1**. Insulin is secreted in response to a rise in blood glucose levels. At a cellular level, glucose uptake is mediated through glucose transporters. GLUT4 is the insulin-responsive transporter of glucose in various cell types in the body, including adipose and muscle cells (Brunetti, 1989, and Nedachi and Kanzaki, 2006). As illustrated in figure 6 below, insulin binds to the transmembrane insulin receptor (INSR) leading to activation of the insulin receptor intrinsic tyrosine kinase. Insulin receptor substrates one and two (IRS1/2) undergo phosphorylation of their tyrosine residues. Phosphorylated IRS proteins serve as multisite docking proteins for various effector molecules including the p85 regulatory subunit of phosphoinositide 3-kinase (PI3K). Multiple downstream effectors result in rapid incorporation of GLUT4 transporters from a cytoplasmic pool to the cell membrane (figure 6) (Nedachi and Kanzaki, 2006; and Sesti 2006).

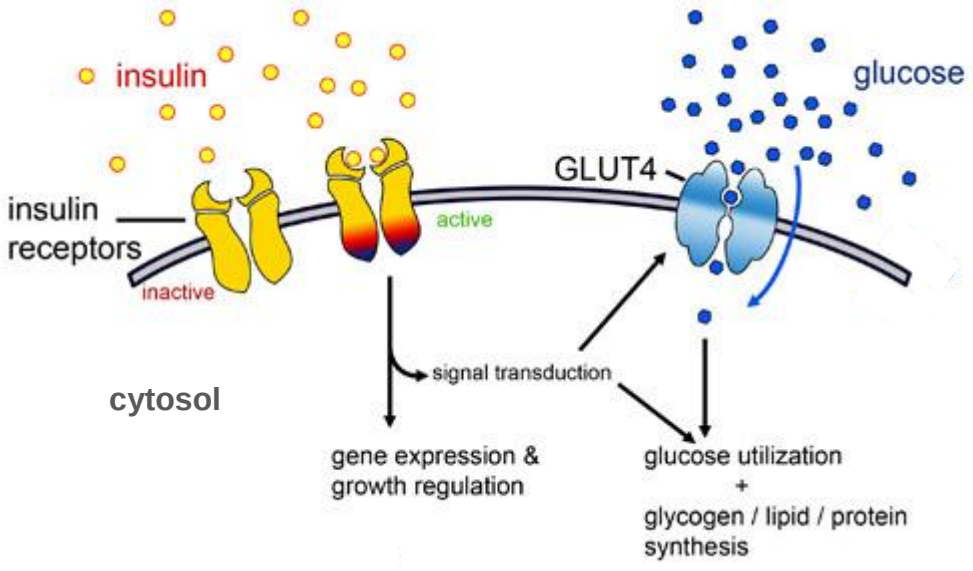

Figure 6. Insulin-mediated GLUT-4 translocation and subsequent glucose uptake into the cell. (Cartailler, 2001)

GLUT4 is the main transmembrane glucose transporter in stimulated glucose uptake in muscle and adipose cells. Basal glucose uptake is regulated by the ubiquitous glucose transporter one (GLUT1) in these cells, as well as glucose sensing GLUT2 in liver and β-cells (Cartailler, 2001; and Nedachi and Kanzaki, 2006).

2.1.1. Defects in type two diabetes mellitus

The socio-economic burden of type two diabetes (T2D) is rapidly increasing, with predictions of worldwide prevalence increasing from 2.8% in 2000 to 4.4% in 2030 (Wild *et al.*, 2004). T2D is characterized by insulin resistance (Reaven, 1988), β-cell failure (Porte, 1991), chronic hyperglycaemia and disturbances in carbohydrate, lipid and protein metabolism (Duckworth, 2001). Insulin resistance in the muscle and liver is characteristic in T2D (DeFronzo, 2004). Despite hyperinsulinemia in the insulin resistant state, the liver continues overproduction of glucose. Insulin-mediated suppression of gluconeogenesis is defective in insulin resistant liver, resulting in increased HGP which further exacerbates the hyperglycaemic conition (DeFronzo, 2004). In T2D, the ability of insulin to inhibit lipase in adipose tissue is reduced (Bays, 2004). The lipase enzyme is responsible for lipolysis in adipose tissue; a process whereby stored triglycerides are released/broken down into FFA and glycerol (Bays, 2004; DeFronzo, 2004; and Chakraborty, 2006). Insulin resistant and T2D patients have been shown to have chronically elevated levels of circulating FFA, which have been demonstrated to be responsible for insulin resistance in muscle and liver (Boden, 1997). Furthermore, chronically elevated FFA impairs insulin secretion (Boden, 1997; and DeFronzo, 2004).

Overt or full blown T2D only develops once the pancreatic β-cells can no longer compensate for the hyperinsulinemic requirement in order to maintain glucose homeostasis. Hyperglycaemia ensues, resulting in a cascade of deleterious physiological

effects including β-cell failure, microvasulature damage, cardiovascular disease, neuropathy and retinopathy (Porte, 1991; and Rahimi *et al*., 2005). Mediators of hyperglycemic induced damage include pro-inflammatory cytokines (e.g. tumor necrosis factor alpha, TNF-α) as well as reactive oxygen and nitrogen species (ROS and RNS respectively).

Insulin-signalling defects in T2D include impaired tyrosine phosphorylation of INSR and IRS1/2 upon insulin stimulation, as well as attenuation of the association of the p85 sub unit of PI3K with IRS1/2 (Cusi *et al*., 2000). Insulin's potential to induce the translocation of GLUT4 from intracellular organelles to the plasma membrane is defective in insulin resistant individuals, thus not facilitating glucose uptake into muscle (and fat) (Bryant *et al.*, 2002; Hoehn *et al.*, 2008).

2.1.2. Role of oxidative stress in type two diabetes mellitus

ROS (and FFA) are proposed to be mediated by intracellular pathways involving several signalling molecules, of which nuclear factor-κB (NF-κB) is one (Bastard *et al*., 2006). These intracellular pathways interact directly with insulin signalling via serine/threonine inhibitory phosphorylation of IRS via the PI3K/protein kinase B (Akt) pathway (Hotamisligil, 2003; Bastard *et al*., 2006). The competitive phosphorylation of IRS inhibits the insulin signalling pathway, causing a reduction in the stimulatory capacity of secreted insulin.

Despite the evolution of internal anti-oxidant defense systems (e.g. small-molecule anti-oxidants, anti-oxidant enzymes and physical barriers), man is still faced with the deleterious consequences of ROS. ROS generated as a result of glucotoxicity (i.e. chronic hyperglycaemia) exert their deleterious effects on deoxyribonucleic acids (DNA), proteins and other biological components through the abstraction of hydrogen atoms, electron

transfer and addition reactions (Zhang *et al*., 2010).

Under normal physiological conditions, key sites of superoxide formation in the mitochondrial membrane are complex one and the ubiquinone-complex three interface. During energy transduction, a small number of electrons “leak” to oxygen prematurely, forming ROS as opposed to oxygen being reduced to water. Diabetes alters these primary sites of superoxide formation so that complex two becomes the primary source of electrons contributing to superoxide formation. This results in a dangerous increase in the normally small amounts ROS produced through “leaking” (Valko *et al.*, 2007). In a study by Gurgul *et al.* (2004) the main source of ROS in the β-cell is attributed to the mitochondrial electron transport chain. Ling *et al.* (2001) describe glucose reacting directly with free amine groups on protein and lipids, finally yielding a diverse group of modifications referred to as advanced glycation end products (AGE). AGE’s act via mitochondrial complex three, resulting in increased ROS production in response to hyperglycaemia.

Li and Shah (2003) describe several lines of evidence supporting nicotinamide adenine dinucleotide phosphate (NADPH) oxidases (through its membrane bound components) as major sources of glucose-induced ROS production in vasculature and kidney cells. Butler *et al.* (2000) proposed xanthine oxidase (XO) as a major source of ROS. Treatment of non-insulin dependent T2D patients with a XO inhibitor reduced levels of oxidized lipids in plasma and improved blood flow. Diabetes is also associated with increased lipoxygenase expression; this results in eicosanoid formation (a process involving natural release of additional ROS) (Brash, 1999).

Hyperglycaemia-induced oxidative stress has also been observed in non-nucleated cells that lack mitochondria and NADPH oxidase (e.g. erythrocytes). Robertson and colleagues

(2003) have considered glucose auto-oxidation as another mechanism of ROS production. Whereby glucose itself (and its metabolites) reacts with hydrogen peroxide in the presence of iron and copper ions to form hydroxyl radicals (shown by *in vitro* studies only).

2.1.3. Role of inflammation in type two diabetes mellitus

The inflammatory state is characterised by secretion of inflammatory cytokines and ROS (Crouvezier *et al.*, 2001). Insulin-stimulated phosphorylation of IRS proteins is the crucially defective step in most cases of systemic insulin resistance (Wellen and Hotamisligil, 2005). Pro-inflammatory effects of cytokines (e.g. TNF-ά), as well as ROS and FFA, are proposed to be mediated by intracellular pathways involving several signalling molecules, of which NF-κB is one (Bastard *et al*., 2006). These intracellular pathways interact with insulin signalling via serine/threonine inhibitory phosphorylation of IRS via the PI3K/Akt pathway (Hotamisligil, 2003; Bastard, 2006).

Kaddai *et al.* (2009) propose that decreased glucose transport in adipocytes from insulin resistant patients could be as a result of decreased GLUT4 levels as well as GLUT4 mislocalisation. This mislocalisation was attributed to a negative correlation between TNF-ά and sortilin one (Sort1) expression (as shown in 3T3-L1 and human adipocytes *in vitro,* and *in vivo* in mice epididymal tissue and subcutaneous tissue of morbidly obese diabetic patients). The role of TNF-ά (as a result of chronic low-grade inflammation) on *Sort1* expression may result in increased lipotoxic effects (adipocyte hypertrophy) since sortilin facilitates lipoprotein lipase degradation in muscle (Nielsen *et al.*, 1999). Sortilin is also a co-receptor for the p75 nerotrophin receptor (p75NTR) and is thus involved in the insulin-responsive glucose transport system in muscle (Ariga *et al.*, 2008).

It is known that TNF-ά stimulates the secretion of interleukin-6 (IL-6) in adipocytes (Rotter

et al., 2003). It has subsequently been demonstrated in 3T3-L1 cells that IL-6 inhibits mRNA expression of GLUT4 and largely increases the expression of GLUT1 (Rotter *et al.*, 2003; Kaddai *et al.*, 2009).

2.2. Defects in pancreatic β-cells in type two diabetes mellitus

2.2.1. Physiology of the endocrine pancreas

The endocrine pancreatic islets of Langerhans are morphologically distinct from the rest of the exocrine pancreatic tissue; they form rounded clusters of cells (figure 7) throughout the pancreas, particularly in the tail (Nunemaker and Satin, 2005; and Stevens and Lowe, 2005).

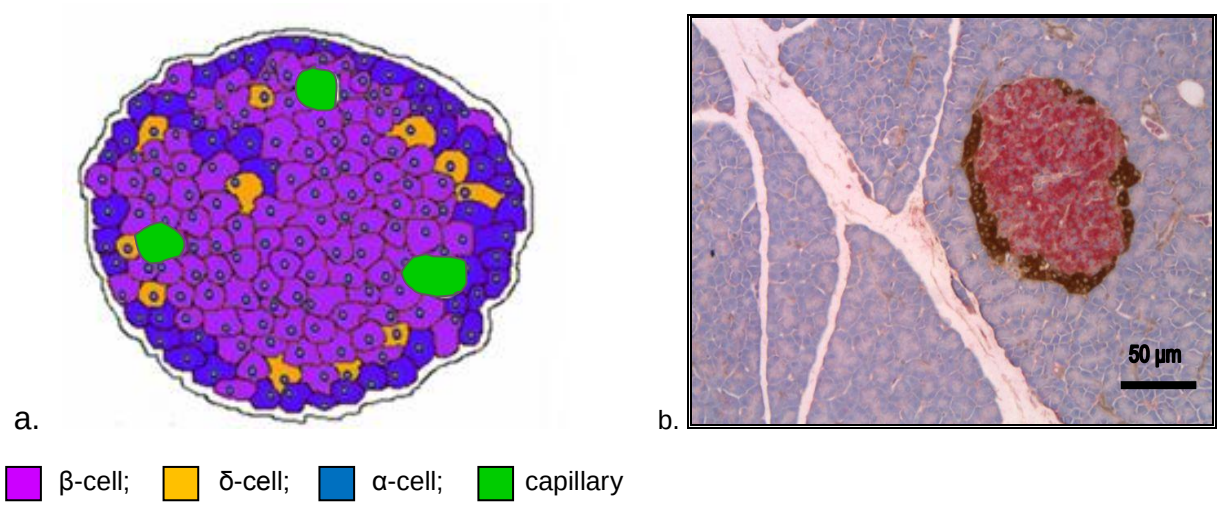

Figure 7. Pancreatic islets of Langerhans. Cellular composition (modified from Nunemaker and Satin, 2005) (a) and histological section stained for insulin (red) and glucagon (brown) at 200 x magnification (Diabetes Discovery Platform, 2010) (b).

The islets are comprised of three main cellular components; i.e. insulin and amylin secreting β-cells, glucagon secreting α-cells and somatostatin secreting delta-cells (δ-cells). Some pancreatic polypeptide secreting PP cells are also found within pancreatic

islets (Nunemaker and Satin, 2005; and Stevens and Lowe, 2005).

Insulin secretion in β-cells is triggered by rising blood glucose levels. GLUT2 senses and transports glucose into the β-cell. Glucose is then phosphorylated, causing a rise in the ATP to adenosine diphosphate (ADP) ratio (figure 8). This rise inactivates the potassium channels, resulting in depolarization of the cell membrane. The calcium channels open, allowing calcium ions to flow into the cell. The ensuing influx of calcium leads to the exocytotic release of insulin from storage granules (Cartailler, 2001).

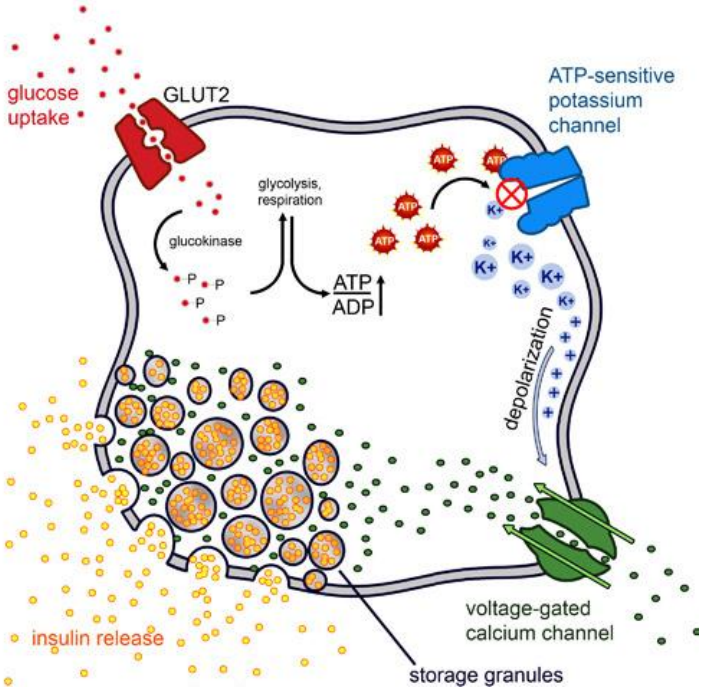

Figure 8. Glucose stimulated insulin secretion in pancreatic β-cells (Cartailer, 2001).

2.2.1. β-cell failure and type two diabetes

β-cell failure is characteristic of T2D, with further deterioration that occurs during the natural course of the disease (Porte, 1991). T2D, as characterized by hyperglycaemia and dyslipidemia, develops when pancreatic β-cells can no longer compensate for the hyperinsulinemic requirement in the preceding insulin resistant state (DeFronzo, 2004).

Autopsy studies by Butler *et al.* (2003) revealed that β-cell neogenesis is not impaired in T2D patients, however increased apoptosis is evident. Suggested factors involved in this neogenesis/apoptosis imbalance include glucotoxicity, insulin resistance within the β-cells, inflammation and oxidative stress (Bonora, 2008). Apart from suppressed insulin response to glucose, islets from T2D were observed to have lower rates of glucose oxidation (Marchetti *et al.*, 2006). Hyperglycaemia has been seen to exacerbate β-cell inflammation and oxidative stress. One of the mechanisms is via the NF-κB pathway which results in increased local expression of inflammatory cytokines (e.g. TNF-ά) (Marchetti *et al.*, 2006 and Bonora, 2008).

One of the hypotheses for induction of β-cell dysfunction focuses on changes in the expression and function of a mitochondrial inner membrane protein, uncoupling protein two (UCP2). Krauss *et al.* (2003) proposed UCP2 activity and expression contribute to an increase in superoxide formation under diabetic conditions. β-cells are particularly sensitive to ROS since they contain low levels of free-radical quenching enzymes such as glutathione peroxidase and superoxide dismutase (Abdollahi *et al.*, 2004).

Brownlee (2003) also demonstrated that hyperglycaemia increased free radical concentration in human islets. Treatment of Zucker fatty rats with antioxidant agents (e.g. N-acetylcisteine and aminoguanidine) prevented abnormalities in insulin gene expression and hyperglycaemia-induced loss of transcription factors (e.g. pancreatic homeobox one, PDX-1) (Tannaka *et al*., 1999).

Since one of the main sources of ROS in the β-cell is attributed to the mitochondrial electron transport chain (Gurgul *et al.,* 2004), chronic stimulation of insulin secretion (induced by hyperglycaemia) increases ROS production and hence oxidative stress.

Changes in β-cell function, as a result of hyperglycaemia, may also be explained by the activation of the endoplasmic reticulum (ER) stress pathway as well as by sustained elevation of cystolic calcium concentrations (Grill and Bjorklund, 2001).

Kahler *et al.* (1993), implicate free radicals (which include the superoxide, hydroxy, hydrogen peroxide and lipid peroxide radicals) in the disease process of T2D. It is known that these ROS are produced as part of the normal biochemical and physiological processes of the body (Arabbi *et al.*, 2004). Increased exposure to adverse environmental and/or dietary xenobiotics (e.g. hyperglycaemia) may increase the production of ROS (Johansen *et al.*, 2005). Long term complications of T2D may be exacerbated by oxygen-free radical activity (e.g. RNS) which can initiate peroxidation of lipids, which in turn stimulates glycation of protein, inactivation of enzymes and alteraltions in the structure and function of cell membranes (Boynes, 1991). Oxidative stress is described as being the result of an imbalance between the generation of oxygen and nitrogen derived radicals and an organism's antioxidant potential (Abdollahi *et al.*, 2004), may validate Logani and Davies' suggestion in 1980 that supplementation with non-toxic antioxidants may have a chemoprotective role in T2D.

2.2.1. The role of nitric oxide in glucose-stimulated insulin secretion and β-cell oxidative stress

Nitric oxide (NO) plays an ambiguous role in physiology in that it is both essential for execution of some physiological processes (e.g. as an endothelial derived relaxing factor and as an intermediate in the synthesis and secretion of insulin at low micromolar concentrations) and that it can be toxic in excess. NO was seen to stimulate insulin gene expression, PI3K activity in both Min6 and freshly isolated pancreatic islets (Campbell *et al*., 2007). NO is most deleterious once it reacts with superoxide radicals to form

peroxynitrite (Paquay *et al*., 2000). Hyperglycaemia is linked with the regulation of NOS expression and the production of peroxynitrite. Protein kinase C activation has been shown by Hink *et al.* (2001) to be a key event in hyperglycaemia-induced NOS upregulation (perhaps mediated by NF-κB). Under *in vitro* conditions, cytokines (e.g. TNF-α, IL-1β) have been demonstrated to increase expression of inducible nitric oxide (iNOS), leading to the generation of NO. Concomitant translocation of NF-κB to the β-cell nucleus results in cell death (Kanitkar *et al*., 2008).

2.3. *In vitro* assay models

In vitro screening assays offer the ability to screen for pharmacokinetic activity of compounds/molecules within a specific, cell type (Van de Venter *et al*., 2008). Muscle derived cell lines, including C2C12 myocyte, and fibroblast derived 3T3-L1 adipocytes, have been shown to be sensitive to insulin stimulation in culture resulting in an increase of GLUT4 translocation and glucose uptake from the culture medium (Brunetti, 1989, and Nedachi and Kanzaki, 2006). These cell lines mimic main tissues involved in peripheral insulin regulated glucose homeostasis and utilisation in mammals, namely muscle and fat. 3T3-L1 adipocytes have also been extensively used in metabolic disease research for over 30 years. These cells have been described as being pivotal in advancing the understanding of basic cellular mechanisms associated with diabetes and related disorders. (ZenBio Inc. 2010). Liver cells, including Chang cells, in contrast to muscle cells, have non-insulin-sensitive glucose transporters and are less sensitive to acute insulin stimulated glucose uptake. Chang cells are a human liver derived epithelial and non-tumorgenic cell line that have been shown to express insulin receptor (Rengarajan *et al*., 2007) and to be responsive to insulin stimulation (Parthasarathy *et al*., 2009).

Erasto *et al.* (2009) demonstrate the ability of all three of the above mentioned cell lines

(i.e. C2C12, Chang and 3T3-L1 cells) to be responsive to extract-stimulated glucose uptake. C2C12 and 3T3-L1 cells responded to insulin stimulation by increasing glucose uptake, and Chang cells exhibited a similar increase in glucose taken up when stimulated with metformin (Erasto *et al*., 2009).

2.4. Current therapies in type two diabetes mellitus

In a review by Jung and colleagues (2006), the authors describe the mechanisms of current T2D therapeutics (both clinical and nutraceuticals). These mechanisms include the ability of an agent to directly stimulate insulin secretion, to inhibit increased release of glucose into the blood (e.g. by inhibition of α-glucosidase, a hormone that facilitates the breakdown of carbohydrates to sugar, or by inhibition of glycogenolysis and gluconeogenesis), to enhance glucose utilisation (e.g. by increasing the concentration and sensitivity of insulin receptors) (Jia *et al*., 2003 and Jung *et al*., 2006). Further ability to reduce free radicals and improve microcirculation offers added benefit to T2D patients (Jung *et al*., 2006).

2.4.1. Clinical pharmacological agents

DeFronzo (2010) describes the goal of pharmacological therapy in T2D as being multifactoral; there should be therapeutic delay in disease progression as well as treat the multiple pathophysiological mechanisms associated with T2D. Insulin therapy and the anti-diabetic drug metformin are commercially available and well characterized treatments for T2D and the latter for insulin resistance (Pearson, 2009, and DeFronzo, 2010). Other oral therapeutic agents include the thiazolidinediones (TZDs), incretin-mimetics and sulfonylureas (Radziuk *et al*., 2003; Pearson, 2009, and DeFronzo, 2010).

Exogenous insulin therapy regulates glucose homeostasis in a similar way to endogenous

insulin secretion. Subcutaneous injection of synthetic insulin decreases HGP (by decreasing gluconeogenesis and glycogenolysis), increases peripheral glucose uptake (in muscle and adipose tissue) and increases lipid synthesis in liver and adipose tissue (Chakraborty, 2006, and DeFronzo, 2010). Risk of hypoglycemia is increased in patients on acute insulin therapy (rapid acting synthetic insulins) since exogenous insulin does not only facilitate increased glucose uptake from the blood, but also suppresses HGP (Gram *et al*., 2010). A study by Azar and Lyons (2010) proposed that insulin therapy may confer added risk for cancer, which may be mediated by signalling through insulin-like growth factor one receptor.

Metformin (and TZDs) act by increasing peripheral insulin sensitivity, as well as by decreasing hepatic gluconeogenesis (Radziuk *et al*., 2003; and DeFronzo, 2010). Metformin has been reported to be active in several different physiological mechanisms which result in amelioration of T2D defects (Perriello *et al*., 1994; Radziuk *et al*., 2003; and DeFronzo 2010). Radziuk *et al.* (2003) described metformin as having a mild ability to inhibit complex one in the mitochondrial respiratory chain. Inhibition of the respiratory chain upregulates expression of GLUT4 and glycolysis in peripheral tissues (Radziuk *et al*., 2003). Perriello and colleagues (1994) implicate the role of metformin in improving systemic lipidemia, lowering circulating FFA thus decreasing fatty acid oxidation. FFA have been implicated in contributing to hyperglycaemia by stimulating gluconeogenesis (Randle *et al*., 1963). Another implication of metformin is in regulation of 5' adenosine monophosphate-activated protein kinase, which plays a role in the stimulation of skeletal muscle fatty acid oxidation and glucose uptake, as well as in the modulation of insulin secretion by pancreatic β-cells (Radziuk *et al*., 2003). With glucose transporters, as well as insulin receptors, being active in cell membranes, membrane integrity is important with fluidity and protein configurations being disturbed in T2D (DeFronzo, 2010). Wiernsperger

(1999) described the ability of metformin to modify the physical state of cell membranes and their related proteins.

2.4.2. Phytotherapy and antioxidant supplementation in type two diabetes mellitus

More than 70% of the South African population use indigenous medicinal plants for either their own health care needs or in cultural practices (van Wyk and Gericke, 2000, and Rampedi and Olivier, 2005). With changes in the socio-economic climate and a new trend in merging Western lifestyle with traditional practices, new interest has been shown in herbal/natural remedies (Mander *et al.,* 1997*)*. Li *et al.* (2004) describe negative side effects of some synthetic anti-diabetic drugs, such as lactic acid intoxication and gastrointestinal upsets. The pharmaceutical industry faces a challenge in that the number of new drugs launched into the market declined by 50% since 1995 (Zhang *et al*., 2010). This lack of development of clinical therapy provides a window of opportunity for the evolution of new therapeutics to keep up with the current trend towards increased risk of degenerative diseases (like T2D and cardiovascular disease) caused by increased oxidative stress due to lifestyle. Uncovering the scientific basis of potential ameliorative effects of natural products has been important in providing the pharmaceutical industry with “lead” compounds which can be synthesized into new clinical therapies (Haslam, 1996).

2.4.2.1. The antidiabetic and/or antioxidant effects of plant extracts *in vitro* and *in vivo*

An *in vitro* study by Erasto *et al*. (2009) demonstrated the ability of *Vernonia amygdalina* (a member of the Asteraceae family to which *A. phylicoides* belongs) to stimulate glucose uptake in cell lines that mimic muscle, liver and adipose (i.e. C2C12, Chang and 3T3-L1). Another extract from a plant in the Asteraceae family, *Stevia rebaudiana* Bertoni, directly

stimulates pancreatic β-cell insulin secretion (Jeppesen *et al*., 2000).

An *in vivo* study by Cao *et al.* (2007) has shown green tea extract as a regulator of gene expression in the glucose uptake (e.g. increase in GLUT2 and GLUT4 expression) and insulin signalling (e.g. increase in IRS1 and IRS2 expression) pathways.

Leopoldini *et al.* (2004) reported that polyphenols derived from green (unfermented) tea (e.g. epicatechins) demonstrate strong anti-oxidant properties, particularly against linoleic acid peroxidation in homogenous solutions. Tea preparations have also been demonstrated to react directly with various types of ROS, such as superoxide radical, peroxy radical, NO and peroxynitrite (Sang *et al*., 2007). Hashimoto *et al*., (2000) demonstrated the metal ion chelating ability of green tea. Chelating of metal ions prevents further generation of free radicals.

A study by Kim *et al.* (1999) demonstrated the ability of flavonoids to inhibit production of NO. If this effect can be replicated in pancreatic β-cells, these cells may be afforded a period of protection from hyperglycaemia induced stress, with the potential to preserve insulin synthetic and secretion properties.

Curcumin, a polyphenolic flavonoid recognized for its potent antioxidant capabilities, has been shown to protect pancreatic islets *in vitro* from cytokine-induced cell dysfunction and death (Kanitkar *et al*., 2007). Using lipopolysaccharide-activated macrophages, isothiocyanate and its indole derivatives (from cruciferous vegetables) have also been shown to have anti-inflammatory properties (Tsai *et al*., 2010).

3. Study Aim

The aims of this study were to determine:

- The *in vitro* effect of *A. phylicoides* aqueous extract on glucose metabolism in cell lines that mimic the three key organs implicated in glucose homeostasis; i.e. muscle (C2C12 myocytes), liver (Chang cells) and adipose tissue (3T3-L1 adipocytes).

- The effect of *A. phylicoides* extract on insulin sensitivity *in vitro* by measuring the expression of genetic markers involved in the insulin signalling cascade.

- The potential *ex vivo* antioxidant and anti-inflammatory effect of the extract in pancreatic β-cells and peripheral mononuclear cells respectively.

- The effect of *A. phylicoides* extract on cultured pancreatic β-cell insulin secretion.

CHAPTER 2

MATERIALS AND METHODOLOGY

MATERIALS

1. Reagents

1.1. *In vitro* experiment reagents

0.3 M NaOH + 1% sodium dodecyl sulphate (SDS) (prepared in the laboratory according to standard protocol; see Appendix I).

- NaOH (Cat No.: 10252; AnalaR Laboratories, Poole, England),
- SDS (Cat No.: 161-0416; BioRad, CA, USA).

1,1-Dimethylbiguanide hydrochloride (metformin) (Cat No.: D150959; Sigma, Stanheim, Germany).

3-Isobutyl-1-methylxanthine (IBMX) (Cat No.: I7018; Sigma, Stanheim, Germany).

3-(4,5-dimethylthiazol-2-yl)-2,5-diphenyltetrazolium bromide (MTT) (Cat No.: M5655; Sigma, Stanheim, Germany).

Absolute ethanol (molecular grade) (Cat No.: E7023; Sigma, Manheim, Germany).

Agilent RNA 6000 Nano kit (Cat No.: 5067-1511; Agilent Technologies, Waldbronn, Germany).

Biovision Assay Kits:

- Glucose Uptake Assay Kit (Cat No.: K606-100; BioVision Incorporated, CA, USA),
- Glycogen Content Kit (Cat No.: K646-100; BioVision Incorporated, CA, USA).

Bovine serum albumin (BSA) (Cat No.: A4919; Sigma, Stanheim, Germany).

Bradford assay kit (Cat No.: 3#500-0203; Bradford BioRad Assay, BioRad Laboratories, California, USA).

Cell culture tested water (Cat No.: W3500; Sigma, Stanheim, Germany).

Cell lines:

- C2C12 (Cat No.: CRL-1772; American Type Culture Collection, VA, USA),
- Chang (Cat No.: CCL-13; American Type Culture Collection, VA, USA),
- 3T3-L1 (Cat No.: CL-173; American Type Culture Collection, VA, USA).

Chloroform (Cat No.: C2432; Sigma, Manheim, Germany).

Dexamethasone (Cat No.: D4902; Sigma, Stanheim, Germany).

D-glucose (Cat No.: G7021; Sigma, Stanheim, Germany).

Dimethyl sulfoxide (DMSO) (Cat No.: D4540; Sigma, Stanheim, Germany)

Dulbecco's modified Eagle's medium base (Cat No.: D5030; Sigma, Stanheim, Germany).

Dulbecco's modified eagle's medium (DMEM) (Cat No.: 12-741F, Lonza, MD, USA) (See Appendix I for constituents).

Dulbecco's phosphate buffered saline (DPBS) (Cat No.: 17-513, Lonza, MD, USA).

Eagle's modified essential medium (EMEM) (Cat No.: 12-662F, Lonza, MD, USA). (See Appendix I for constituents).

GenElute™ Mammalian Total RNA kit (Cat No.: RTN350; Sigma, Stanheim, Germany).

Glucose-D-[^{14}C (U)] (Cat No.: NECO42X050UC, Perkin Elmer, MA, USA).

Heat inactivated fetal calf serum (FCS) (Cat No.: 1050-064; GIBCO, Invitrogen, Auckland, New Zealand).

High capacity cDNA kit (Cat No.: 4369913; Applied Biosystems, CA, USA).

Horse serum (HS) (Cat No.: 14-103E, Lonza, MD, USA).

Insulin solution from bovine pancreas; 10 mg/ml in 25 mM HEPES buffer, pH8.2 (Cat No.: I0516; Sigma, Stanheim, Germany).

Isopropanol (Cat No.: I9516; Sigma, Manheim, Germany).

Millex GP syringe-driven filter units (Cat No.: SLGP033RS; Millipore, MA, USA).

$NaHCO_3$ (Cat No.: S3817; Sigma, Stanheim, Germany).

Polymerase chain reaction probes (Applied Biosystems, CA, USA):

- Insulin receptor (INSR); Human (Accession No.: NM_000208.2), mouse (Accession No.: NM_010568)
- Insulin receptor substrate one (IRS1); Human (Accession No.: NM_005544.2), mouse (Accession No.: NM_010570)
- Insulin receptor substrate two (IRS2); Human (Accession No.: NM_003749.2), mouse (Accession No.: NM_001081212.1)
- Phosphoinositide-3-kinase (PI3K); Human (Accession No.: NM_181523.1), mouse (Accession No.: NM_001024955.1)
- Glucose transporter four (GLUT4); (Accession No.: NM_001042), mouse (Accession No.: NM_009204.2)
- Beta Actin (ActB); Human (Part No.: 4326315E-0805013), mouse (Part No.: 4352341E-0808009)
- Glyceraldehyde 3-phosphate dehydrogenase (GAPDH); Human (Part No.: 4326317E-0810028), mouse (Part No.: 4352339E-0806018)

Power SYBR Green (Cat No.: 4367659; Applied Biosystems, CA, USA).

RNase-free water (Cat No.: 1039480; Qiagen, Hilden, Germany).

RNase-free wipes (Cat No.: 9786; Ambion, Applied Biosystems, CA, USA).

RNase inhibitor (Cat No.: N8080119; Applied Biosystems, CA, USA).

RNeasy mini kit (Cat No.: 74106; Qiagen, Hilden, Germany).

Sorenson’s Buffer pH 10.5 (prepared in the laboratory according to standard protocol; see Appendix I).

- Glycine (Cat No.: 2139410; AnalaR Laboratories, Poole, England),
- NaCl (Cat No.: AB006404.500; Merck, Midrand, South Africa),
- NaOH (Cat No.: 10252; AnalaR Laboratories, Poole, England).

TRI Reagent (Cat No.: 93289; Sigma, Manheim, Germany).

Trypan blue (Cat No.: T93595; Sigma, Stanheim, Germany).

Trypsin (Cat No.: 17-161F, Lonza, MD, USA) (See Appendix I for constituents).

TURBO DNA-free kit (Cat No.: 1907; Ambion, Applied Biosystems, CA, USA).

1.2. *Ex vivo* experiment reagents

^{125}I-labeled rat insulin RIA kit (Cat No.: RI-13K; Linco research, St Charles, MO).

26 gauge cannula catheter (Cat No.: NM126; Neotec Medical Industries, Singapore).

BD OptEIA™ Rat TNF-alpha ELISA kit (Cat No.: 560479; BD Biosciences, Woodmead, South Africa).

Collagenase P type I from *Clostridium histolyticum* (C0130; Sigma, Stanheim, Germany).

Dihydrofluorescein diacetate (DAF) (Cat No.: 292648; Sigma, Stanheim, Germany).

Geneticin (Cat No.: 11464990; Roche Diagnostics, IN, USA).

Hanks Balanced Salt Solution (HBSS) (Cat No.: 14025; GIBCO, Invitrogen, Auckland, New Zealand).

Histopaque (1.119 g/L) (Cat No.: 11191; Sigma, Stanheim, Germany).

Krebs-Ringer bicarbonate HEPES buffer (KRBH) (prepared in the laboratory according to standard protocol; see Appendix I).

- NaCl (Cat No.: S5886; Sigma, Stanheim, Germany),
- $NaHCO_3$ (Cat No.: S3817; Sigma, Stanheim, Germany),
- KCl (Cat No.: P5405; Sigma, Stanheim, Germany),
- $MgCl_2$ (Cat No.: M4880; Sigma, Stanheim, Germany),
- $CaCl_2$ (Cat No.: C5670; Sigma, Stanheim, Germany),
- Bovine serum albumin (BSA) (Cat No.: A4919; Sigma, Stanheim, Germany),
- 10 mM HEPES Buffer (Cat No.: 3344; Highveld Biological, Gauteng, South Africa).

L-Glutamine (Cat No.: G8540; Sigma, Stanheim, Germany).

Lipopolysaccharides from *E.coli* (LPS) (Cat No.: L6529; Sigma, Stanheim, Germany).

Penicilin- streptomycin mixture (Cat No.: 17602; Lonza, MD, USA)

RPMI 1640 Medium (Cat No.: 12-702F; Lonza, MD, USA).

Sodium pentobarbital euthanase (Bayer Pty. Ltd., Animal Health Division, Isando, South Africa).

Vacutainer® Ethylenediaminetetraacetic acid (EDTA) blood collection tubes (Cat No.: 368861; BD Biosciences, Woodmead, South Africa).

2. Equipment

2100 PCR Expert Software (Applied Biosystems, CA, USA).

2720 Thermal cycler (Applied Biosystems, CA, USA).

7500 RT PCR System (Applied Biosystems, CA, USA).

ELX800 absorbance microplate reader (Bio Tek Instruments Inc; Friedrichshall, Germany).

FACSCaliber™ (BD Biosciences, MD, USA).

FLX800 fluorescence microplate reader (Bio Tek Instruments Inc.; Friedrichshall, Germany).

Nanodrop ND-1000 spectrophotometer (Nanodrop, Thermo Scientific; DE, USA).

Qiagen TissueLyser (Retsch Technology; Haan, Germany).

3. Software packages

7500 System Software v.1.4.0 (Applied Biosystems; CA, USA).

Gen5 v.1.05 (BioTek Instruments Inc.; Friedrichshall, Germany).

GraphPad Prism v.5.01 (GraphPad Software Inc.; CA, USA).

WinMDI v.2.8 (Purdue University; IN, USA).

METHODOLOGY

1. Source and preparation of *Athrixia phylicoides* extract

A. phylicoides fine twigs and leaves, harvested in June 2005 in the Bushbuckridge area (Limpopo, South Africa), was identified by the South African National Botanical Institute (SANBI) and supplied by Prof Jana Olivier, University of South Africa. A freeze-dried aqueous extract of twigs and leaves of *A. phylicoides* (ARC401) was prepared on a pilot-scale by Dr Dalene De Beer, Nietvoorbij, Agricultural Research Council of South Africa. The extract was prepared by boiling dried fine twigs and leaves in five batches of 1.4 kg/20 L water for 10 minutes. After filtration the extract was concentrated using reverse osmosis and freeze-dried. The batch of dry extract was stored in the dark, under vacuum desiccation, at room temperature (20-24°C).

1.1. Preparation of extract for *in vitro* and *ex vivo* assays

Fresh solutions of the extract were reconstituted in cell culture tested water prior to each assay at a stock concentration of 1 mg/ml. The extract solution was sterile filtered by passing the solution through a sterile, low affinity 0.22 µm syringe driven filter unit. The sterile 1 mg/ml stock was diluted to the required assay concentrations in base DMEM (without phenol red, pyruvate, L-glutamine and glucose) supplemented with 8 mM D-glucose, 3.7 g/L $NaHCO_3$ and 0.1% BSA.

2. *In vitro* experimental procedure

2.1. Source and storage of cell lines

Cryo-vials containing C2C12, Chang or 3T3-L1 cells, originally obtained from the American Type Culture Collection, were cryo-preserved in freshly prepared freezing medium containing cryo-protectant (7% DMSO) in the vapour phase of a liquid nitrogen tank.

2.2. C2C12 cell line

2.2.1. Thawing and counting of C2C12 cells

A vial of C2C12 cells was removed from the nitrogen tank and thawed in a circulating water bath at 37°C with gentle agitation until only a very small piece of ice was left. The cell suspension in the vial was immediately aspirated using a 3 ml disposable Pasteur pipette and dispensed into 10 ml of fresh, warm DMEM supplemented with 10% FCS. To remove DMSO, the cell suspension was centrifuged at 800 x g for 5 minutes. The supernatant was discarded and the cells re-suspended in 10 ml fresh DMEM supplemented with 10% FCS. Cell concentration and viability was determined using a haemocytometer (figure 9).

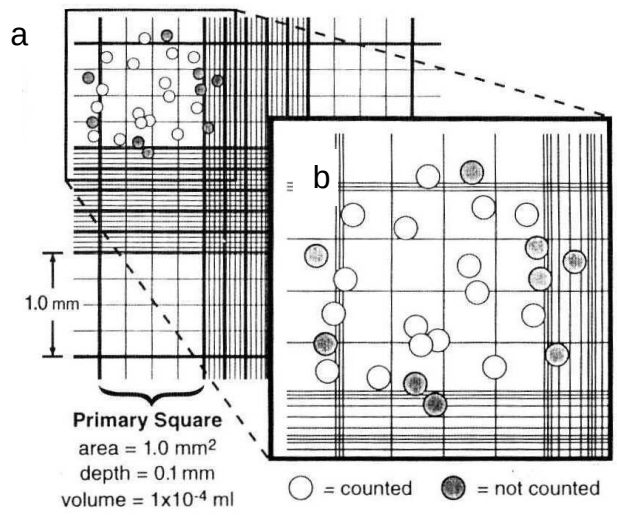

Figure 9. Haemocytometer chamber (**a**) and a 1 mm^2 grid within the chamber (**b**) (PK Group standard protocol, 2004).

2.2.1.1. Cell viability

Cell viability was determined by staining a 100 µl sample of the cell suspension with 100 µl of 0.4% trypan blue in DPBS solution in a 1.5 ml tube. A 10 µl sample of the stained cell suspension was pipetted under the coverslip of the two chambers of the haemocytometer. The number of cells in three 1 mm^2 grids per chamber of the haemocytometer were counted and the average of the six counts was used to determine the total number of cells per milliliter. The membranes of viable cells exclude the blue trypan dye, and damaged or dead cells take up the stain. The number of viable cells was calculated by deducting the blue stained, non-viable cells from the total number of cells. Only cells with a viability of greater than 85% were used.

C2C12 cells were seeded at 2 500 cells/cm^2 into a 75 cm^2 cell culture flask in 18 ml DMEM supplemented with 10% FCS and were incubated at 37°C in humidified air with 5% CO_2 until the following day.

2.2.2. Sub-culture of C2C12 cells

Cells were refreshed with DMEM supplemented with 10% FCS the following day and two days later were sub cultured into three 75 cm^2 culture flasks at 2 500 cells/cm^2 in order to obtain sufficient cells for each experiment. C2C12 cells are known to differentiate rapidly and form contractile myotubes that produce characteristic muscle proteins and myofibrils. During sub-culture, cells were not allowed to become confluent (i.e. less than 70% confluence) as this depletes the myocytic population. In order to loosen cells from the flask culture surface, all media was aspirated and cells were washed with 8 ml warm (37°C) DPBS and incubated for 7 minutes in 2 ml 0.25% Trypsin-versene at 37°C in humidified air with 5% CO_2. Trypsinisation was stopped with the addition of 8 ml fresh DMEM supplemented with 10% FCS. A 100 µl sample of the cell suspension was counted and the

three flasks seeded at 2 500 cells/cm^2. Two of the sub cultured flasks were used to seed assay multi-well plates or flasks and the third was sub cultured for further experiments. For this experiment C2C12 cells were sub cultured and assayed up to a passage number of 19. Thereafter, a new vial of cells was thawed as described above as required. C2C12 cells were seeded at 15 625 cells/cm^2 for assay purposes into multi-well plates as described in the experimental procedure of each assay.

2.2.3. Differentiation of C2C12 cells

Differentiation of C2C12 cells was achieved by refreshing media with DMEM supplemented with 2% HS as opposed to the FCS added in normal cell culture. Since horse serum contains less growth factors than fetal calf serum, proliferation was reduced and myotubule formation was initiated. Cells were differentiated three days after being seeded into the assay plates/flasks. Differentiated C2C12 cells were characterised by a distinct change in morphology; from single, flat, poly-glonal shaped cells to spindle shaped myocytes and multi-nucleate, densely packed myotubules. The evening prior to the respective assay, cells were serum starved by replacing the media with DMEM supplemented with 0.5% HS. Assays were performed on the fifth day after seeding.

2.3. Chang cell line

2.3.1. Thawing of Chang cells

Chang cells were thawed and the cells in suspension were immediately aspirated using a 3 ml disposable Pasteur pipette and dispensed into 10 ml of fresh, EMEM supplemented with 10% FCS. Cell density and viability was determined as described in section **2.2.1.** and viable Chang cells were seeded at 3 000 cells/cm^2 into a 75 cm^2 cell culture flask. The flask, with a total media volume of 18 ml, was incubated at 37°C in humidified air with 5% CO_2 until the following day.

2.3.2. Sub-culture of Chang cells

Chang cells were refreshed with EMEM supplemented with 10% FCS the following day. Two days later the cells were sub cultured into three 75 cm^2 culture flasks at 3 000 cells/cm^2 in order to obtain sufficient cells for each experiment. Two of the sub cultured flasks were used to seed assay plates and the third was sub cultured for further experiments. In this study cells were sub cultured and assayed up to a passage number of 19. In order to avoid contact inhibition, cultures were not allowed to become confluent. After 19 passages, a new vial of cells was thawed as required. Chang cells were seeded at 18 750 cells/cm^2 for assay purposes into multi-well plates or flasks as described in the experimental procedure of each assay. The evening prior to the respective assay, cells were serum starved by replacing the media with EMEM supplemented with 0.5% FCS. Assays were performed on the fifth day after seeding.

2.4. 3T3-L1 cell line

2.4.1. Thawing of 3T3-L1 cells

3T3-L1 cells are embryogenic pre-adipocytes developed through clonal isolation. As described for C2C12 cells above, 3T3-L1 cells were thawed and the cells in suspension were immediately aspirated using a 3 ml disposable Pasteur pipette and dispensed into 10 ml of fresh, warm DMEM supplemented with 10% FCS. Cell density and viability was determined as described in section **2.2.1.** and viable 3T3-L1 cells were seeded at 2 000 cells/cm^2 into a 75 cm^2 cell culture flask. The flask, with a total media volume of 18 ml, was incubated at 37°C in humidified air with 5% CO_2 until the following day.

2.4.2. Sub-culture of 3T3-L1 cells

Seeded cells were refreshed with DMEM supplemented with 10% FCS the following day and two days later were sub cultured into three 75 cm^2 culture flasks at 2 000 cells/cm^2 in order to obtain sufficient cells for each experiment. Two of the sub cultured flasks were used to seed assay plates and the third was sub cultured for further experiments. In this study, 3T3-L1 cells were sub cultured and assayed up to a passage number of 19. Thereafter, a new vial of cells was thawed as required. 3T3-L1 cells were seeded at 12 500 cells/cm^2 for assay purposes into multi-well plates as described in the experimental procedure of each assay.

2.4.3. Differentiation of 3T3-L1 cells

To induce the adipocyte phenotype, 3T3-L1 cells were refreshed prior to reaching confluence (on day three) with adipogenic media (DMEM with 10% FCS was supplemented with 16 µM insulin, 0.6 µM dexamethasone and 0.1 mM IBMX). The transition from fibroblastic, progenitor mesenchymal cells to rounded, fully functional fat-producing adipocytes requires two cell divisions in the adipogenic media, thus cells were refreshed for a further three days with the supplemented, adipogenic media. 3T3-L1 cells were then cultured in normal DMEM supplemented with 10% FCS for two days. The evening prior to the respective assay, cells were serum starved by replacing the media with DMEM supplemented with 0.5% FCS. Assays on 3T3-L1 cells were performed on the eighth day after seeding.

2.5. Glucose Uptake Determination – Glucose oxidase fluorimetric method (method modified from Van de Venter *et al*., 2008)

Cells (C2C12, Chang and 3T3-L1) were seeded into 24 well culture plates and were maintained as described in section **2.1** at 37°C in humidified air with 5% CO_2 until the day

of the experiment (i.e. day five for C2C12 and Chang cells and day eight for 3T3 cells).

On the day of the experiment, cells were rinsed with DPBS in order to remove leftover medium and glucose. Cells were then serum and glucose starved in DPBS for 30 minutes at 37°C in humidified air with 5% CO_2 as this pre-sensitizes the cells. DPBS was aspirated and DMEM containing 8 mM glucose and 0.1% BSA was added to each well and, according to the plate layout (figure 10), either insulin (1.0 µM), metformin (1.0 µM), vehicle control (cell culture tested water) or ARC401 extract (0.025, 0.05, 0.1 µg/µl) was added. C2C12 cells were incubated for one hour, and Chang and 3T3 cells for three hours at 37ºC in humidified air with 5% CO_2.

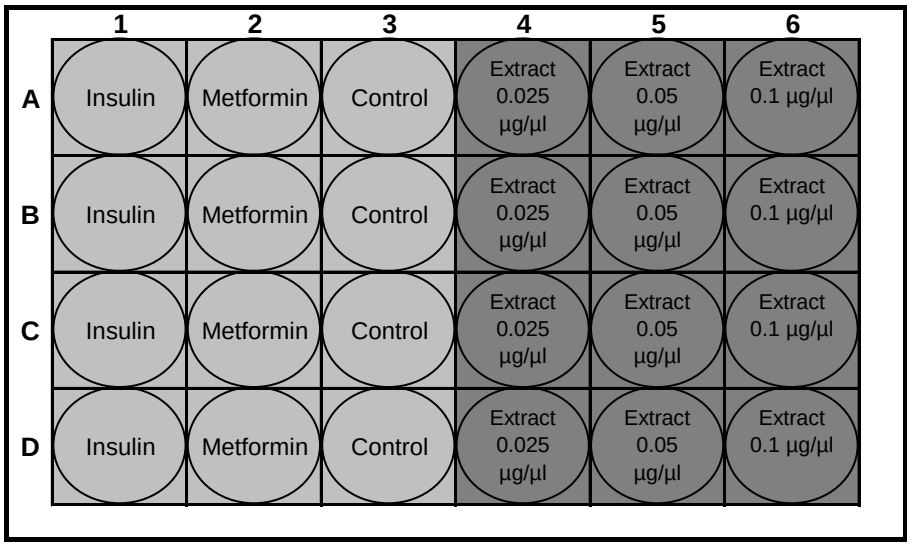

Figure 10. Glucose uptake plate layout

2.5.1. Fluorimetric glucose concentration determination in the media

Glucose concentration of the media remaining in each well was determined by a fluorimetric glucose oxidase method (Biovision Glucose Uptake Assay Kit) following one or three hours incubation. A 4 µl medium sample was removed from each well and was

diluted 1 in 100 in ddH_2O. Ten microlitres of the diluted sample was transferred to a 384 well plate and 10 µl of kit reaction mix was added. The plate was incubated for 30 minutes at 37°C in the dark. The resulting reaction produced a pink solution which was fluorimetrically measured (Ex/Em 530/590) on a BioTek Flx800 plate reader. A glucose standard curve (supplied in the kit) was prepared for each plate read. The actual glucose concentration (µg/well) was calculated by plotting the fluorescent measurement of each sample on the standard curve using Gen5 software v.1.05. A blank reading was obtained from an empty well and subtracted from each glucose value.

2.6. Glucose oxidation and glycogen content assays (methods modified from Gray and Flatt, 1998, and Huijing, 1970 respectively)

Cells (C2C12, Chang and 3T3-L1) were seeded into three six well culture plates and were maintained at 37°C in humidified air with 5% CO_2 until the day of the experiment (i.e. day five for C2C12 and Chang cells and day nine for 3T3 cells).

On the day of the experiment, cells were rinsed with DPBS in order to remove leftover medium and glucose. Cells were then serum and glucose starved in DPBS for 30 minutes at 37°C in humidified air with 5% CO_2. DPBS was aspirated and DMEM containing 8 mM glucose, 0.1% BSA and 0.5 µCi of glucose-D-[^{14}C (U)] was added to each well. According to the plate layout (figure 11), either insulin (1.0 µM), metformin (1.0 µM), vehicle control (water) or extract (0.025, 0.05, 0.1 µg/µl) was added.

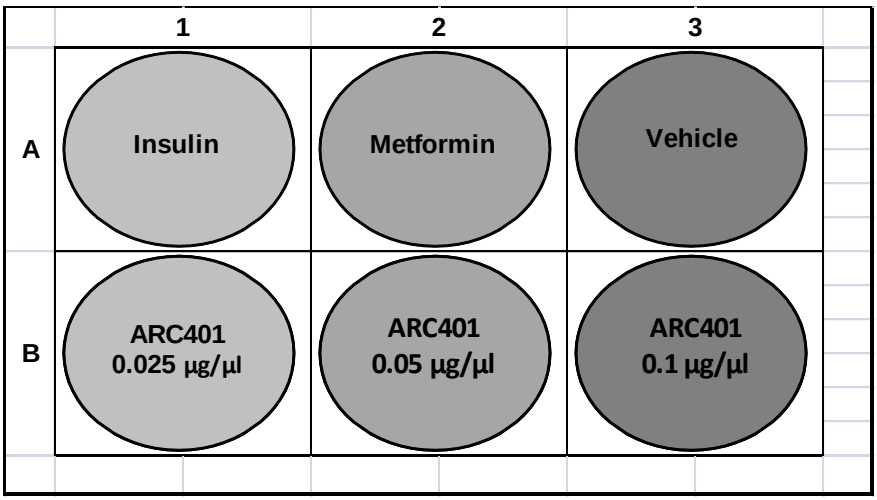

Figure 11. Glucose oxidation assay and glycogen content determination plate layout

2.6.1. ^{14}C glucose oxidation assay (method adapted from Gray and Flatt, 1998)

For this assay the sterile 1 mg/ml ARC401 stock was diluted in DMEM with phenol red to eliminate cell samples that may be compromised due to NaOH leakage from the filter paper used (as described below). Filter paper (Whatman no.1) moistened with 0.1 M NaOH was cut into well-size discs and placed over each well to trap ^{14}C released by cells during glucose oxidation. C2C12 cells were incubated for one hour, and Chang and 3T3 cells for three hours at 37ºC in humidified air with 5% CO_2. The respective filter paper discs were removed and placed in scintillation vials with 1 ml ddH_2O and 5 ml Ultima Gold liquid scintillation fluid. Samples were equilibrated overnight in the 2200CA Tri-carb Series liquid scintillation and cpm and dpm values measured the following day. Each sample was read for 1 minute. An average of two cpm and two dpm values were used per sample. Sample readings were normalised according to a standard curve for radioactive carbon (^{14}C) that is installed in the 2200CA Tri-carb system.

2.6.2. Glycogen content determination (method adapted from Huijing, 1970)

The cells were rinsed with warm (37°C) DPBS and trypsinised (0.5 ml 0.25% trypsin-versene per well for 2 minutes at 37°C in humidified air with 5% CO_2). Trypsinisation was stopped using ice cold DPBS. The cell suspension was counted using a haemocytometer (as described in section **2.1**) and 1 x 10^6 cells were removed and centrifuged (800 x g for 5 minutes at 4°C). The resultant pellet was resuspended in 200 µl ddH_2O. The cell suspension was homogenized using a Qiagen TissueLyser (20/s for 2 minutes) and then boiled for 5 minutes to inactivate glycogen degrading enzymes such as phospho-glucomutase and glycogen phosphorylase. The boiled samples were spun at 13 000 x g for 5 minutes and 50 µl of the supernatant was transferred to a 96 well plate and glycogen content was determined using a colourimetric glycogen assay kit from BioVision. To the 50 µl supernatant sample, 2 µl of hydrolysis enzyme mix (provided in the kit) was added and the samples incubated at room temperature in the dark for 30 minutes. This was also done for the standards which were provided in the kit. Fifty microlitres of kit reaction mix was added to each sample and to the standards. Plates were incubated at room temperature for 30 minutes. The resulting pink solution was colourimetrically measured (absorbance was read at 577 nm on a BioTek® ELX 800 plate reader). The actual glycogen content was calculated by plotting the absorbance measurement of each sample on the standard curve. Results were normalised per million cells. Three independent experiments with three replicates per extract concentration and control were performed per cell line.

2.7. Protein determination assay (method modified from Bradford, 1976)

Protein determinations were performed for the assessment of radio-labeled deoxy-glucose uptake using the Bradford method according to the manufacturer's instructions (Bradford Biorad Assay, Biorad Laboratories, USA). A 5 µl sample of lysed cells from each well/flask or bovine serum albumin (BSA) standards (supplied with the kit) was added to wells of a

96-well plate, followed by 250 µl of Bradford reagent. Plates were incubated in the dark for 10 minutes and absorbance was read at 570 nm on a BioTek® ELX 800 plate reader. The actual protein concentration was calculated by plotting the absorbance measurement of each sample on the BSA standard curve.

2.8. Chang cell MTT (3-(4,5-Dimethylthiazol-2-yl)-2,5-diphenyltetrazolium bromide) cytotoxicity assay (method modified from Mossman, 1983)

Chang cells were seeded into 96 well culture plates and were maintained at 37°C in humidified air with 5% CO_2 until the day of the experiment (i.e. day five).

On the day of the experiment, cells were rinsed with DPBS in order to remove leftover medium and glucose. Cells were then serum and glucose starved in DPBS for 30 minutes at 37°C in humidified air with 5% CO_2. DPBS was aspirated and DMEM containing 8 mM glucose and 0.1% BSA was added to each well, as well as vehicle control (water) and ARC401 extract at increasing concentrations (0.0125, 0.025, 0.05, 0.1, 1.0 µg/µl) according to the plate layout (figure 12).

	1	2	3	4	5	6	7	8	9	10	11	12
A	Blank	Blank	Blank	Blank	Blank	Blank	Blank	Blank	Blank	Blank	Blank	Blank
B	Blank	Vehicle	0.0125 µg/µl	0.025 µg/µl	0.05 µg/µl	0.1 µg/µl	1 µg/µl	Blank	Blank	Blank	Blank	Blank
C	Blank	Vehicle	0.0125 µg/µl	0.025 µg/µl	0.05 µg/µl	0.1 µg/µl	1 µg/µl	Blank	Blank	Blank	Blank	Blank
D	Blank	Vehicle	0.0125 µg/µl	0.025 µg/µl	0.05 µg/µl	0.1 µg/µl	1 µg/µl	Blank	Blank	Blank	Blank	Blank
E	Blank	Vehicle	0.0125 µg/µl	0.025 µg/µl	0.05 µg/µl	0.1 µg/µl	1 µg/µl	Blank	Blank	Blank	Blank	Blank
F	Blank	Vehicle	0.0125 µg/µl	0.025 µg/µl	0.05 µg/µl	0.1 µg/µl	1 µg/µl	Blank	Blank	Blank	Blank	Blank
G	Blank	Vehicle	0.0125 µg/µl	0.025 µg/µl	0.05 µg/µl	0.1 µg/µl	1 µg/µl	Blank	Blank	Blank	Blank	Blank
H	Blank	Blank	Blank	Blank	Blank	Blank	Blank	Blank	Blank	Blank	Blank	Blank

Figure 12. MTT cytotoxicity plate layout

The plates were incubated at 37°C in humidified air with 5% CO_2 for 24 hours. All media was aspirated and 200 µl of fresh DMEM containing 8 mM glucose and 0.1% BSA (without phenol red) as well as 50 µl MTT solution (2 mg/ml DPBS) was added to each well and plates incubated for one hour. Once incorporated into the cells, the tetrazolium bromide is reduced in active mitochondria by mitochondrial dehydrogenase to formazan crystals. The non-solubilised formazan crystals formed over the one hour incubation period were dissolved in 200 µl DMSO and 25 µl Sorensen's glycine buffer pH 10.5. The resulting purple formazan solution was colourimetrically measured (absorbance was read at 570 nm on a BioTek® ELX 800 plate reader). Samples of ARC401 at the various concentrations tested were dissolved in media without phenol red and the absorbance read at 570 nm. To eliminate non-specific reaction between the extract, at the given concentrations, and the MTT solution, the optical density of extract dissolved in base DMEM containing 8 mM glucose and 0.1% BSA (without phenol red) as well as MTT solution was measured. These values were subtracted from the respective optical density of the samples per concentration tested. Three independent experiments with six replicates per extract concentration and control were performed.

2.9. Ribonucleic acid (RNA) extraction, complementary DNA synthesis (cDNA) and real-time polymerase chain reaction

Cells (C2C12, Chang and 3T3-L1) were seeded into four 75 cm^2 flasks and were maintained at 37°C in humidified air with 5% CO_2 until the day of the experiment (i.e. day five for C2C12 and Chang cells and day nine for 3T3 cells).

On the day of the experiment, cells were rinsed with DPBS in order to remove leftover medium and glucose. Cells were then serum and glucose starved in DPBS for 30 minutes at 37°C in humidified air with 5% CO_2. DPBS was aspirated and DMEM containing 8 mM

glucose and 0.1% BSA was added to each of the five flasks. To flask A, insulin was added to yield a final concentration of 1.0 µM, to flask B metformin (1.0 µM), to flask C vehicle control (water) and to flask D ARC401 extract (0.05 µg/µl). C2C12 cells were incubated for one hour, and Chang and 3T3-L1 cells for three hours at 37ºC in humidified air with 5% CO_2. All media was then aspirated and cells trypsinised (2 ml 0.25% trysin-versene per flask). Trypsinisation was stopped with 8 ml ice cold DPBS per flask and the DPBS cell suspensions were frozen at -20ºC until the total number of experiments were completed (i.e. three independent experiments per cell line).

2.9.1. RNA Extraction (method modified from Chomczynski and Sacchi, 1987)

When all 36 cell samples were collected, the DPBS cell suspensions were spun down (800 x g for 5 minutes at 4°C) and supernatants aspirated. The cell pellets were resuspended in 1 ml TRI Reagent and transferred to 2 ml PCR tubes. The TRI reagent protects RNA by deactivating RNases which may still be active at 0°C. The samples were given abbreviated labels as shown in table in appendix II.

All cell samples were homogenized using a Qiagen TissueLyser (20/s for 1 minute), rested on ice for 1 minute and homogenized again for 1 minute at 20 oscillations per second. The work surfaces used for all molecular work, as well as the equipment (e.g. pipettes) was wiped down with 70% ethanol and RNase free wipes. Cell samples were kept on ice throughout the RNA extraction, cDNA synthesis and reverse transcription-polymerase chain reaction (RT-PCR) processes in order to preserve RNA integrity. The homogenates were then spun at 12 000 x g for 10 minutes at 4°C. The supernatant, containing the RNA, was transferred to new 2 ml tubes. Two hundred micro liters of chloroform was added to each tube and the tubes shaken for 3 minutes. Tubes were then centrifuged at 12 000 x g for 15 minutes at 4°C. The upper aqueous phase, containing the RNA was transferred to a

new 1.5 ml tube; with special precaution taken not to disturb the white interphase (containing DNA) or the pink/red organic phase (containing lipid and proteins) (figure 13).

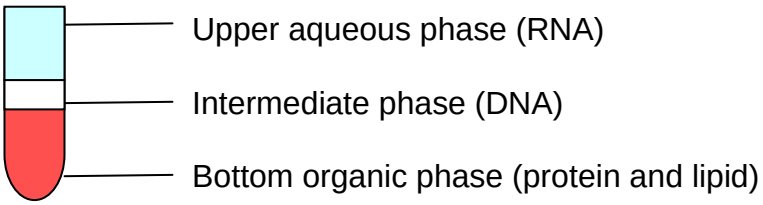

Figure 13. Chloroform partitioning of RNA into aqueous supernatant by centrifugation. The upper aqueous phase containing the RNA was mixed with 500 µl isopropanol to precipitate RNA and incubated at -20°C overnight.

2.9.1.1. RNA purification

The following morning, tubes were removed from -20°C and centrifuged at 12 000 x g for 20 minutes at 4°C. The supernatants were discarded and the RNA pellets washed twice in 75% ethanol and allowed to partially dry. The partially-dried pellets were each re-dissolved in 100 µl RNase-free water. The suspensions were incubated at 55°C for 10 minutes on a heating block to promote solubilisation. RNA clean-up was done using a RNeasy mini kit from Qiagen. Three hundred and fifty microlitres of RLT lysis buffer (supplied in kit) and 250 µl molecular grade absolute ethanol was added to each RNA solution. The entire volume of each sample was transferred to an RNeasy spin column placed in a 2 ml collection tube (supplied in kit). Samples were spun at 12 000 x g for 15 seconds at room temperature and the flow through discarded. Each RNA sample was retained in the respective column membrane. RPE buffer (supplied in kit) was diluted with four volumes of molecular grade absolute ethanol and 500 µl added to each spin column. The columns were spun for 15 seconds at 12 000 x g at room temperature. The flow through was

discarded and a further 500 µl RPE buffer added to each column before spinning for another 15 seconds at 12 000 x g at room temperature. Each column was transferred to a new 2 ml collection tube and spun at 12 000 x g for 1 minute at room temperature. The RNeasy spin columns were transferred to new 1.5 ml collection tubes and 40 µl RNase-free water was added directly to each spin column membrane in order to elute RNA. Columns were allowed to stand for 1 minute and were then spun for 1 minute at 12 000 x g at room temperature. A further 40 µl RNase-free water was added directly to each spin column membrane and columns spun for 1 minute at 12 000 x g at room temperature. RNA yields were quantified using a Nanodrop ND-1000 spectrophotometer using absorption at 260 nm (A_{260}). An A_{260} reading of 1 is equivalent to approximately 40 µg/ml of single-stranded RNA. An A_{260}/A_{280} ratio of 2.0 indicates very pure RNA samples, with no protein contamination. An A_{260}/A_{240} of 1.4 indicates very pure RNA samples, with no salt contamination. The instrument was blanked using 2 µl of RNase-free water and three measurements per sample were read. The Nanodrop spectrophotometer uses the Beer-Lambert law to calculate UV absorbance by nucleic acid, where A_{260} = ECl (A = absorbance; E = extinction coefficient; C = concentration of nucleic acid; l = path length of the spectrophotometer cuvette). The extinction coefficient for RNA is 0.025 $(mg/ml)^{-3}cm^{-2}$ and the path length of the spectrophotometer cuvette is typically 1 cm. The average of the three measurements was used in calculations performed in Excel (see table in appendix II) for DNase treatment and determining RNA integrity on an Agilent chip.

2.9.1.2. Determining RNA Integrity

Although the A_{260}/A_{280} and the A_{260}/A_{240} spectral ratios obtained from the Nanodrop indicate the protein and organic contamination of the RNA samples, true integrity and RNA quality is best determined by running RNA samples on an electrophoretic gel. The Agilent RNA 6000 Nano kit was used to determine RNA integrity. In the evaluation of both RNA

integrity and concentration, the Agilent 2100 Bioanalyser employs a combination of microfluidics, capillary electrophoresis and fluorescent dye that binds to nucleic acid. Nucleic acid fragments were separated based on their size as they were driven through the RNA chip electrophoretically. The RNA 6000 Nano dye, marker and filtered gel (supplied in the kit) were removed and allowed to equilibrate to room temperature. The Nano dye was vortexed for 10 seconds and spun down at 13 000 x g for 10 minutes at room temperature. One microlitre of Nano dye was added to the 65 µl filtered gel aliquot and the solution vortexed well and then spun at 13 000 x g for 10 minutes at room temperature. The RNA samples were denatured by placing samples on a heating block set at 70°C for 2 minutes. Electrodes on the Agilent Bioanalyser were cleaned and decontaminated using 350 µl of RNase-free water and 350 µl RNaseZap respectively. Gel-dye mix, Nano marker (to confirm electrophoretic drive), RNA ladder and samples were loaded into the respective wells of the Agilent chip and the chip vortexed for 1 minute at 1 159 x g. The RNA ladder was used as a reference standard and was composed of six RNAs ranging 25 – 500 ng/µl. The chip was read using 2100 Expert Software within 5 minutes of preparation. Size and mass information was determined by the fluorescence of RNA molecules as they move through the channels of the chip. The 2100 Expert Software compared the peak areas of the RNA samples to the combined area of the six RNA ladder peaks in order to determine RNA concentration. The software generated both a gel-like image and an electropherogram. The ratio of the two major ribosomal RNA species (i.e. 18S and 28S; 1:2) was used to determine potential degradation of RNA (figure 14). A RNA integrity number (RIN) of 9.2 was considered good (intact, non-degraded total RNA) and a RIN of less than six was considered poor (partially degraded total RNA).

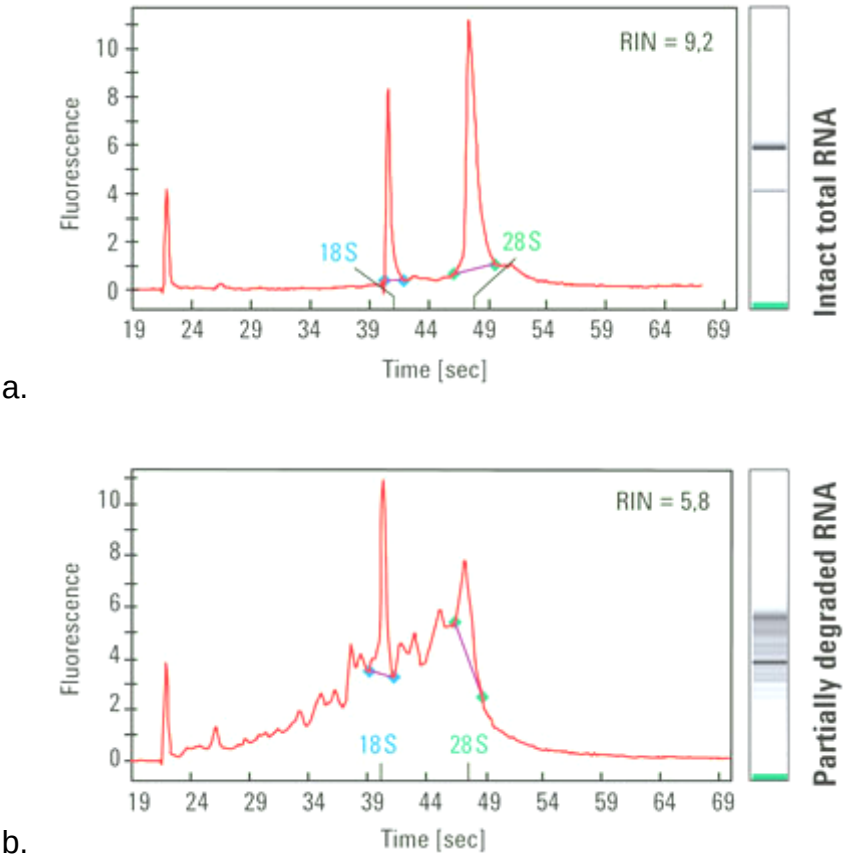

Figure 14. Electropherogram. Showing the characteristic signature of a high quality total RNA (100 ng) sample (a) and low quality total RNA sample (100 ng) (b).

2.9.1.3. DNase Treatment

A 20 µg sample of RNA was made up to 42 µl with RNase-free water according to the table in appendix II. Forty two micro litres of samples that had a total RNA content of less than 20 µg were used as required.

To the diluted RNA, 5 µl of DNase buffer and 1.5 µl of Turbo DNase (as provided in the TURBO DNA-free kit from Ambion) was added and the mix incubated for 45 minutes at 37°C. An additional 1.5 µl of Turbo DNase was added to each sample with further 45 minutes incubation at 37°C. To stop the reaction, DNase inactivation reagent (provided in the kit) was added to the samples (10 µl per sample). Samples were centrifuged at 10 000

x g for 1.5 minutes and the supernatant (RNA) was transferred to a fresh 0.5 ml tube. DNA-free RNA concentrations were determined using a Nanodrop spectrophotometer as described in section **2.9.1**.1.

2.9.1.4. Reverse Transcription Complimentary DNA Synthesis

Complementary DNA (cDNA) was synthesized from the RNA extracted from the C2C12, Chang and 3T3-L1 cells. The reaction was catalysed by the enzyme reverse transcriptase. Reverse transcriptase generates the complementary DNA based on the pairing of RNA base pairs (A, U, G, C) to their DNA compliments (T, A, C, G respectively). Deoxynucleoside triphosphates (dNTPs) (T, A, C, G) are added to the RNA samples with the reverse transcriptase enzyme. Random primers are also added to initiate the reverse transcriptase enzyme transcription of cDNA. High capacity cDNA kit components were thawed on ice. A 1 µg sample of RNA was made up to a total volume of 10 µl with RNase-free water according to the table in appendix II in MicroAmp optical 96 well reaction plates. A negative (-ve) water control as well as two positive (+ve) controls (1 µg of Ambion mouse and 1 µg of Ambion human RNA control template) were prepared with the cell RNA samples. Mouse and human positive controls were used since C2C12 and 3T3-L1 cells are mouse-derived and Chang cells human-derived. All tubes were prepared in duplicate (i.e. a +ve and –ve reverse transcription control).

Two reverse transcription (RT) mastermixes were prepared according to kit instructions. The mastermixes were prepared as follows:

Positive RT Mastermix (per reaction) – 2 µl RT buffer
0.8 µl dNTP mix
2 µl random primers
1 µl RNase inhibitor
3.2 µl nuclease-free water
1 µl reverse transcriptase

Negative RT Mastermix (per reaction) – 2 µl RT buffer
0.8 µl dNTP mix
2 µl random primers
1 µl RNase inhibitor
4.2 µl nuclease-free water

Mastermix was required for 38 samples (including controls) so 44 reactions were made per RT Mastermix. All reagents for the Mastermixes were provided in the High capacity cDNA kit. The respective Mastermixes were added to the 1 µg RNA samples (10 µl per sample) and the plate sealed. The 96 well plates were spun for 30 seconds at 3 000 x g to eliminate air bubbles. A 2720 Thermal cycler was used to amplify the RNA and was programmed as follows:

Step 1 - 75°C (10 minutes)

Step 2 - 37°C (120 minutes)

Step 3 - 85°C (5 seconds)

Step 4 - 4°C (∞)

The reaction volume was set to 20 µl, sample tubes were placed into the thermal cycler and the programme run. The first step in the thermal cycler allowed for the activation of the reverse transcriptase enzyme. Annealing of the dNTPs followed in the second step and extension of the sequence occured in the third. The fourth step cooled the newly synthesised cDNA to 4°C. Newly synthesized cDNA samples were removed within 30 minutes after the completion of Step 4 and was then stored at -20°C.

2.9.1.5. Testing cDNA

cDNA was thawed on ice and work surfaces prepared by wiping with 70% ethanol. To confirm positive cycling prior to the identification and quantification of our desired sequences (i.e. those coding for insulin receptor, insulin receptor substrates 1 and 2, phosphoinositide-3-kinase and glucose transporter 4) the cDNA was tested using β-actin primers (forward and reverse). β-actin was used as it is a well known stably expressed gene that occurs in all tissue. The non-specific fluorescent dye SYBR green was used to confirm double stranded DNA (SYBR green intercalates with double stranded DNA). Two PCR reaction mixes were prepared per sample as follows:

Mouse β-actin (Act B) Reaction Mix - 12.5 µl SYBR green
1 µl mouse Act B forward primer (10 µM)
1 µl mouse Act B reverse primer (10 µM)
9.5 µl nuclease-free water

Human β-Actin (Act B) Reaction Mix - 12.5 µl SYBR green
1 µl human Act B forward primer (10 µM)
1 µl human Act B reverse primer (10 µM)
9.5 µl nuclease-free water

Since primers (and Syber green) were used to test the cDNA the dissociation step was added in the PCR programme run by 7500 RT-PCR System Sequence Detection Software version 1.4.

According to the sample key (table in the appendix II) plate layout (figure 15), 1 µl of positive and negative cDNA samples and 24 µl of respective reaction mix was added to each well. The 96 well PCR plate was agitated for 5 minutes at 500 oscillations and spun down at 1 811 x g for 30 seconds and Real-Time PCR was run on a 7500 RT-PCR System.

	1	2	3	4	5	6	7	8	9	10	11	12
A	1+	1-	9+	9-	26+	26-	34+	34-	13+	13-	23+	23-
B	2+	2-	10+	10-	27+	27-	35+	35-	14+	14-	24+	24-
C	3+	3-	11+	11-	28+	28-	36+	36-	15+	15-	25+	25-
D	4+	4-	12+	12-	29+	29-	37+	37-	16+	16-	39+	39-
E	5+	5-			30+	30-	38+	38-	17+	17-	20+	20-
F	6+	6-			31+	31-	20+	20-	18+	18-		
G	7+	7-			32+	32-			21+	21-		
H	8+	8-			33+	33-			22+	22-		

Figure 15. cDNA PCR test plate layout.

2.9.2. Real Time-PCR (RT-PCR)

Polymerase chain reaction was used to amplify and quantify targeted DNA molecules. The DNA molecules (genes) of interest were insulin receptor (INSR), insulin receptor substrates 1 and 2 (IRS1 and IRS2), PI3K and glucose transporter 4 (GLUT4). Amplified DNA were detected and quantified as the reaction progressed in real time. Sequence-specific probes for each of the genes of interest were used (rather than primers). Since

reporter probes offer higher specificity and enables quantification even in the presence of non-specific DNA amplification. DNA probes consist of oligonucleotides labeled with a fluorescent reporter which is cleaved once the probe hybridizes with its complimentary DNA target. The probe also has a quencher of fluorescence attached at the opposite end to the fluorescent reporter which prevents detection of fluorescence if the reporter is not cleaved. cDNA synthesized in section **2.9.1.4.** was diluted 1:3 in nuclease-free water and kept on ice. Standard curves were prepared for the C2C12 and 3T3-L1 cells using 1 µg of mouse Ambion cDNA. Serial dilutions were made in nuclease-free water and 0.8 µl pipetted in duplicate into a 96 well PCR plate according to the plate layout below (figure 16). Standard curves were similarly prepared for Chang cells using 1 µg of human Ambion cDNA.

a.

	1	2	3	4	5	6	7	8	9	10	11	12
A	100	100	1+	9+	1+	9+	26+	34+	26+	34+		
B	10	10	2+	10+	2+	10+	27+	35+	27+	35+		
C	1	1	3+	11+	3+	11+	28+	36+	28+	36+		
D	0.1	0.1	4+	12+	4+	12+	29+	37+	29+	37+		
E	0.01	0.01	5+		5+		30+	38+	30+	38+		
F	0.001	0.001	6+		6+		31+	20+	31+	20+		
G	0.000	0.000	7+		7+		32+		32+			
H	NTC	NTC	8+		8+		33+		33+			

b.

	1	2	3	4	5	6	7	8	9	10	11	12
A	100	100	13+	23+	13+	23+						
B	10	10	14+	24+	14+	24+						
C	1	1	15+	25+	15+	25+						
D	0.1	0.1	16+	39+	16+	39+						
E	0.01	0.01	17+	20+	17+	20+						
F	0.001	0.001	18+		18+							
G	0.000	0.000	21+		21+							
H	NTC	NTC	22+		22+							

Figure 16. RT-PCR plate layouts for each of the six genes of interest. i.e. INSR, IRS1,

IRS2, PI3K and GLUT4; for C2C12 and 3T3-L1 cells (a) and Chang cells (b).

A PCR reaction mix was prepared per gene of interest. The reaction mix contained the respective assay probe in a Taq polymerase assay master mix as follows per probe per sample:

PCR Reaction Mix - 5 µl Master mix

0.5 µl Probe assay

3.7 µl nuclease-free water

PCR reaction mix was required for 42 Chang cDNA samples (including standards). The diluted cDNA samples (0.8 µl) were pipetted into a 96 well PCR plate according to the plate layout above in duplicate. Similarly, 0.8 µl of the respective human and mouse cDNA Ambion was added to the 96 well plates. To each of the wells (including the standards), 9.2 µl of PCR reaction mix was added. The 96 well plate/s were agitated for 5 minutes at 500 oscillations per minute and centrifuged for 30 seconds at 1 811 x g. Real-Time PCR was run on a 7500 RT-PCR. Data was analysed using 7500 System Software v.1.4.0. Data was expressed relative to GAPDH and Actβ house-keeping genes.

3. *Ex vivo* experimental procedure

Age matched, one year old, adult, male Wistar rats of similar body weight (250-300 g) were housed in a controlled environment (12 hour light/dark cycle at 22±2°C). Rats were maintained on a standardized laboratory diet according to the Medical Research Council Animal Unit standard operating procedures. The rats were anaethetised with 15 mg/kg sodium pentobarbital by intraperitoneal injection. A mid-line abdominal incision (figure 17a) was made and 24 ml of blood was collected (pooled from three rats) from the abdominal vena cava in EDTA tubes (figure 17b) for use in section **3.3.** below. Pancreata were harvested for use in section **3.2.** below.

a. 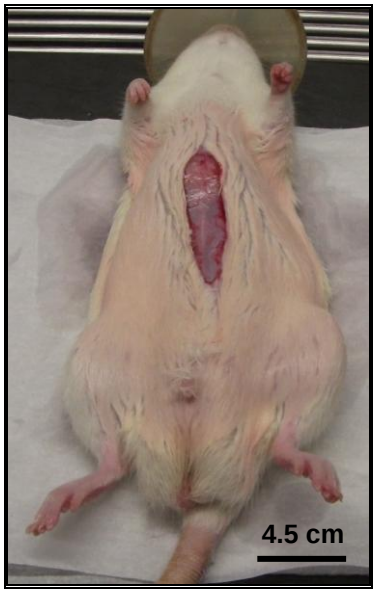

b. 

Figure 17. Mid-line abdominal incision (a) and blood collection (b) in a Wistar rat. (Diabetes Discovery Platform, 2010)

3.1. Animal ethics

All animal procedures were performed in accordance with the ethical code of conduct as prescribed by the latest South African Medical Research Council (MRC) “Guidelines on ethics for medical research: use of animals in research”. This study was approved by the Ethical Committee for Research on Animals (ECRA) (approval no. 09/09).

3.2. Pancreatic islet and β-cell experimental procedure

3.2.1. Isolation and culture of rat pancreatic islets (method adapted from Gotoh, Maki *et al.*, 1987)

The main pancreatic duct was identified by reflecting the duodenal loop, thereby exposing the main pancreatic duct and ampullae (figure 18).

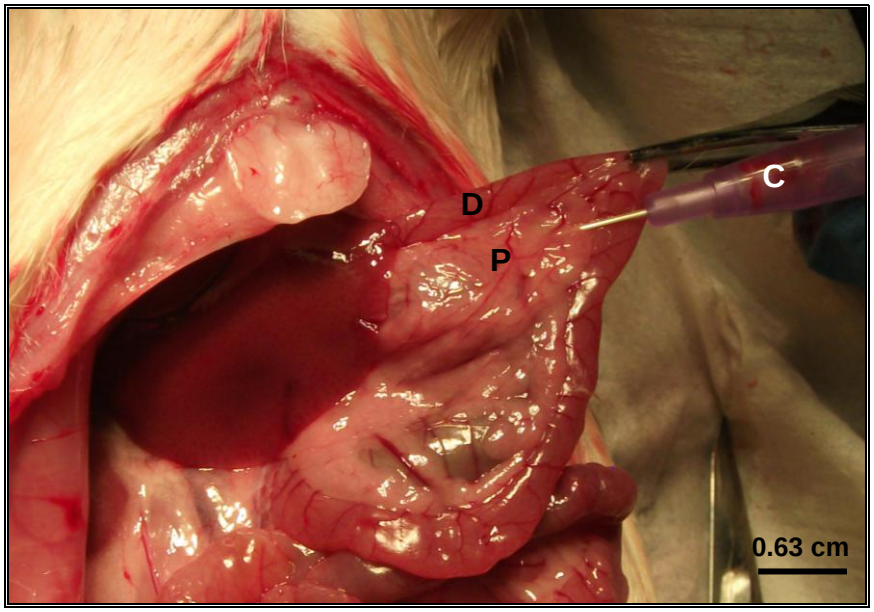

Figure 18. Reflection of the duodenal loop (D), exposing the pancreas (P) to allow for ductal cannullation (C). (Diabetes Discovery Platform)

Rat pancreata were distended with 6 ml ice cold HBSS containing 1 mg/ml collagenase P via the main pancreatic duct using a 26 gauge neonatal canula under a stereo microscope. The pancreata were then carefully excised (figure 19) and placed in a sterile 50 ml tube on ice with a further 5 ml of collagenase P solution. Pancreata were carefully removed from along the gastrointestinal tract and the spleen. Visible excess fat was removed.

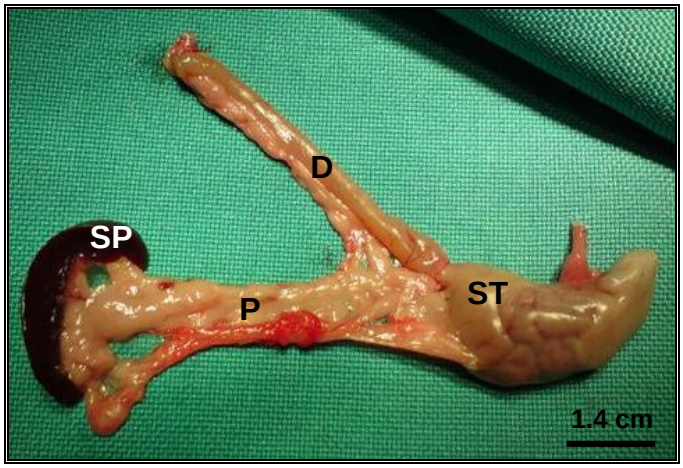

Figure 19. Distended rat pancreas (P) semi-excised; attached to the spleen (SP), duodenum (D) and stomach (ST). (Diabetes Discovery Platform)

Five pancreata were pooled to form one sample. The excised pancreata were digested at 37ºC in a circulating water bath for 30 minutes with intermittent shaking. The digestate was washed in 10 ml cold HBSS containing 0.1% BSA (HBSS/BSA), filtered through a 500 µm nylon mesh and centrifuged at 600 x g for 15 minutes. The pellet was again washed and centrifuged in 10 ml HBSS/BSA, the pellet was resuspended, layered onto a Histopaque gradient (15 ml Histopaque 1.119 g/l containing the digested pancreas tissue with 15 ml HBSS/BSA layered on top) and centrifuged at 800 x g for 20 minutes at 4°C with the brake off. The islets were recovered from the HBSS/BSA layer, washed with HBSS and cultured for 24 hours in DMEM containing 5.5 mM glucose supplemented with 10% FCS, 40 µg/ml geneticin, penicillin (100IU) and streptomycin (100 µg/ml) at 37ºC in

humidified air with 5% CO_2. The following day approximately 1 000 islets were handpicked using a 100 µl pipette under a stereo microscope and cultured for 24 hours in two petri dishes in DMEM containing 5.5 mM glucose supplemented with 10% FCS, 40 µg/ml geneticin, penicillin (100IU) and streptomycin (100 µg/ml). To one of the petri dishes, 0.05 µg/µl ARC401 was added to the culture medium.

3.2.2. Glucose-stimulated insulin release assay (method modified from Henningsson *et al*., 2002)

Cultured islets were washed and incubated for 30 minutes at 37ºC and 5% CO_2 with KRBH containing 2.8 mM glucose. The islets were equally separated into the wells of a six well plate incubated for two hours at 37ºC in humidified air and 5% CO_2 with KRBH containing either 2.8 mM, 17 mM or 35 mM glucose according to the plate layout (figure 20).

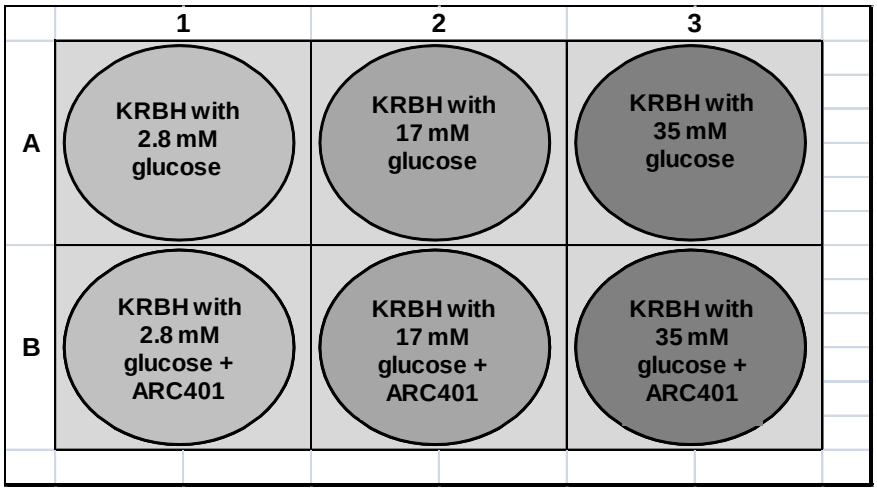

Figure 20. Isolated rat islet plate layout for the measurement of glucose-stimulated insulin secretion

Islets pre-exposed for 24 hours to ARC401 extract were seeded in row B and islets incubated without ARC401 for 24 hours were seeded into row A. After 15 minutes and 120 minutes, 200 µl KRBH was removed and the insulin concentration determined by radioimmunoassay (RIA) using a ^{125}I-labeled rat insulin RIA kit. Unlabelled antigen (i.e. insulin in culture media) is added to fixed concentrations of labeled tracer antigen (^{125}I-labeled insulin) and antiserum (guinea pig anti-rat insulin). Unlabeled antigen competes with labeled tracer antigen for binding sites on the antibody; the amount of tracer bound to the antibody decreases with increasing concentrations of unlabeled antigen. The amount of unlabeled antigen is quantified relative to a standard curve which was set up using increasing concentrations (0.1 – 10 ng/ml) of standard unlabeled antigen.

3.2.3. Flowcytometric determination of nitric oxide (NO) (method adapted from Strijdom *et al*., 2004)

Immediately after the glucose-stimulated insulin release assay, a single cell suspension of β-cells was obtained by trypsinising the islets with 0.5 ml 0.25% trypsin-versene solution for 4 minutes, or until single cells could be seen under a stereo microscope. The single β-cell suspensions were incubated with either 2.8 mM glucose or 35 mM glucose as well as 10 mM DAF fluorescent nitric oxide (NO) label per well for two hours at 37ºC in humidified air and 5% CO_2 (see plate layout, figure 21).

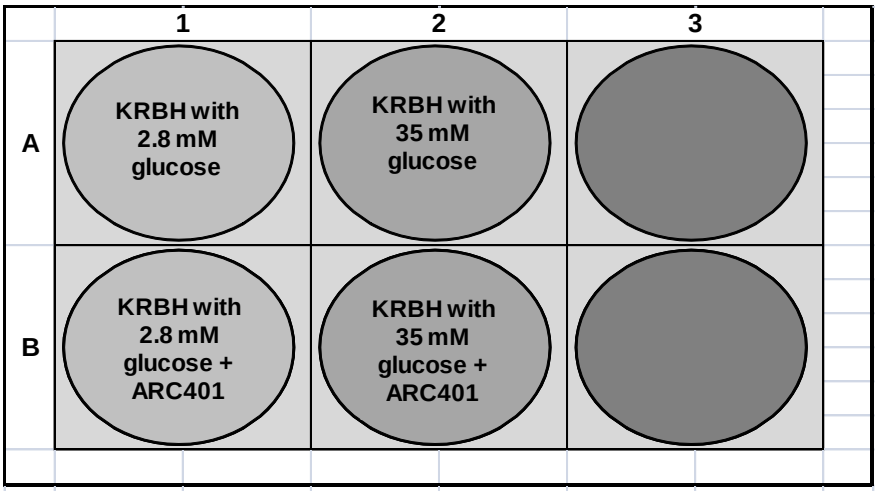

Figure 21. Isolated rat islet plate layout for the determination of nitric oxide produced by β-cells.

β-cells were then washed with 5 ml per well warm (37°C) HBSS/BSA and intracellular fluorescence of the oxidized form of DAF, DAF-triazol (DAF-2T) was quantified by flow cytometry, using a 488 nm laser to interrogate the individual β-cells (events) and a 530 nm emission wavelength detector (FL1). WinMDI v. 2.8 was used to analyse data. Forward and side scatter data for 20 000 events was collected. β-cells were gated by their high side scatter properties and their mean fluorescence intensity calculated as a percentage of the control.

3.3. Production of tumor necrosis factor alpha (TNF-α) by peripheral blood mononuclear cells (PMBCs) (method adapted from Wisman *et al*., 2008)

3.3.1. Preparation of blood samples

Blood collected from age matched, adult male Wistar rats in section **3.** above was used to isolate peripheral blood mononuclear cells (PBMCs). Eight milliliters of whole blood was collected from anaethetised into Vacutainer® tubes containing 7.2 mg of EDTA to prevent clotting. The blood of three rats was pooled to yield a 24 ml sample. Each blood sample

was diluted 1:2 in DPBS and kept on ice. In order to retrieve the PBMCs from the whole blood, 24 ml of the diluted blood sample was layered over 12 ml Histopaque (1.119 g/l) in a 50 ml centrifuge tube. The tube was then centrifuged at 530 x g for 15 minutes at 4°C with the brake off. PBMCs (and platelets) were extracted from the second graduated layer between the Histopaque and the plasma layers (figure 22).

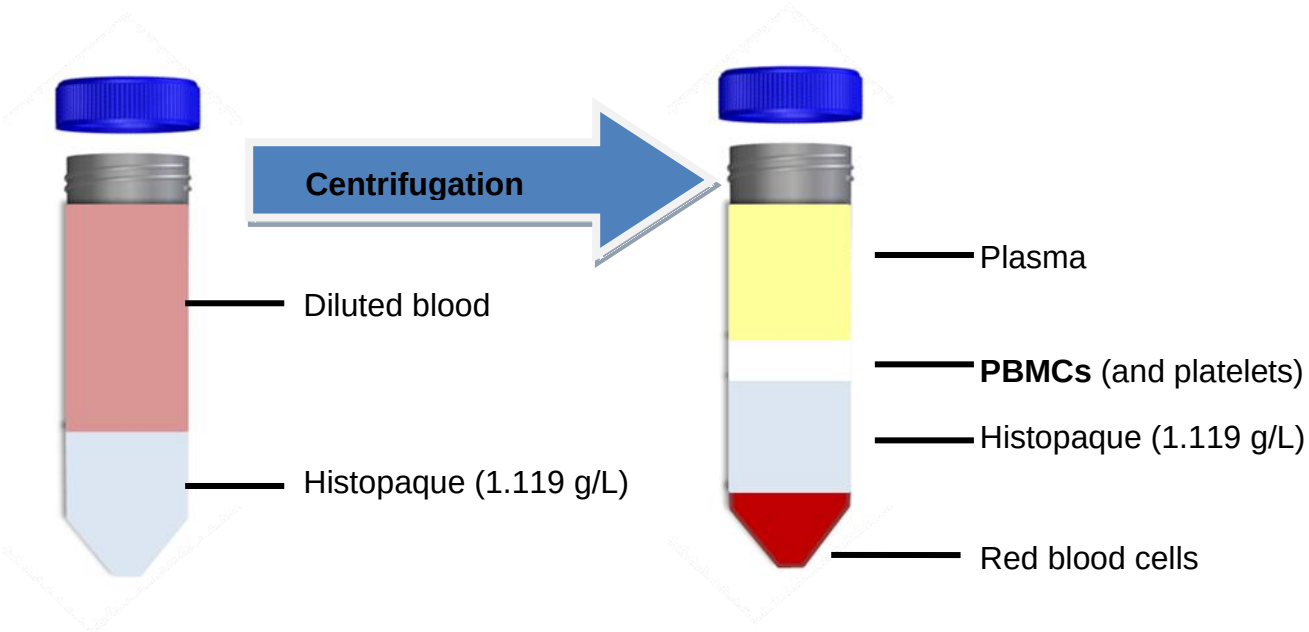

Figure 22. Histopaque gradient centrifugation and isolation of peripheral mononuclear cells (PBMCs)

In order to remove platelets, a further 10 ml of cold DPBS was added to the PBMCs and the samples centrifuged at 130 x g for 15 minutes at 4°C. The supernatant was aspirated and the pellet re-suspended in DPBS followed by centrifugation at 130 x g for 15 minutes at 4°C. The supernatant was aspirated and the pellet re-suspended in RPMI 1640 supplemented with 2 g/L sodium bicarbonate, 10% FCS, 2 mM L-glutamine, penicillin (100 IU) and streptomycin (100 µg/ml). PBMC's were counted using a haemocytometer and seeded at 1 x 10^6 cells/ml in a 24 well cell culture plate with RPMI 1640 supplemented media with 0.05 µg/µl ARC401 extract and lipopolysaccharides (LPS) according to the

plate layout below (figure 23). The plate was incubated for 24 hours at 37ºC with humidified air and 5% CO_2.

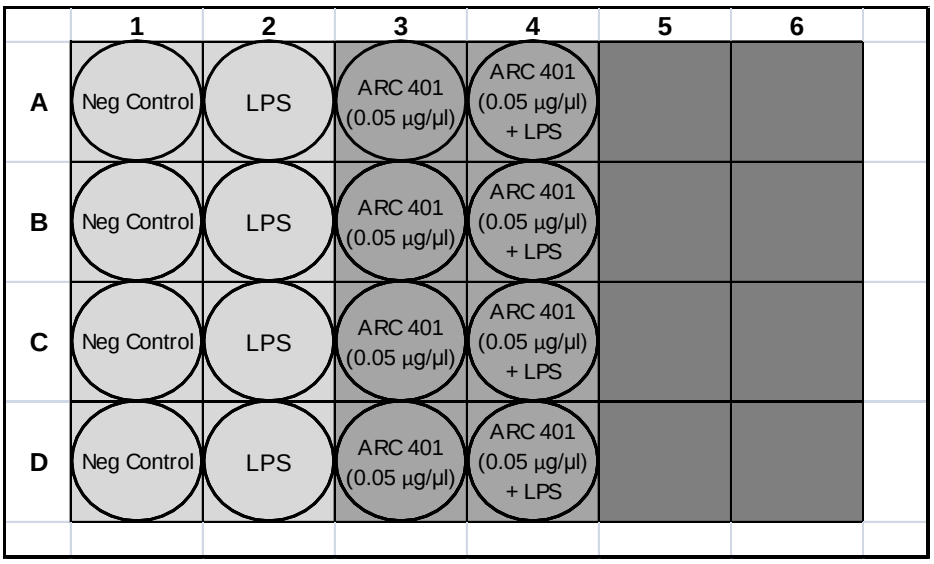

Figure 23. PBMC plate layout.

The next day contents of the wells were transferred to 2 ml microfuge tubes and a 100 µl sample per well was collected to determine cell viability as described in section **3.3.3.** below. The remaining contents in the microfuge tubes were centrifuged at 10 000 x g for 15 minutes. The supernatants were collected into 1.5 ml microfuge tubes and frozen at -20°C for use in a sandwich ELISA assay to quantify TNF-α. One experiment with four replicates per treatment was performed.

3.3.2. Enzyme-linked immune absorbent assay (ELISA)

A BD Biosciences OptEIA sandwich enzyme-linked immune absorbent assay (ELISA) kit was used to quantify TNF-α produced by the PBMCs. Frozen culture medium supernatants were added to the ELISA plate (100 µl/well). The plates were pre-coated with anti-rat TNF-α monoclonal antibody, which binds TNF-α in the culture medium. Standards

(provided in the kit) were also added to the respective wells. The plates were sealed and incubated at room temperature for 2 hours. The wells were then washed four times with 300 µl/well wash buffer (supplied in the kit) and 100 µl/well detection antibody (biotinylated anti-rat TNF-α phage Fab antibody) was added. Plates were then sealed and incubated at room temperature for 1 hour. The washing step described above was repeated and 100 µl/well enzyme working reagent (streptavidin-horseradish peroxidase conjugate with BSA) was added. Avidin-biotin was used to amplify signal since numerous biotin molecules can be conjugated to the specific antibody (one molecule of avidin non-covalently binds four biotinylated proteins). The plate was resealed and incubated at room temperature for 30 minutes. After incubation, the wash step was repeated and 100 µl/well 3, 3', 5, 5'-tetramethylbenzadine (TMB) One-step substrate reagent (provided in the kit) was added and plates incubated in the dark at room temperature for 30 minutes. The TMB reagent produces a blue color which was in direct proportion to the amount of TNF-α present. Thereafter, 50 µl/well of Stop solution (provided in the kit) was added to stop the reaction, changing the solution colour to yellow. The absorbance of the resultant yellow solution was read at 450 nm on a BioTek plate reader.

3.3.3. Cell viability

Peripheral blood mononuclear cell viability was determined as described in section **2.2.1.1.** by staining the 100 µl sample obtained in section **3.3.1.** above 100 µl of 0.4% Trypan blue in DPBS solution in a 1.5 ml tube. A 10 µl sample of the stained cell suspension was pipetted under the coverslip of the two chambers of the haemocytometer. The number of cells in three 1 mm^2 grids per chamber of the haemocytometer were counted and the average of the six counts was used to determine the total number of viable cells per well.

4. Statistical analysis

All *in vitro* work was done with three repeats in three independent experiments. Significant differences between groups were determined using the multivariate analysis of variance (ANOVA) statistical assessment. A one way ANOVA was used instead of a simple t-test in order to avoid false-positive type-I errors that may arise from multiple two-sample t-tests. A Dunnett's post hoc test was also performed if $p<0.05$, comparing the treatment group means to that of the vehicle control. Specific attention was given to correct sample size, controls and avoidance of type-II errors. Statistical significance was obtained when the p-value was less than 0.05. A non-parametric Spearman's correlation was performed on data in order to determine possible extract concentration related trends. Relative gene expression was analysed using fold change compared to the vehicle control samples. A 1.5 fold change was regarded as meaningful. Statistical analysis was not performed on pancreatic islet and β-cell results as the experiment was not repeated. Nitric oxide production, as measured by diaminofluorescein diacetate triazol fluorescence, was analysed using fold change compared to the control group not pretreated with ARC401. Significant differences between groups compared to the negative control in the PBMC TNF-α quantification assay was analysed using ANOVA and a Dunnett's post hoc test was also performed. Graph Pad Prism v.5.01 was used for all statistical analyses.

CHAPTER 3

RESULTS

1. Differentiation of C2C12 myoblasts and 3T3 pre-adipocytes into myocytes and adipocytes, respectively

Since HS contains less growth factors than fetal calf serum, proliferation of C2C12 myoblasts was arrested. Differentiation to myocytic phenotype with myotubule formation was initiated by substituting 10% fetal calf serum in the medium with 2% horse serum. Differentiated C2C12 cells are characterised by a distinct change in morphology; from single, flat, poly-glonal shaped cells (figure 24a) to spindle shaped myocytes and multi-nucleate, densely packed myotubules which are similar to normal muscle fibres, with contractile ability (figure 24b). Fully differentiated C2C12 cells were characterized morphologically by the condensation of neighboring myocytes into myotubules.

a. 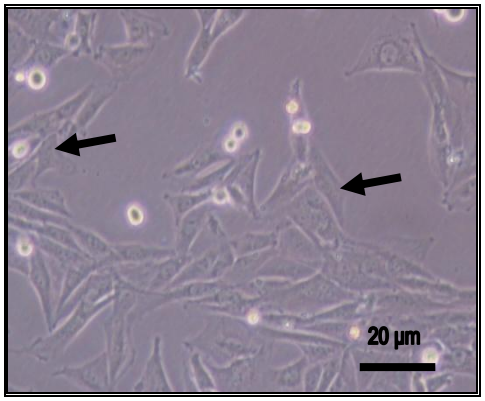

b. 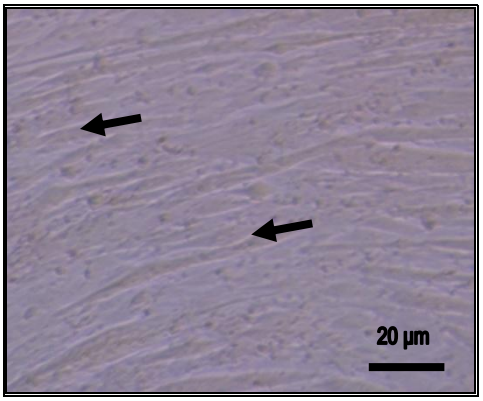

Figure 24. Myocyte and myotubule formation in C2C12 cells.

C2C12 myoblasts prior to differentiation on day two (arrow indicates single poly-glonal myoblast) (**a**) and spindle-shaped C2C12 myocytes with multi-nucleate, densely packed myotubules after differentiation on day five (arrows indicate condensed myotubules) (**b**) at 400 x magnification.

To induce the adipocyte phenotype, 3T3-L1 cells were refreshed prior to reaching confluence with adipogenic media (DMEM with 10% FCS was supplemented with 16 µM insulin, 0.6 µM dexamethasone and 0.1 mM isobutylmethylxanthine). The transition from fibroblastic, progenitor mesenchymal cells (figure 25a) to rounded, fully functional fat-producing adipocytes (figure 25b and c) required two cell divisions in the adipogenic media. Fully differentiated adipocytes were characterised morphologically with the observation of fat/lipid droplets in the cell cytoplasm.

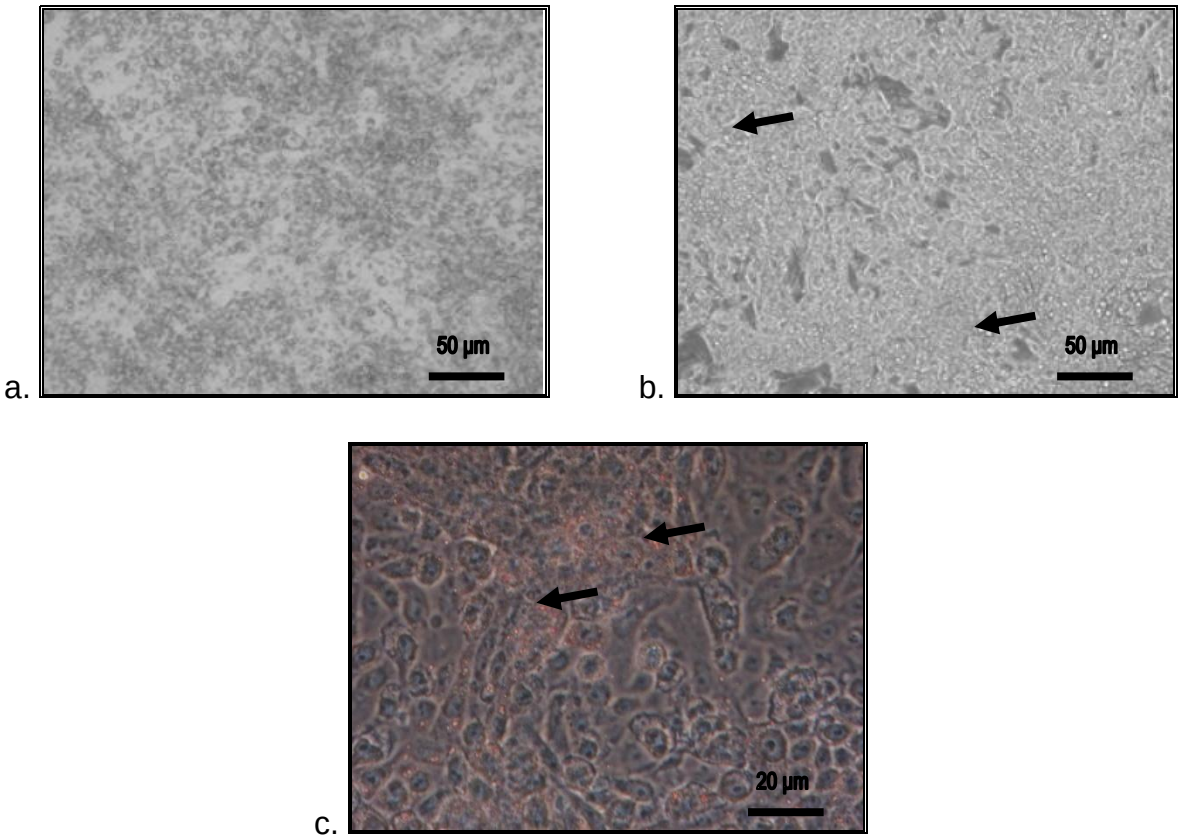

Figure 25. Adipocyte formation in 3T3-L1 fibroblasts.

3T3-L1 fibroblasts prior to differentiation on day three (a) and 3T3-L1 adipocytes after differentiation on day six (b) at 200 x magnification (ZenBio Inc, 2010); 3T3-L1 adipocytes during differentiation on day four (c) with lipid stained in red with Oil RedO at 400 x magnification. Arrows indicate lipid accumulation.

2. *Athrixia phylicoides* aqueous extract (ARC401) and cellular glucose uptake

The glucose oxidase fluorimetric was used to determine the amount of glucose taken up by C2C12, Chang and 3T3-L1 cells following acute exposure to ARC401 and positive controls. Chang and 3T3-L1 cells were acutely exposed for three hours to 1 μM insulin, 1 μM metformin, water vehicle and increasing concentrations of ARC401 (0.025, 0.05 and 0.1 μg/μl). C2C12 cells were acutely exposed for one hour.

Measurement of glucose removed from the media by the cell lines showed that, compared to the water control, ARC401 significantly increased the amount of glucose taken up by C2C12 cells at 0.025, 0.05 and 0.1 μg/μl (183.4% ± 32.6, $p<0.01$; 228.3% ± 66.2, $p<0.001$; 161.7% ± 8.5, $p<0.05$) (figure 26). In Chang cells ARC401 significantly increased the amount of glucose taken up at 0.05 and 0.1 μg/μl (134.5% ± 2.5, $p<0.05$; 130.9% ± 5.8, $p<0.05$) (figure 27). In 3T3-L1 cells ARC401 significantly increased the amount of glucose taken up at 0.025 and 0.05 μg/μl (143.5% ± 10.3, $p<0.001$; 134.7% ± 18.8, $p<0.01$) (figure 28). In C2C12, Chang and 3T3-L1 cells the insulin (301.3% ± 12.3, $p<0.001$; 155.1% ± 44.5, $p<0.01$; 188.0% ± 40.7, $p<0.001$) and metformin (206.8% ± 1.8, $p<0.01$; 171.4% ± 44.3, $p<0.01$; 188.5% ± 13.4, $p<0.001$) (figures 26-28) positive controls significantly increased glucose taken up from the media. Insulin and maximal ARC401 glucose uptake stimulation was 1.9 and 1.7 fold higher in C2C12 myocytes compared to Chang cells, and 1.6 fold higher in C2C12 cells compared to 3T3-L1 adipocytes.

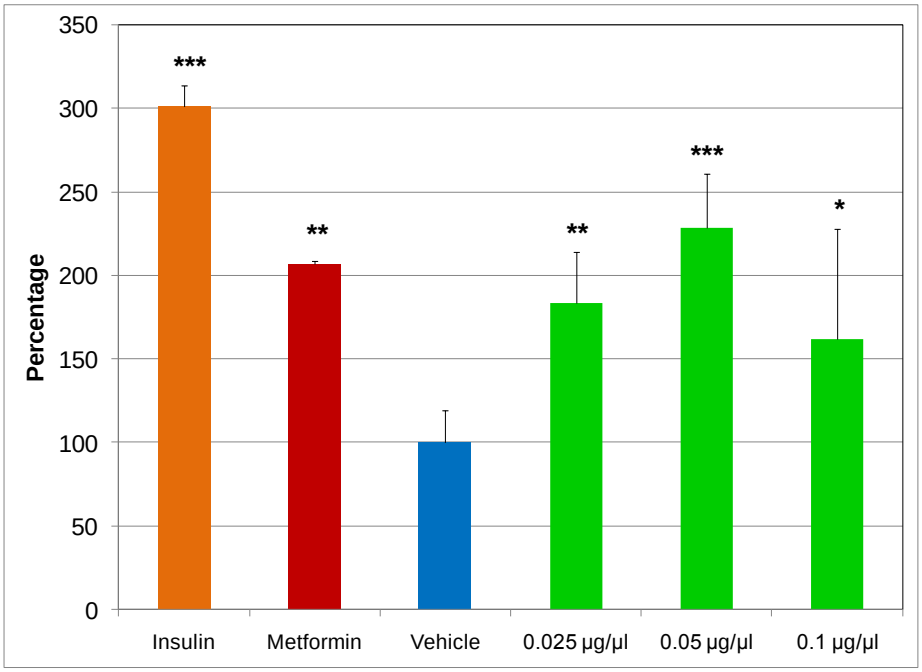

Figure 26. Percentage glucose taken up from the media by C2C12 myocytes following acute exposure to ARC401 at increasing concentrations and controls (insulin, metformin and water vehicle). Results are mean values of three independent experiments + standard deviation. * $p<0.05$, ** $p<0.01$, *** $p<0.001$ compared to vehicle control.

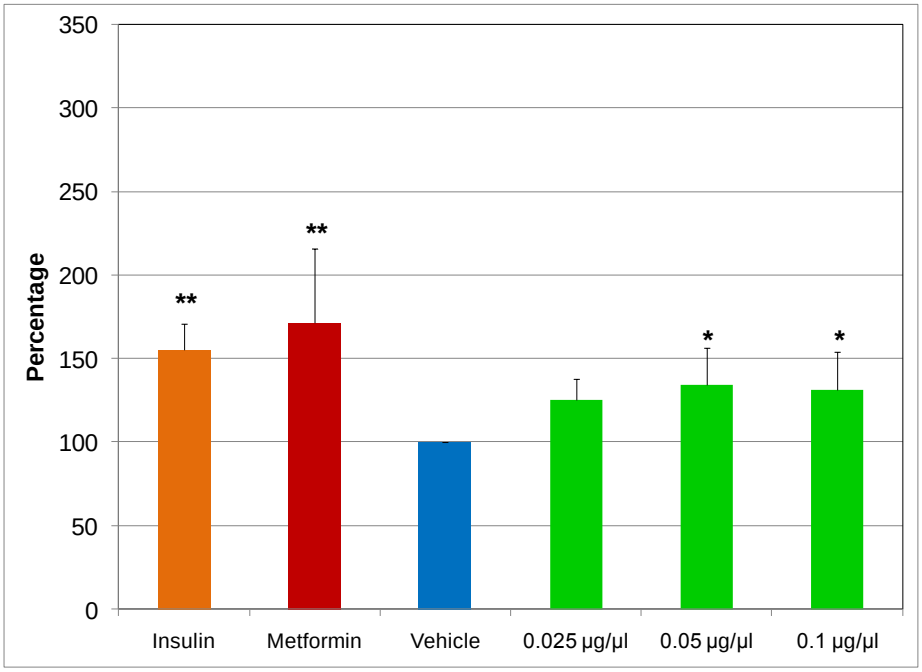

Figure 27. Percentage glucose taken up from the media by Chang cells following acute exposure to ARC401 at increasing concentrations and controls (insulin, metformin and water vehicle). Results are mean values of three independent experiments + standard deviation. * $p<0.05$, ** $p<0.01$ compared to vehicle control.

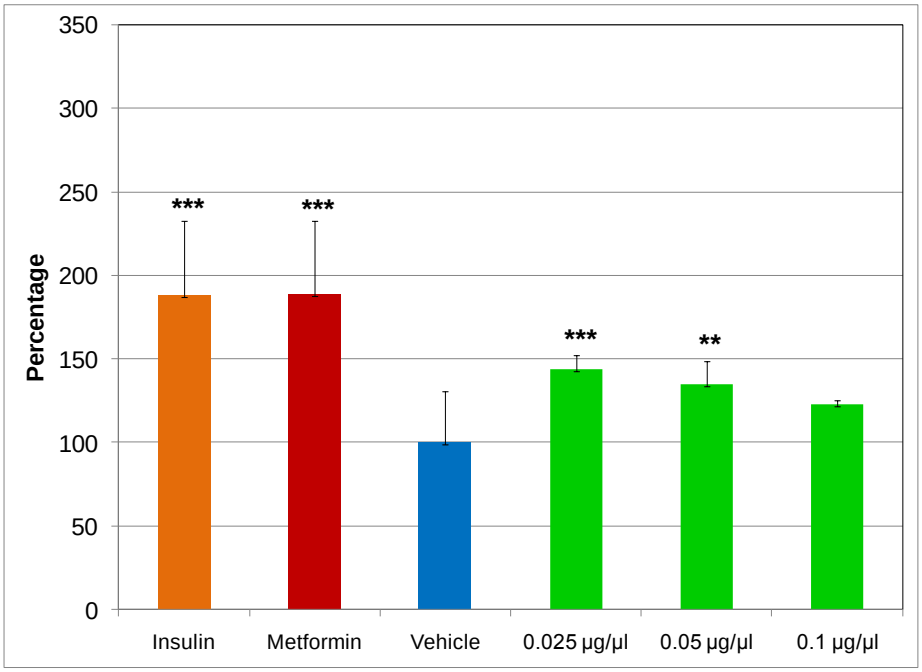

Figure 28. Percentage glucose taken up from the media by 3T3-L1 adipocytes following acute exposure to ARC401 at increasing concentrations and controls (insulin, metformin and water vehicle). Results are mean values of three independent experiments + standard deviation. ** p<0.01, *** p<0.001 compared to vehicle control

3. Glucose oxidation and glycogen content assays

The effect of ARC401 on glucose utilization in C2C12, Chang and 3T3-L1 cells was assessed by measuring the amount of glucose stored as glycogen and the amount of glucose oxidized to CO_2. Intracellular glycogen content was measured using a colorimetric assay kit in cells acutely exposed to increasing concentrations of ARC401 (0.025, 0.05 and 0.1 µg/µl) as well as 1 µM insulin, 1 µM metformin, water vehicle. C2C12 myocytes were acutely exposed for one hour. Chang cells and 3T3-L1 adipocytes were acutely exposed for three hours.

3.1. ^{14}C-glucose oxidized to $^{14}CO_2$ by C2C12, Chang and 3T3-L1 cells

The oxidation of ^{14}C-glucose to $^{14}CO_2$ by C2C12 myocytes was significantly increased following acute exposure to ARC401 at 0.05 and 0.1 µg/µl (2806.3 fmol/1x10^6 cells ± 751, $p<0.05$; 2919.3 fmol/1x10^6 cells ± 428, $p<0.01$). Acute exposure of C2C12 myocytes to ARC401 at 0.025 µg/µl had no effect on ^{14}C-glucose oxidation to $^{14}CO_2$. Positive controls, 1 µM insulin and 1 µM metformin, increased oxidation in of ^{14}C-glucose to $^{14}CO_2$ in C2C12 myocytes. The increased oxidation induced by metformin was statistically significant (2905.9 fmol/1x10^6 cells ± 729.6, $p<0.05$) (figure 29). The oxidation of ^{14}C-glucose to $^{14}CO_2$ by Chang cells was significantly increased following acute exposure to ARC401 at 0.05 and 0.1 µg/µl (3115.7 fmol/1x10^6 cells ± 743.6, $p<0.05$: 4476.7 fmol/1x10^6 cells ± 1620, $p<0.05$); as seen in the C2C12 cells. Acute exposure of Chang cells to ARC401 at 0.025 µg/µl had no effect on ^{14}C-glucose oxidation to $^{14}CO_2$. Positive controls, 1 µM insulin and 1 µM metformin, increased oxidation of ^{14}C-glucose to $^{14}CO_2$ in Chang cells (figure 30). ARC401, at the concentrations tested, showed some inhibition of oxidation of ^{14}C-glucose to $^{14}CO_2$ by 3T3-L1 cells. Insulin and metformin positive controls had no effect on glucose oxidation in 3T3-L1 cells following acute exposure (figure 31).

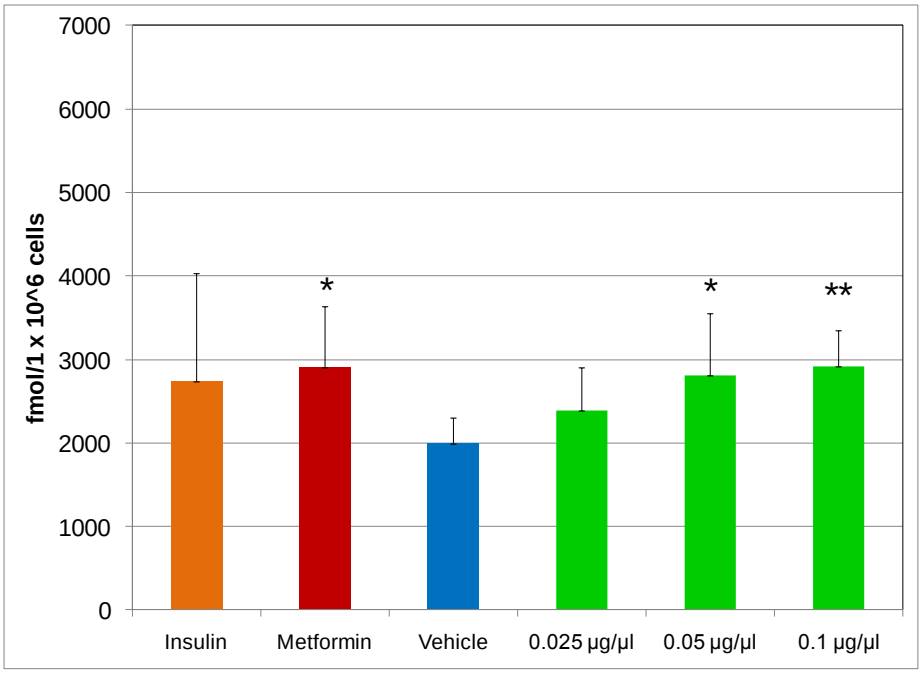

Figure 29. ^{14}C-glucose oxidized to $^{14}CO_2$ by C2C12 myocytes during acute exposure to ARC401 at increasing concentrations and controls (insulin, metformin and water vehicle). Results are mean values of three independent experiments + standard deviation. * p<0.05, ** p<0.01 compared to vehicle control.

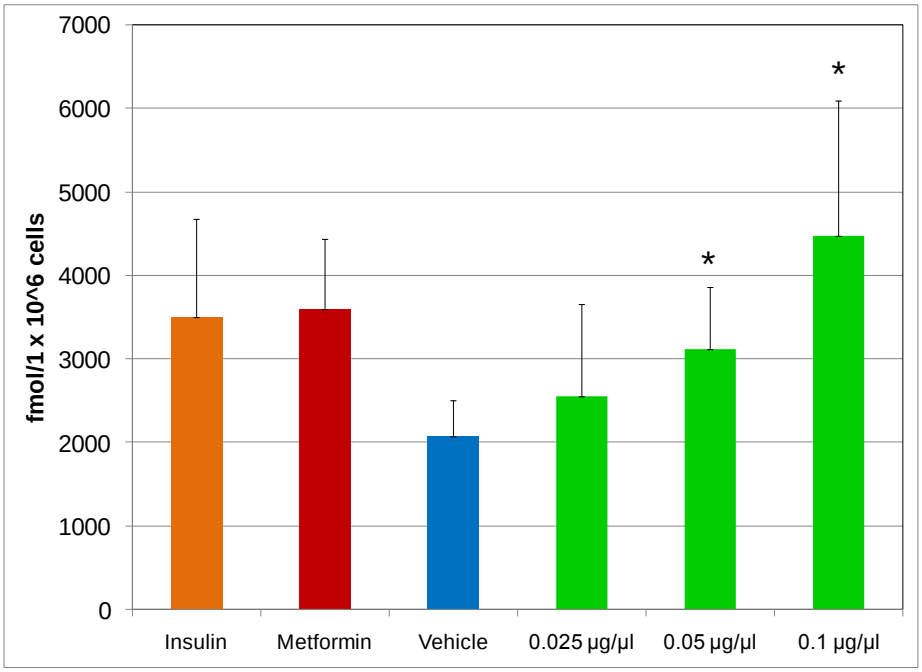

Figure 30. ^{14}C-glucose oxidized to $^{14}CO_2$ by Chang cells during acute exposure to ARC401 at increasing concentrations and controls (insulin, metformin and water vehicle). Results are mean values of three independent experiments + standard deviation. * p<0.05 compared to vehicle control.

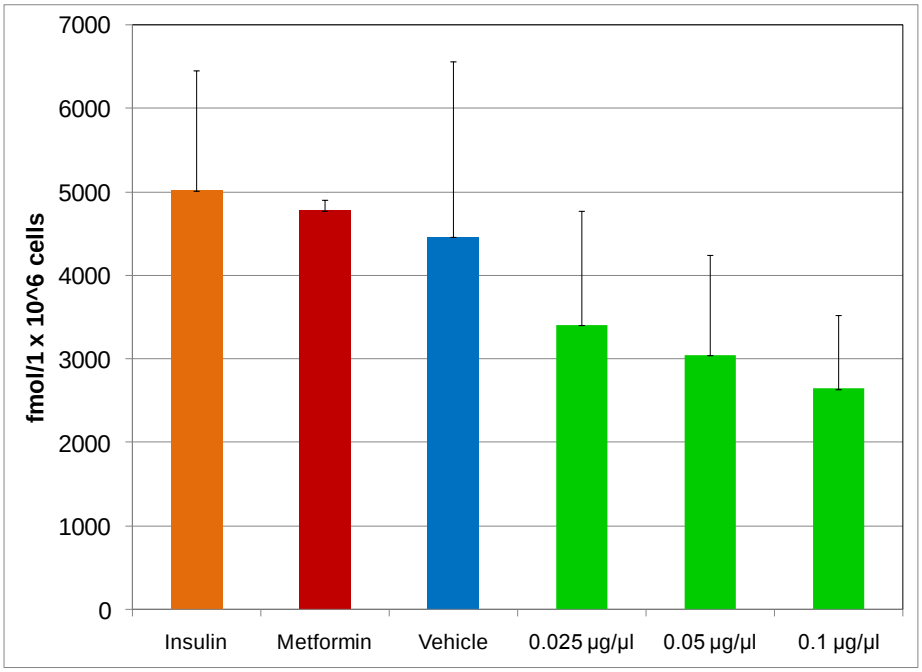

Figure 31. ^{14}C-glucose oxidized to $^{14}CO_2$ by 3T3-L1 adipocytes during acute exposure to ARC401 at increasing concentrations and controls (insulin, metformin and water vehicle). Results are mean values of three independent experiments + standard deviation.

3.2. Glycogen content determination in C2C12 and Chang cells

ARC401, only at the highest concentration tested (0.1 µg/µl), increased glycogen storage in C2C12 myocytes, although not significantly (figure 32). The 1 µM insulin positive control also non-significantly increased glycogen storage in the C2C12 myocytes, whereas 1 µM metformin control reduced the amount of glycogen stored. ARC401 significantly increased glycogen storage at all three concentrations tested in Chang cells (13.6 µg/1x10^6 cells ± 0.7, $p<0.05$; 12.7 µg/1x10^6 cells ± 1.8, $p<0.05$; 12.7 µg/1x10^6 cells ± 1.6, $p<0.05$) (figure 33). Both insulin and metformin postitive controls also significantly increased glycogen storage in the Chang cells (12.7 µg/1x10^6 cells ± 1.5, $p<0.05$; 13.3 µg/1x10^6 cells ± 4, $p<0.01$). The assay kit used in this study was not able to detect the amount of glycogen stored by the 3T3-L1 adipocytes.

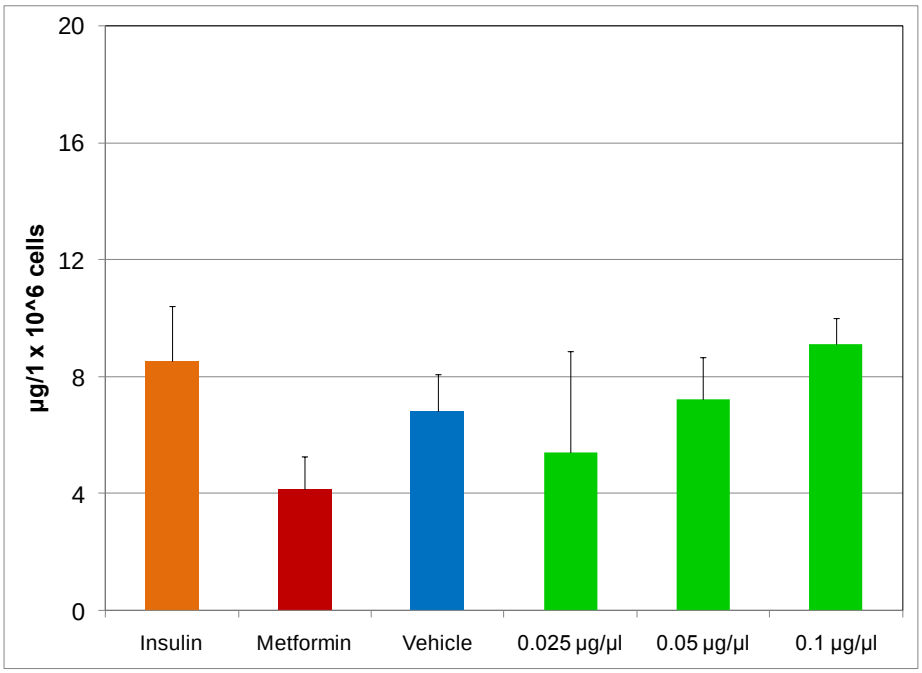

Figure 32. Glycogen content of C2C12 myocytes following acute exposure to ARC401 at increasing concentrations and controls (insulin, metformin and water vehicle). Results are mean values of three independent experiments + standard deviation.

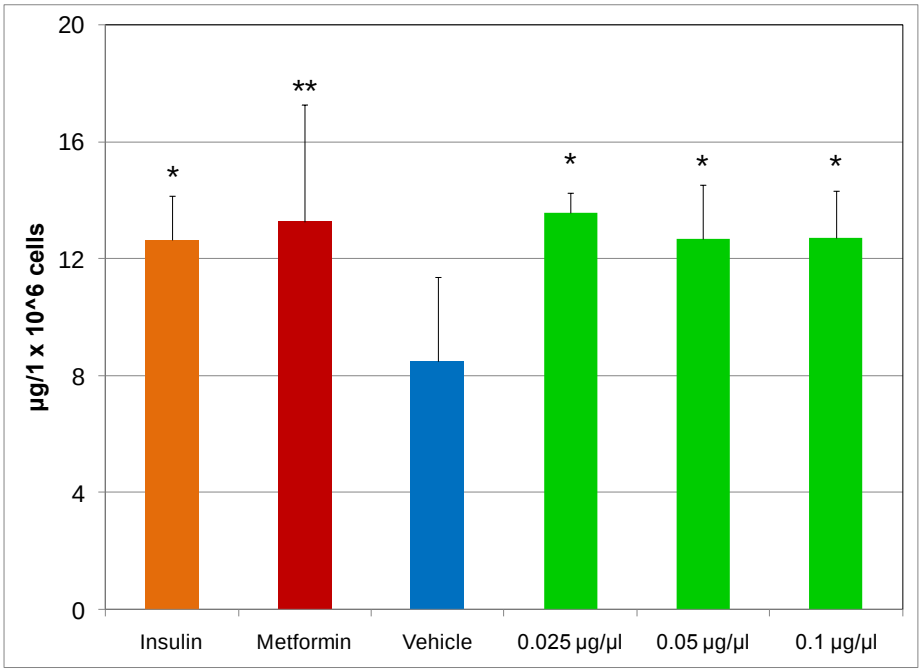

Figure 33. Glycogen content of Chang cells following acute exposure to ARC401 at increasing concentrations and controls (insulin, metformin and water vehicle). Results are mean values of three independent experiments + standard deviation. * $p<0.05$, ** $p<0.01$ compared to vehicle control.

4. Chang cell MTT (3-(4,5-Dimethylthiazol-2-yl)-2,5-diphenyltetrazolium bromide) cytotoxicity assay

Following chronic exposure (24 hours), the mitochondrial activity of Chang cells, as determined by the MTT assay, remained consistent and comparable with the water vehicle control at all concentrations of ARC401 tested except the highest (1 µg/µl) (0.28 nm ± 0.03, $p<0.01$). At 1 µg/µl mitochondrial activity was significantly reduced when compared to the water vehicle control (figure 34).

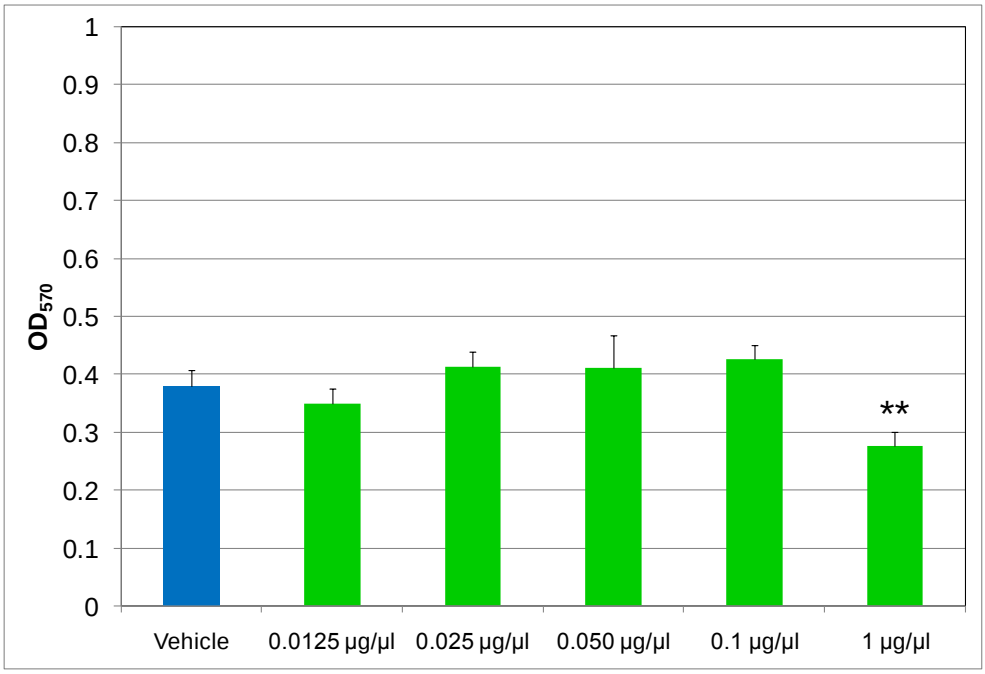

Figure 34. MTT of Chang cells following chronic exposure to water vehicle control and ARC401 at increasing concentrations. Results are mean values of three independent experiments + standard deviation. ** $p<0.01$ compared to vehicle control.

5. RNA extraction, complementary DNA synthesis (cDNA) and real-time polymerase chain reaction

The effect of ARC401 on insulin signalling gene expression in C2C12, Chang and 3T3-L1 cells was assessed by extracting RNA from cells acutely exposed to ARC401 (0.05 µg/µl) as well as 1 µM insulin, 1 µM metformin, water vehicle. C2C12 myocytes were acutely exposed for one hour. Chang cells and 3T3-L1 adipocytes were acutely exposed for three hours. RNA was extracted using a Tri-reagent based method modified from Chomczynski and Sacchi (1987). RNA was purified and DNase treated. Agilent RNA 6000 Nano kit was used to determine RNA integrity. The 2100 Expert Software compared the peak areas of the RNA samples to the combined area of the six RNA ladder peaks in order to determine RNA concentration. Complementary DNA (cDNA) was synthesized from the RNA extracted and mouse and human positive controls were used since C2C12 and 3T3-L1 cells are mouse-derived and Chang cells human-derived. To confirm positive cycling prior to the identification and quantification of our desired sequences the cDNA was tested using β-actin primers (forward and reverse). Polymerase chain reaction was used to amplify and quantify targeted DNA molecules. The DNA molecules (genes) of interest were insulin receptor (INSR), insulin receptor substrates 1 and 2 (IRS1 and IRS2), PI3K and glucose transporter 4 (GLUT4). Amplified DNA were detected and quantified as the reaction progressed in real time.

5.1. Agilent bioanalyser one dimensional gels

Samples obtained from C2C12 myocytes in the first two experiments (A1-A5 and B1-B5) showed distinct 28s and 18s bands. The 28s band of the samples obtained from the third experiments in C2C12 myocytes (C1-C5) was not as defined. Bands of the C5 sample were not clearly visible (figure 35). RNA extracted from Chang cells showed distinct and crisp 28s and 18s bands with the exception of sample F2, which was subsequently excluded from the rest of the PCR process (figure 36). RNA extracted from 3T3-L1 cells showed distinct 28s and 18s bands. Sample I2 showed lower intensity bands (figure 37).

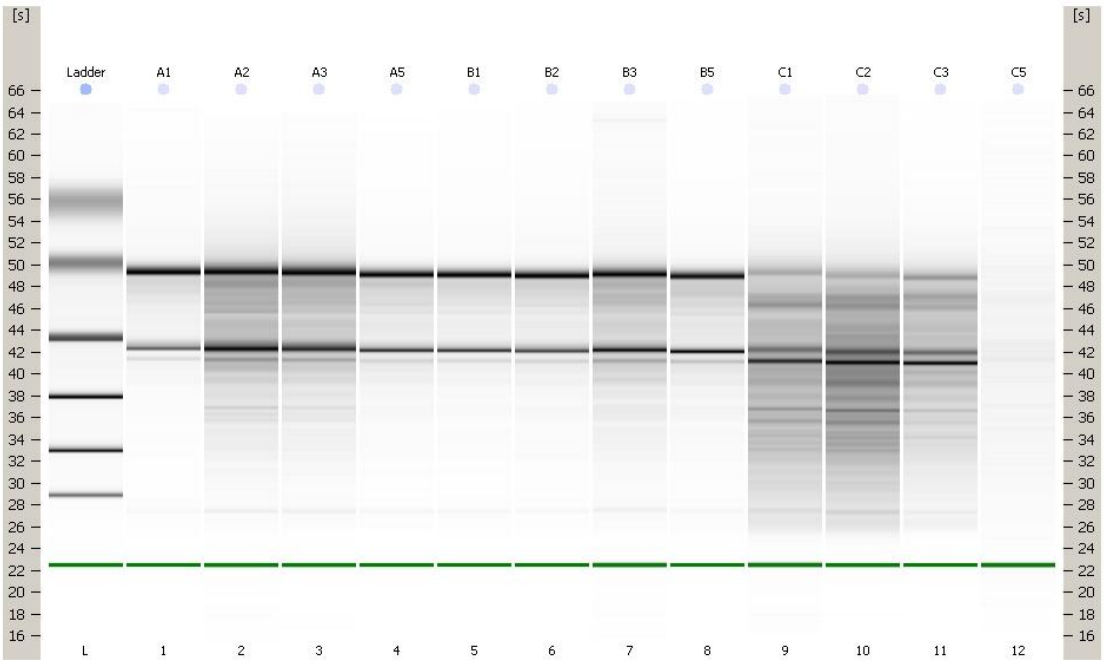

Figure 35. Agilent bioanalyser one dimensional gel of RNA extracted from C2C12 myocytes following acute exposure to insulin (A1, B1, C1), metformin (A2, B2, C2) water vehicle control (A3, B3, C3) and ARC401 (A5, B5, C5).

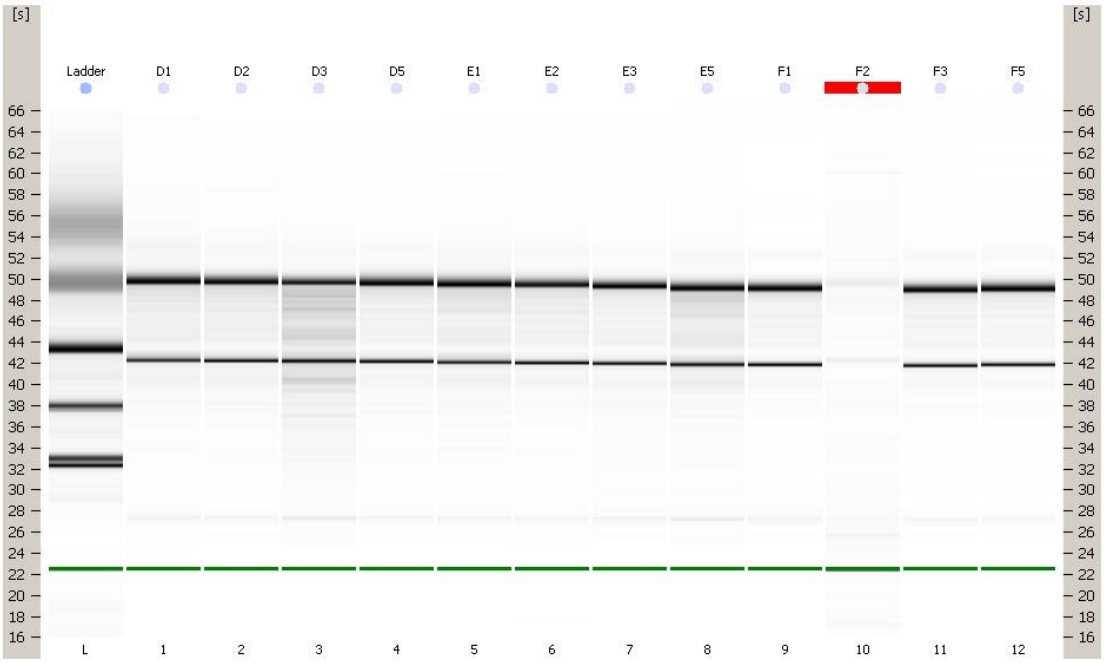

Figure 36. Agilent bioanalyser one dimensional gel of RNA extracted from Chang cells following acute exposure to insulin (D1, E1, F1), metformin (D2, E2, F2) water vehicle control (D3, E3, F3) and ARC401 (D5, E5, F5).

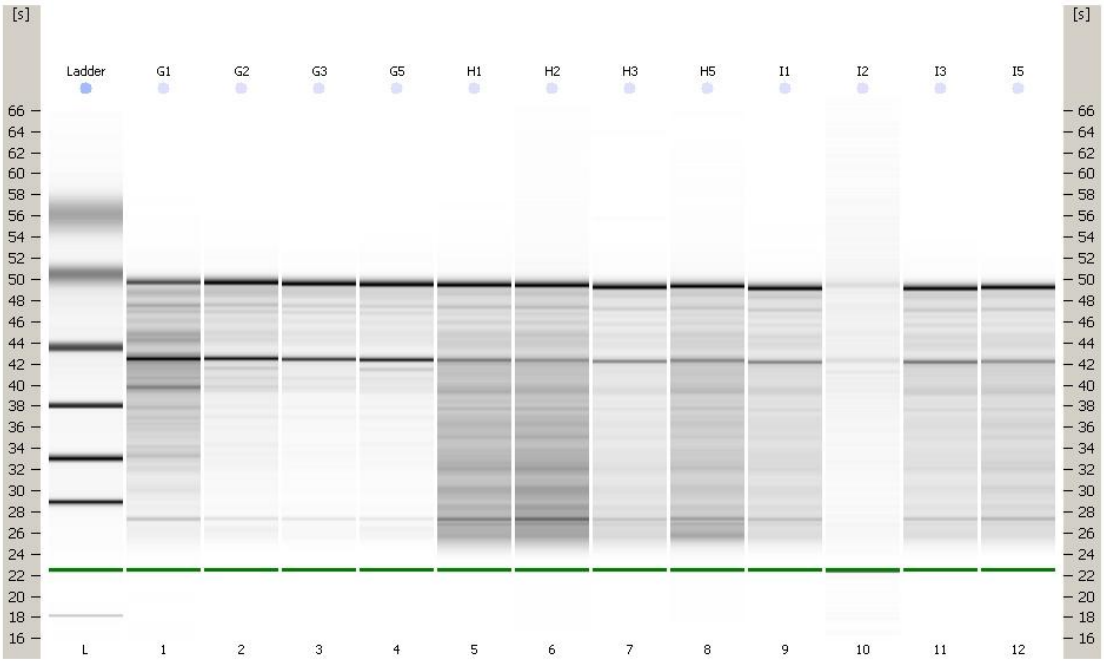

Figure 37. Agilent bioanalyser one dimensional gel of RNA extracted from 3T3-L1 adipocytes following acute exposure to insulin (G1, H1, I1), metformin (G2, H2, I2) water vehicle control (G3, H3, I3) and ARC401 (G5, H5, I5).

5.2. Dissociation curves of cDNA synthesized from RNA extracted from C2C12, Chang and 3T3-L1 cells acutely exposed to ARC401

All cDNA samples showed positive cycling, with dissociation curve peaks for each cell line falling within a tight band (figure 38). In the Chang cells (figure 39), the positive human Ambion control peaked approximately 2°C before that of the samples, which were clustered together. The 3T3-L1 adipocyte peaks were also clustered together (figure 40). C2C12 myocytes peaked approximately 2°C below Chang cells and 3T3-L1 adipocytes (figure 41).

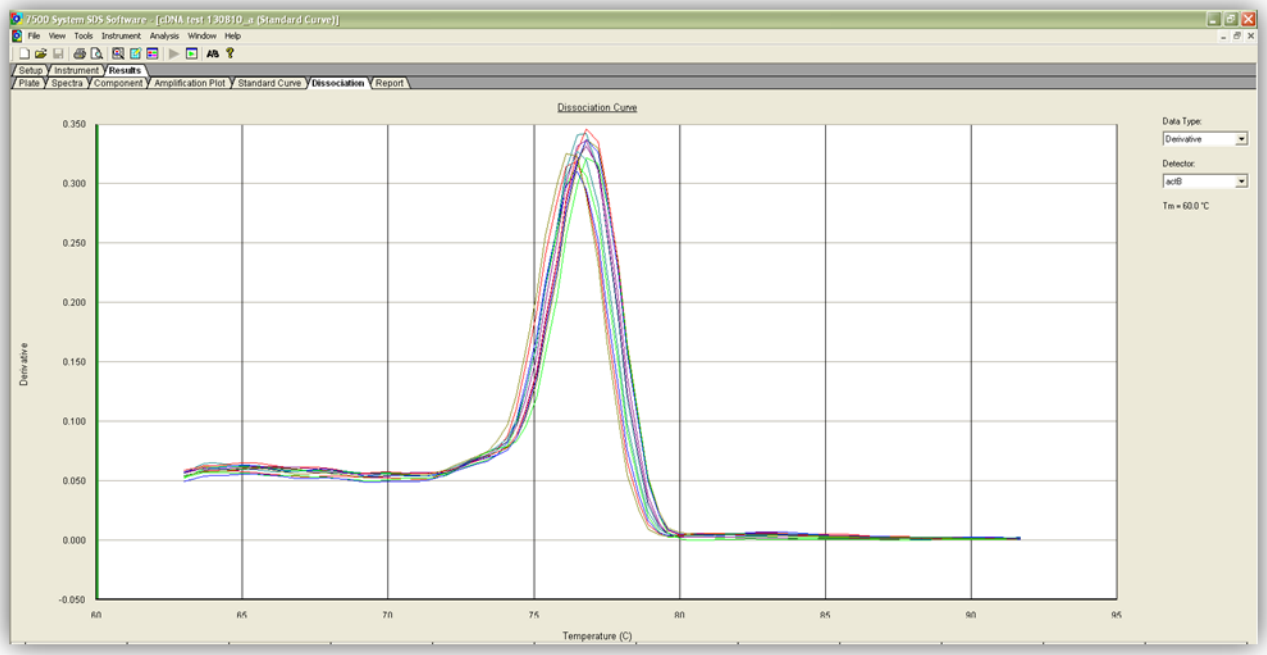

Figure 38. Dissociation curve of cDNA extracted from C2C12 myocytes when probed with β-actin forward and reverse primers.

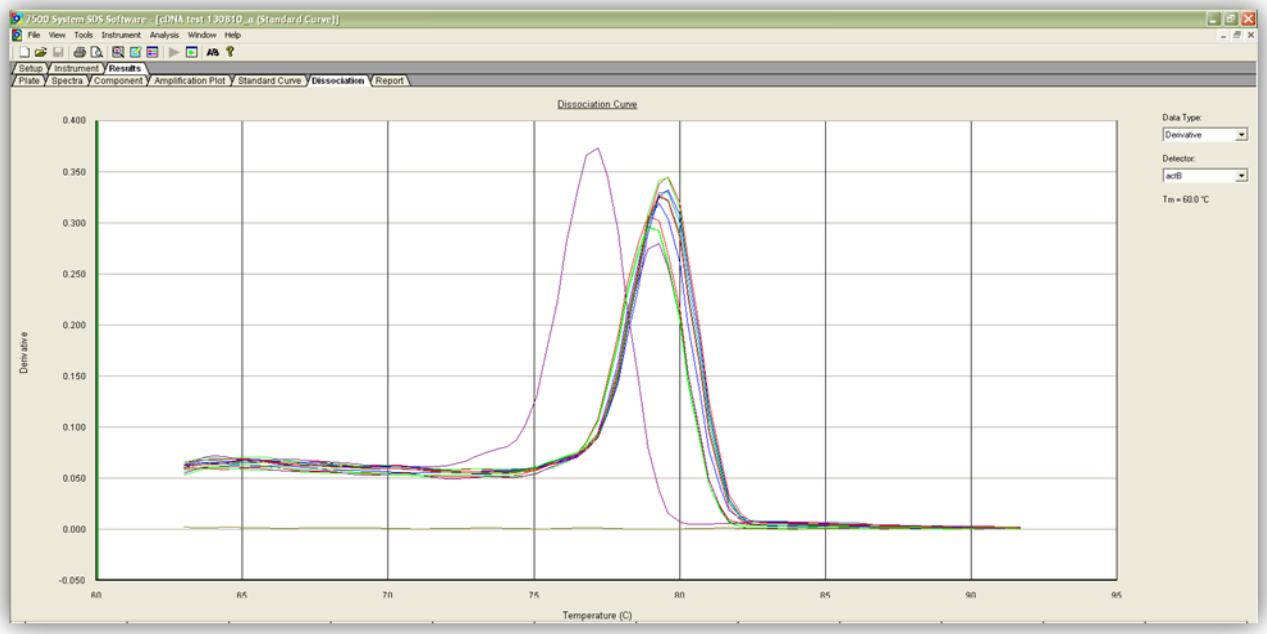

Figure 39. Dissociation curve of cDNA extracted from Chang cells when probed with β-actin forward and reverse primers.

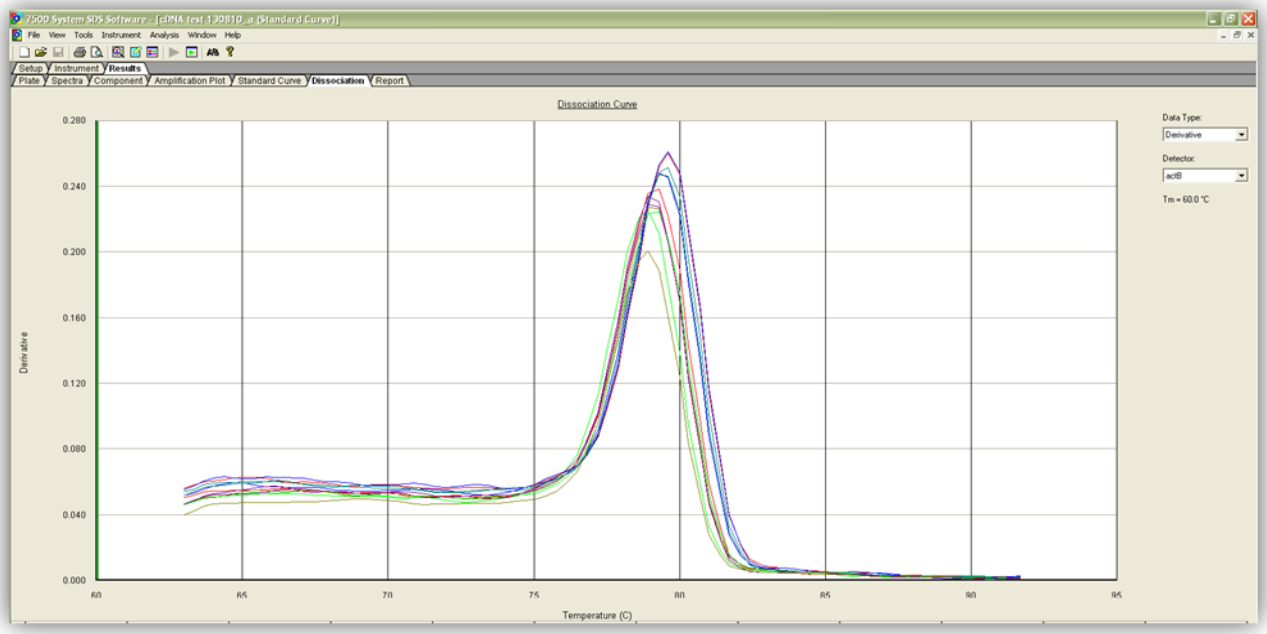

Figure 40. Dissociation curve of cDNA extracted from 3T3-L1 adipocytes when probed with β-actin forward and reverse primers.

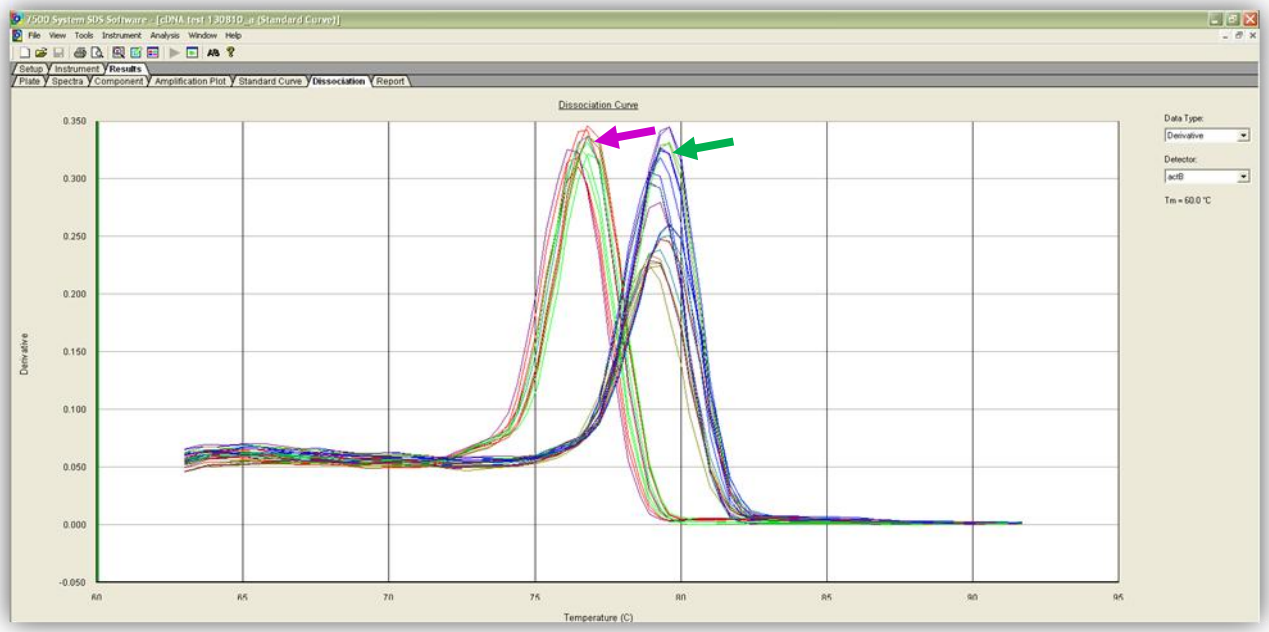

Figure 41. Dissociation curve of cDNA extracted from C2C12 myocytes, Chang cells and 3T3-L1 adipocytes when probed with β-actin forward and reverse primers. C2C12 myocytes peak (purple arrow) approximately 2°C below Chang cells and 3T3-L1 adipocytes (green arrow).

5.3. Insulin signalling gene expression

Polymerase chain reaction was used to amplify and quantify targeted DNA molecules synthesized from C2C12 myocyte and Chang cell RNA. The DNA molecules (genes) of interest were INSR, IRS1, IRS2, PI3K and GLUT4. Genes of interest were expressed relative to two house-keeping genes actin-β and GAPDH). Amplified DNA were detected and quantified as the reaction progressed in real time. The probes used were not effective in 3T3-L1 cells.

5.3.1. Insulin receptor (INSR) PCR assay

ARC401 increased INSR expression 2.7 fold compared to the water vehicle control in C2C12 myocytes (figure 42). The insulin and metformin positive controls also increased INSR expression in the C2C12 myocytes 3 and 2.4 fold respectively. ARC401 had no effect on INSR expression in Chang cells (figure 43). The insulin positive control increased INSR expression and metformin had no effect on INSR expression in the Chang cells.

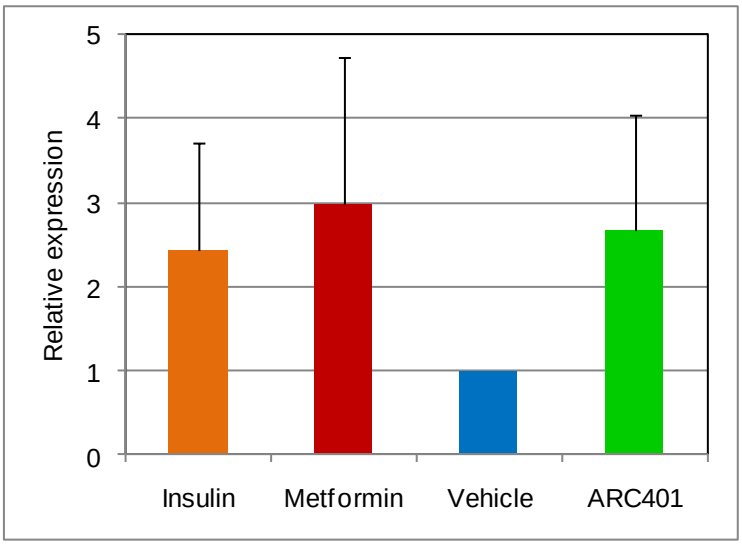

Figure 42. Relative expression of insulin receptor (INSR) of C2C12 myocytes following acute exposure to ARC401 controls (insulin, metformin and water vehicle). Results are the mean of two independent experiments + standard deviation.

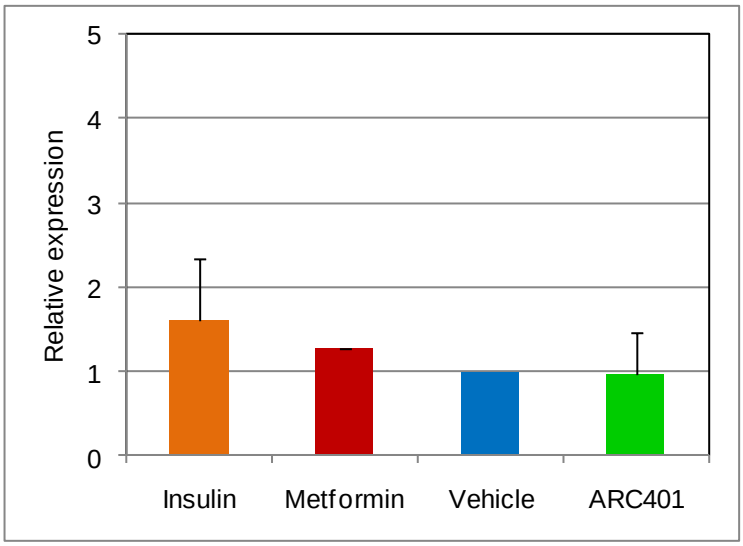

Figure 43. Relative expression of insulin receptor (INSR) of Chang cells following acute exposure to ARC401 controls (insulin, metformin and water vehicle). Results are the mean of two independent experiments + standard deviation.

5.3.2. Insulin receptor substrate one (IRS1) PCR assay

ARC401 had no effect on IRS1 expression in C2C12 myocytes (figure 44). The insulin and metformin positive controls each showed a 1.5 fold increase in IRS1 expression in the C2C12 cells. ARC401, as well as metformin, decreased IRS1 expression in Chang cells (figure 45). The insulin positive control had no effect on IRS1 expression in the Chang cells.

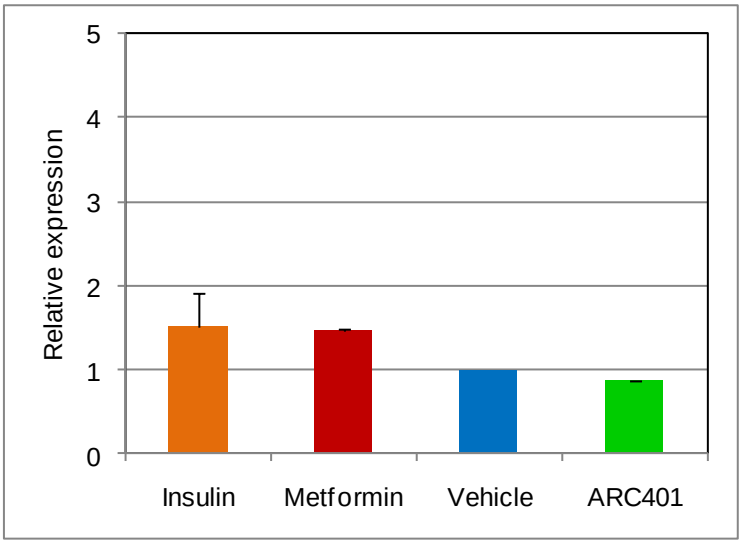

Figure 44. Relative expression of insulin receptor substrate one (IRS1) of C2C12 myocytes following acute exposure to ARC401 controls (insulin, metformin and water vehicle). Results are the mean of two independent experiments + standard deviation.

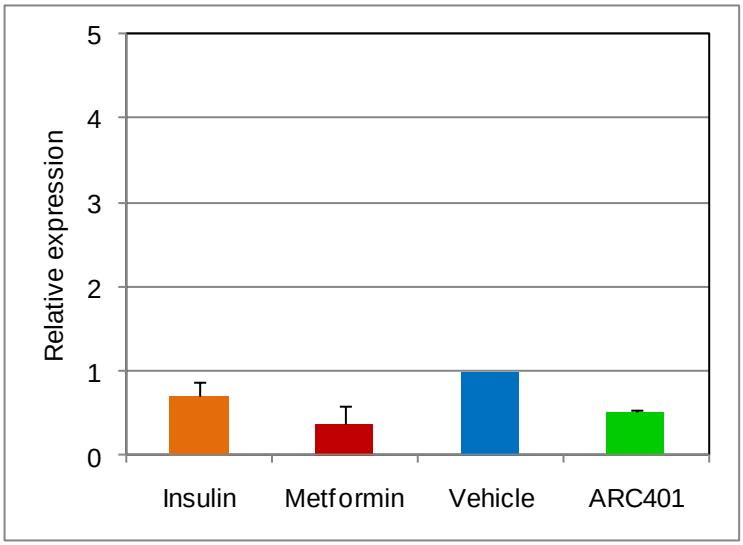

Figure 45. Relative expression of insulin receptor substrate one (IRS1) of Chang cells following acute exposure to ARC401 controls (insulin, metformin and water vehicle). Results are the mean of two independent experiments + standard deviation.

5.3.3. Insulin receptor substrate two (IRS2) PCR assay

ARC401 had no effect on IRS1 expression in C2C12 myocytes (figure 46). The insulin positive control showed a 1.7 fold increase in IRS2 expression. Metformin positive control had no effect in the C2C12 myocytes. ARC401, as well as metformin, had no effect on IRS2 expression in Chang cells (figure 47). The insulin positive control increased IRS2 expression in the Chang cells.

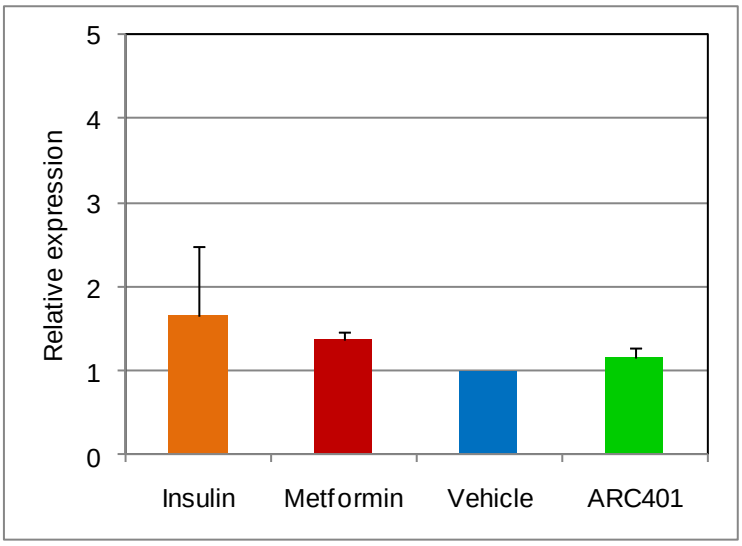

Figure 46. Relative expression of insulin receptor substrate two (IRS2) of C2C12 myocytes following acute exposure to ARC401 controls (insulin, metformin and water vehicle). Results are the mean of two independent experiments + standard deviation.

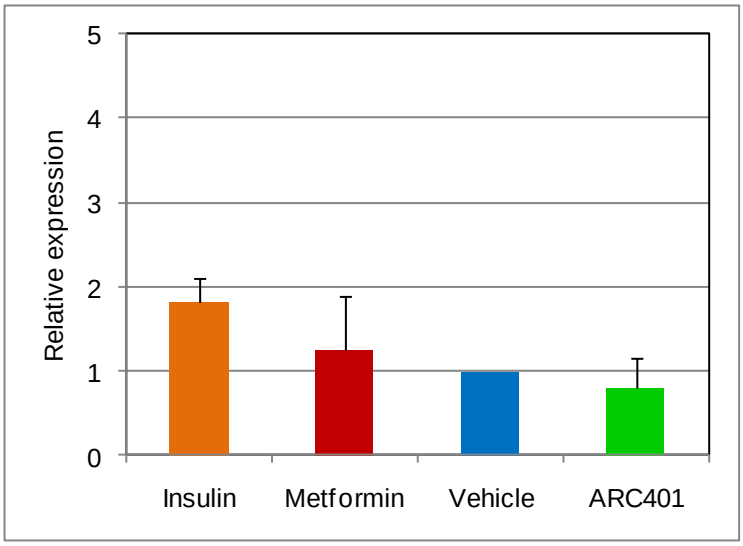

Figure 47. Relative expression of insulin receptor substrate one two (IRS2) of Chang cells following acute exposure to ARC401 controls (insulin, metformin and water vehicle). Results are the mean of two independent experiments + standard deviation.

5.3.4. Phosphoinositide-3-kinase (PI3K) PCR assay

ARC401 had no effect on PI3K expression in C2C12 myocytes (figure 48). The insulin and metformin positive controls also had no effect on PI3K expression in C2C12 myocytes. ARC401, as well as positive controls insulin and metformin, had no effect on PI3K expression in Chang cells (figure 49).

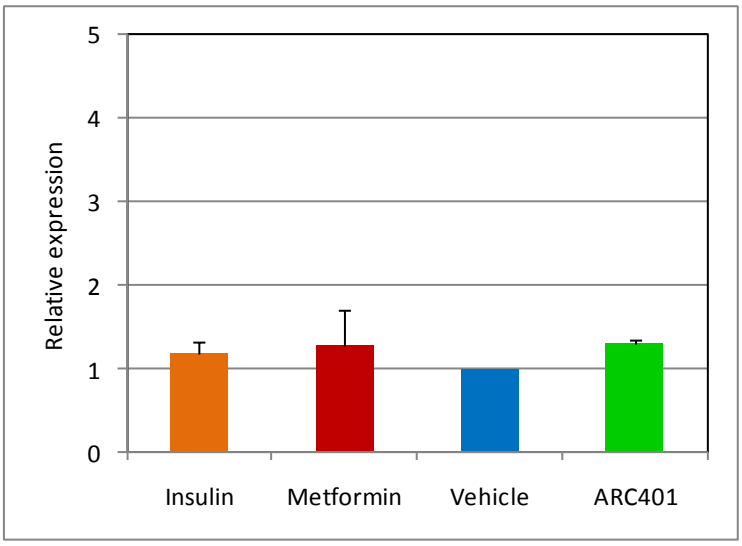

Figure 48. Relative expression of phosphoinositide-3-kinase (PI3K) of C2C12 myocytes following acute exposure to ARC401 controls (insulin, metformin and water vehicle). Results are the mean of two independent experiments + standard deviation.

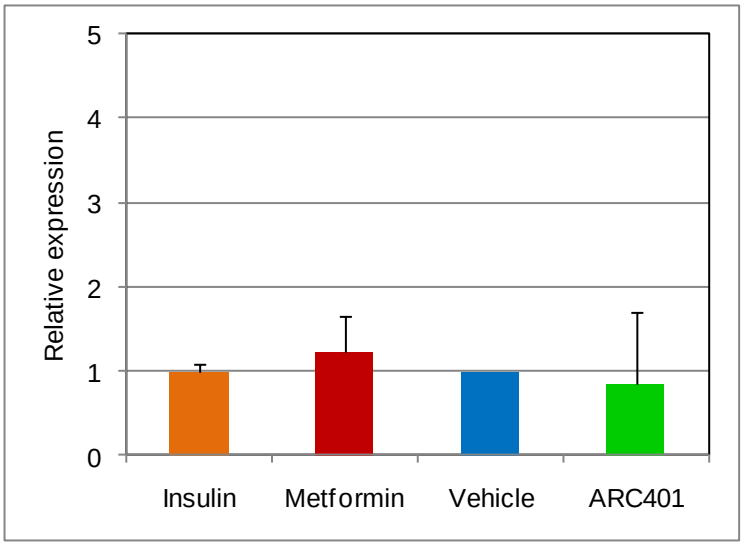

Figure 49. Relative expression of phosphoinositide-3-kinase (PI3K) of Chang cells following acute exposure to ARC401 controls (insulin, metformin and water vehicle). Results are the mean of two independent experiments + standard deviation.

5.3.5. Glucose transporter 4 (GLUT4) PCR assay

ARC401 increased GLUT4 expression 2 fold compared to the water vehicle control in C2C12 myocytes (figure 50). The insulin and metformin positive controls also increased GLUT4 expression in the C2C12 myocytes 1.4 and 1.9 fold respectively.

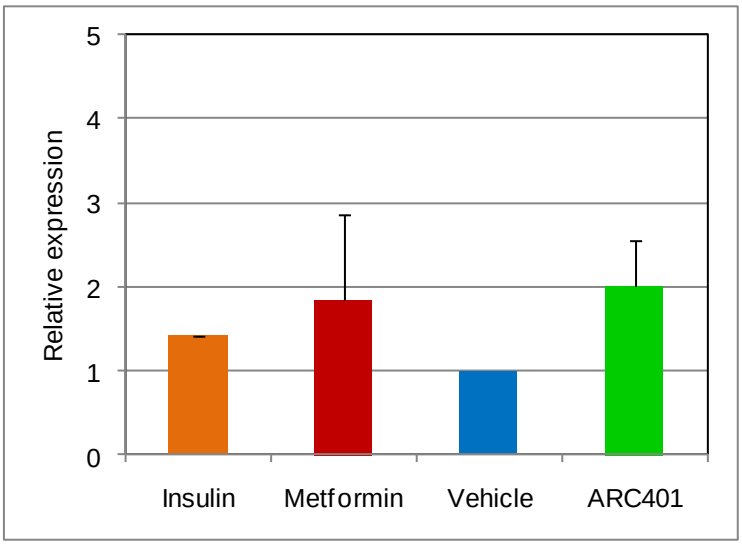

Figure 50. Relative expression of glucose transporter 4 (GLUT4) of C2C12 myocytes following acute exposure to ARC401 controls (insulin, metformin and water vehicle). Results are the mean of two independent experiments + standard deviation.

6. Pancreatic islet and β-cell assays

Pancreata were isolated from adult, male Wistar rats and islets retrieved by histopaque centrifugation. The isolated islets were cultured overnight and a glucose-stimulated insulin release assay was performed the following day. Prior to the glucose-stimulated insulin release assay, individual islets of medium to large size (approximately 30-60 µm) were hand-picked under a stereo-microscope in order to obtain a more purified sample (figure 51). Isolated islets were then trypsinised to retrieve individual β-cells, which were used in the flow cytometric determination of nitric oxide (as measured by diaminofluorescein-triazol fluorescence), in response to hyperglycaemia (figure 52).

a. 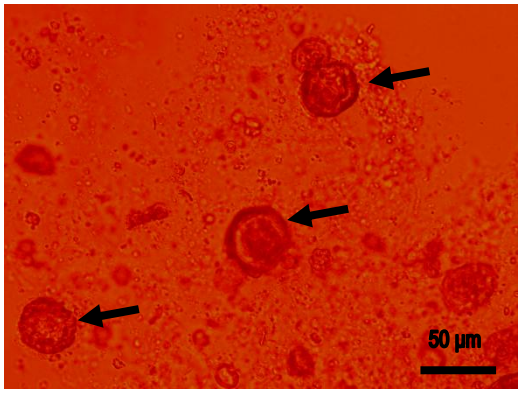

b. 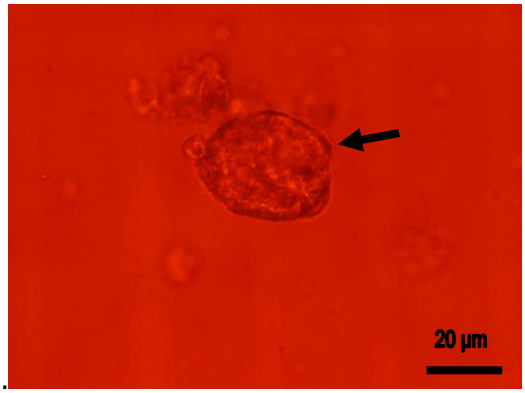

Figure 51. Isolated rat pancreatic islets (arrows) on the day of isolation at 200 x magnification (a) and after being hand-picked the day after isolation at 400 x magnification (b).

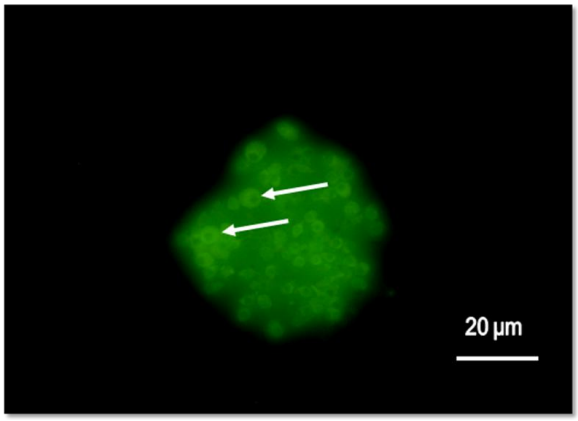

Figure 52. Diaminofluorescein-triazol (DAF-2T) fluorescence of a cluster of β-cells. Individual β-cells are indicated by the arrows.

6.1. Glucose-stimulated insulin release assay

Freshly isolated rat pancreatic islets were pre-exposed to ARC401 (0.05 µg/µl) and then acutely stimulated (120 minutes) with increasing glucose concentrations (2.8 mM, 17 mM and 35 mM). Insulin secreted into the medium was measured after 15 minutes and 120 minutes of glucose stimulation. ARC401 reduced both first phase (15 min) and second phase (120 min) insulin response in β-cells by 0.9 fold at low glucose (2.8 mM) concentrations (figure 53). At higher glucose concentrations (17 mM and 35 mM), ARC401 increased the first phase insulin response by 1.2 and 1.9 fold respectively. Similarly, ARC401 decreased second phase insulin response at 17 mM and 35 mM glucose concentrations by 0.7 and 0.6 fold respectively.

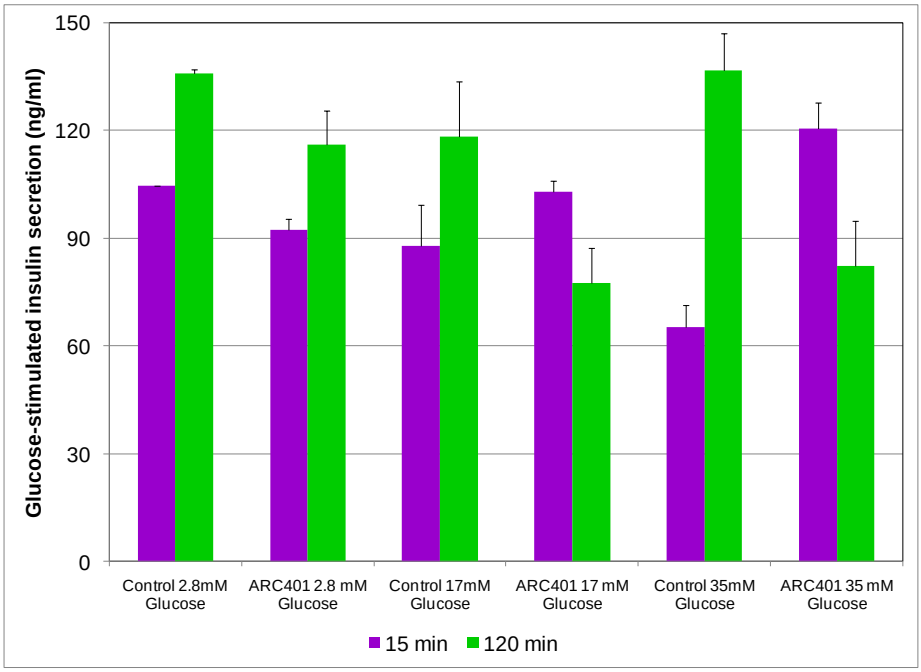

Figure 53. Insulin secretion at 15 and 120 minutes following glucose-stimulation in pancreatic islets pre-exposed to ARC401. Results are the mean + standard deviation of one experiment with two replicates.

6.2. Flowcytometric determination of nitric oxide (NO)

The single β-cell suspensions were acutely exposed to non-stimulatory (2.8 mM glucose) and hyper-stimulatory glucose (35 mM glucose) and incubated with 10 mM DAF fluorescent nitric oxide (NO). Intracellular fluorescence of the oxidized form of DAF, DAF-triazol (DAF-2T) was quantified by flow cytometry. B-cells were gated into region one (R1) due to their higher granularity (SSC-Height) and/or larger size (FSC-Height) (figure 54). The black population to the bottom left of figure 54 represents cellular debris, miscellaneous endothelial cells and other islet cells. High glucose concentration (35 mM) increased DAF-2T fluorescence (i.e. nitric oxide production) in β-cells 1.3 fold compared to β-cells incubated in KRBH containing 2.8 mM glucose (figure 55). ARC401 decreased DAF-2T fluorescence (i.e. nitric oxide production) in β-cells 0.5 fold compared to β-cells incubated in KRBH containing 2.8 mM glucose only (figure 56). ARC401 had no effect on

DAF-2T fluorescence (i.e. nitric oxide production) in β-cells compared to β-cells incubated in KRBH containing 35 mM glucose only (figure 57).

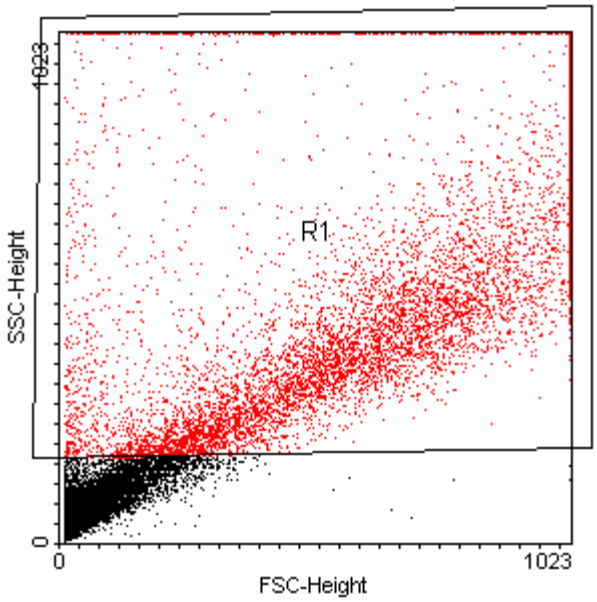

Figure 54. B-cell population gating on a forward scatter (FSC-Height) side scatter (SSC-Height) dot plot.

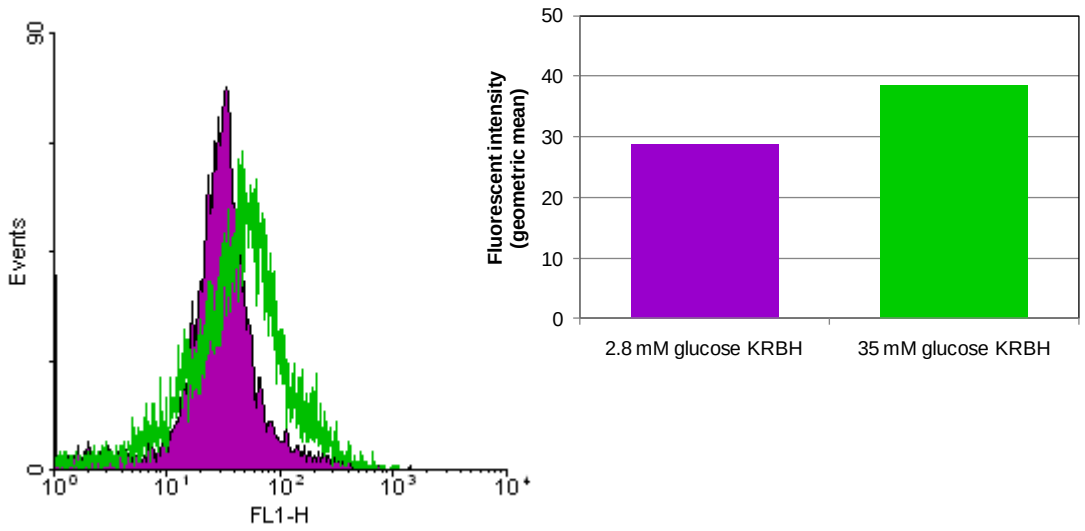

Figure 55. Region one gated DAF-2T fluorescence in β-cells incubated in 2.8 mM (purple) and 35 mM (green outline) glucose in KRBH.

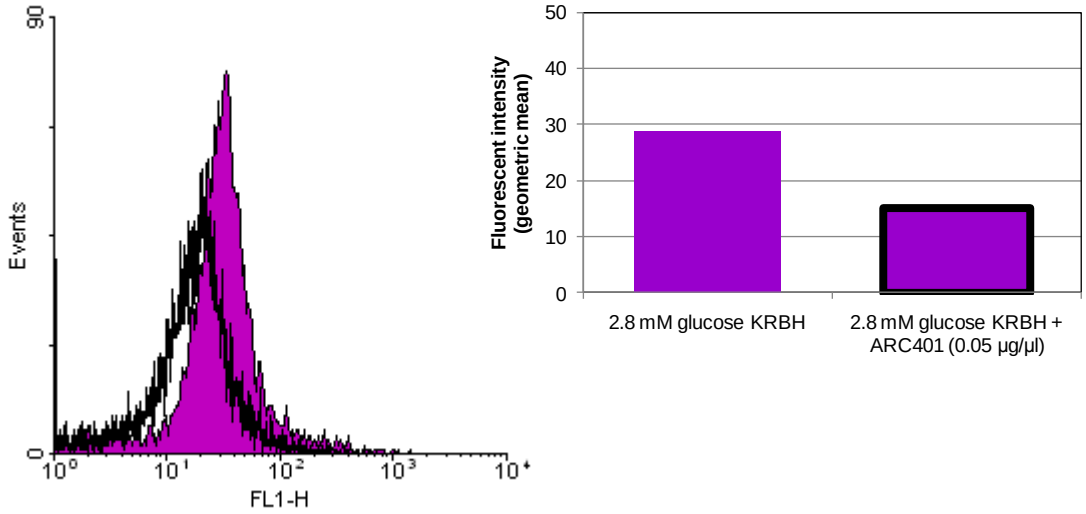

Figure 56. Region one gated DAF-2T fluorescence in β-cells incubated in 2.8 mM glucose (purple) and with ARC401 (0.05 µg/µl) (black outline) KRBH.

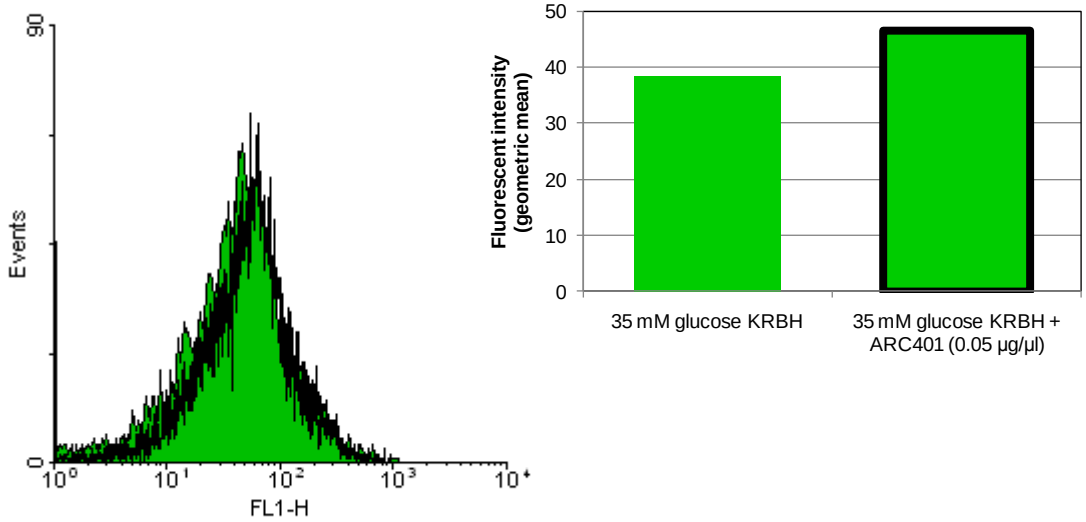

Figure 57. Region one gated DAF-2T fluorescence in β-cells incubated in 35 mM glucose (green) and with ARC401 (0.05 µg/µl) (black outline) in KRBH.

7. Production of tumor necrosis factor alpha (TNF-α) by peripheral blood mononuclear cells (PMBCs)

Peripheral blood mononuclear cells (PBMCs) were retrieved by histopaque centrigugation from whole blood drawn from adult, male Wistar rats. TNF-α production by PBMCs following 24 hour chronic incubation with 0.05 µg/µl ARC401 extract and 2ng/ml lipopolysaccharides (LPS) was measured in the culture media using an ELISA kit. PBMC viability was determined using a trypan blue exclusion viability assay.

7.1. PBMC viability

The number of viable cells per well was comparable across all treatments (figure 58). ARC401 was not toxic to PBMCs, nor was LPS.

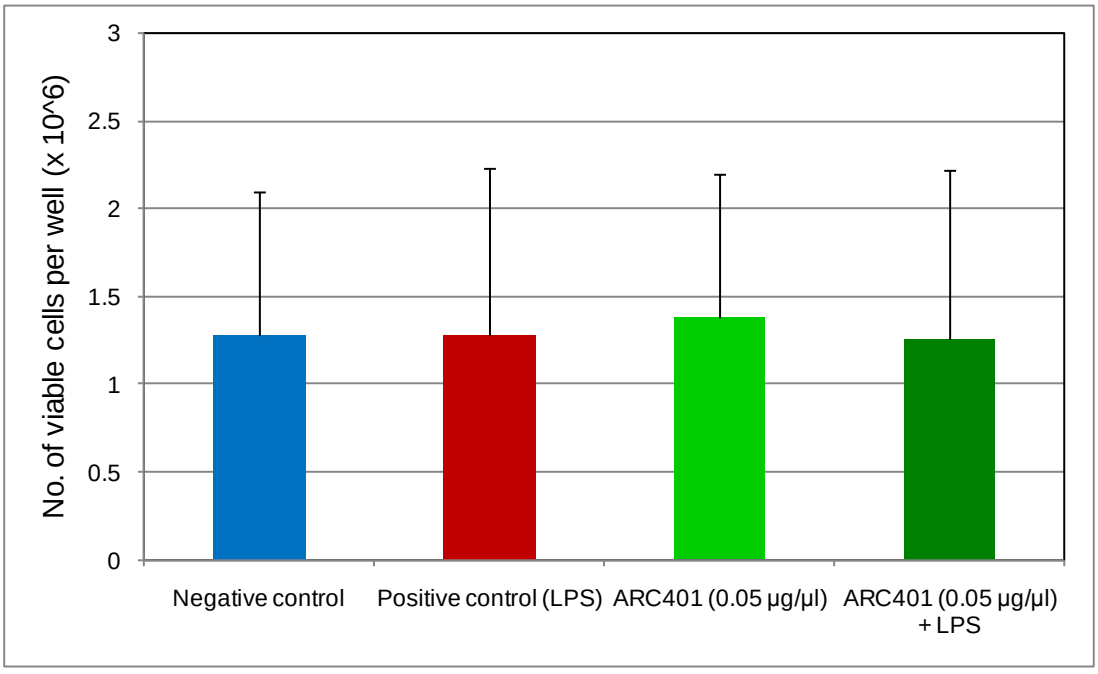

Figure 58. Viable PBMCs per well following chronic exposure to ARC401 extract and LPS. Results are the mean of four replicates in one experiment + standard deviation.

7.2. Quantification of TNF-α produced by PBMCs

ARC401 extract had no effect on TNF-α production by isolated rat PBMCs with or without LPS stimulation (figure 59). LPS significantly increased TNF-α production by isolated rat PBMCs.

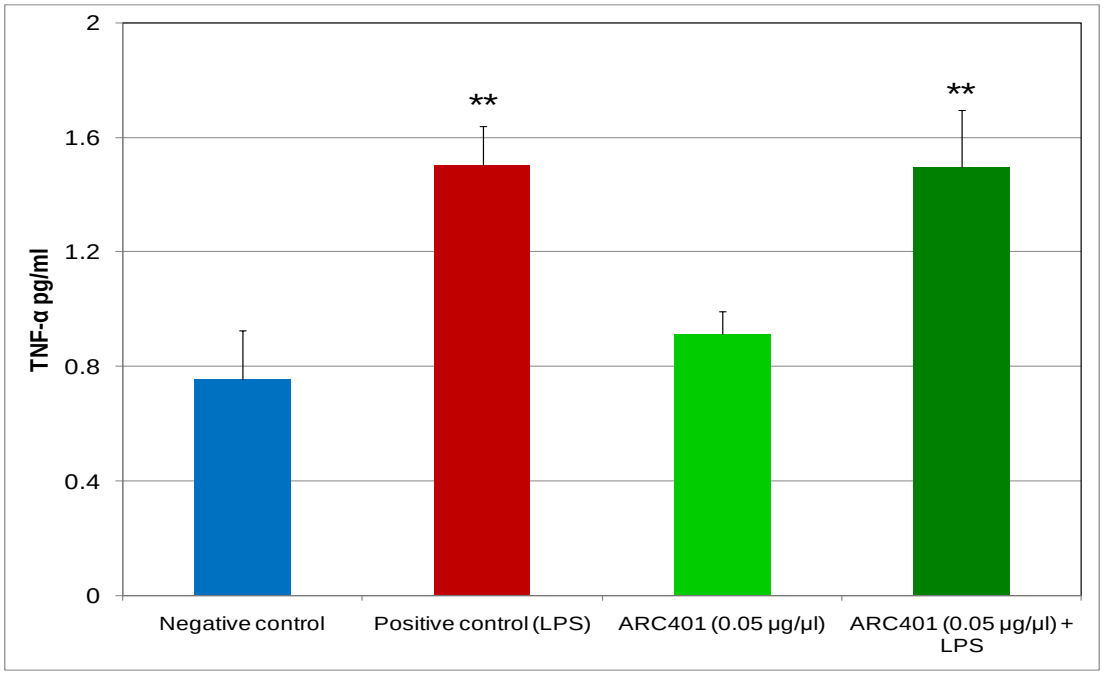

Figure 59. TNF-α production in PBMCs following chronic exposure to ARC401 extract and LPS. Results are the mean of four replicates in one experiment + standard deviation. * $p<0.05$, ** $p<0.01$ compared to negative control.

8. Summary of results

8.1. Summary of *in vitro* results

8.1.1. Glucose uptake and metabolism

Table 1. Summary of the effect of ARC401 in C2C12, Chang and 3T3-L1 cells

	Glucose uptake	Glucose oxidation	Glycogen content	Insulin signalling gene expression
C2C12	↑↑↑	↑↑	-	↑INSR ↑GLUT4
Chang	↑	↑	↑	-
3T3-L1	↑↑	-	-	-

↑ = p <0.05 **OR** fold change > 1.5; ↑↑ = p < 0.01; ↑↑↑ = p < 0.001 at maximal stimulatory concentration of ARC401.

8.1.2. Chang cell cytotoxicity

ARC401 reduced mitochondrial activity at the highest concentration tested (1 µg/µl).

8.2. Summary of *ex vivo* results

8.2.1. Glucose stimulated insulin secretion

ARC401 increased first phase insulin secretion of β-cells in hyperglycemic conditions, although the increase was not significant.

8.2.2. NO production

ARC401 did not reduce NO production induced by hyperglycaemia.

8.2.3. Anti-inflammatory effect in PBMCs

ARC401 did not reduce TNF-α production of PBMCs stimulated with LPS.

CHAPTER 4

DISCUSSION

1. *Athrixia phylicoides* aqueous extract (ARC401) and muscle cell glucose uptake and metabolism

C2C12 myoblasts were morphologically differentiated into spindle shaped myocytes which then fused to form multi-nucleate, densely packed myotubules. The differentiated myocytes have increased levels of the insulin-sensitive GLUT4 and mimic normal physiological glucose uptake in muscle tissue (Cartailler, 2001).

1.1. ARC401 increases glucose uptake in differentiated C2C12 myocytes acutely exposed to the extract

Significantly increased glucose uptake following acute exposure to 1 µM insulin positive control confirmed that the differentiated C2C12 myocytes are sensitive to insulin or insulin-like stimulation. The 1 µM metformin positive control also demonstrated significantly increased glucose uptake, further demonstrating sensitivity of the myocytes to glucose transport stimulation by a known anti-diabetic drug. Acute exposure of the C2C12 myocytes to ARC401 extract increased glucose uptake in the C2C12 cells at all three concentrations tested. Maximal stimulation of glucose uptake was achieved at the 0.05 µg/µl concentration, with the stimulatory activity lower at the low concentration (0.025 µg/µl) and attenuated at the high concentration (0.1 µg/µl). The attenuated glucose uptake activity at the 0.1 µg/µl concentration could be related to saturation of or changes to the stimulatory pathway. Glucose uptake data in the C2C12 cells indicate that ARC401 extract is highly active in muscle; Van de Venter *et al.* (2008) described extracts with the ability to stimulate glucose uptake in muscle cells by more than 150%, as very active.

1.2. ARC401 increases glucose metabolism in differentiated C2C12 myocytes acutely exposed to the extract

The increased glucose taken up by the C2C12 myocytes was actively oxidized to CO_2 and energy (ATP and NADH). Although the glycogen content of C2C12 myocytes was not significantly increased by ARC401, a dose related increase in intracellular glycogen content was found with increasing concentrations of extract. Increasing plasma concentrations of insulin have been previously correlated with predominating glycogen synthesis (DeFronzo, 2004). At the highest concentration tested (0.1 µg/µl), ARC401 increased glycogen storage comparable with that of insulin-stimulated storage. The oxidation of ^{14}C-glucose to $^{14}CO_2$ by C2C12 myocytes was significantly increased following acute exposure to ARC401 at 0.05 and 0.1 µg/µl. The maximal stimulatory effect of ^{14}C-glucose oxidation to $^{14}CO_2$ at the two high doses was similar to that of insulin and metformin positive controls. Increase in glucose oxidation may be as a result of insulin-like stimulation by ARC401 of pyruvate dehydrogenase, which plays a pivotal role in glucose oxidation (DeFronzo, 2004).

1.3. ARC401 increases insulin receptor (INSR) and glucose transporter four (GLUT4) expression in differentiated C2C12 myocytes acutely exposed to the extract

Gene expression PCR analysis showed that ARC401 increased INSR expression 2.7 fold. The insulin positive control also increased INSR expression in the C2C12 myocytes 3 fold. Furthermore, ARC401 increased GLUT4 expression 2 fold, with insulin positive control increasing GLUT4 expression in the C2C12 cells 1.4 fold. These data suggest that ARC401 stimulated glucose uptake via INSR and GLUT4 in an insulin-mimetic manner. With defects in GLUT4 incorporation into the plasma membrane being characterized as one of the well-defined defects in glucose uptake in type II diabetes (Bryant *et al.*, 2002;

Hoehn *et al.*, 2008), increased gene expression and subsequent increased protein expression of GLUT4 have therapeutic implications. ARC401 stimulated increased glucose uptake and metabolism in C2C12 myocytes, the concurrent increase in INSR and GLUT4 in these cells demonstrates potential insulin-mimetic properties of ARC401. However, the protein expression of these insulin-signalling genes needs some interrogation in order to determine potential alternative, non-insulin stimulatory pathway/s. Post-transcriptional modification of proteins (e.g. phosphorylation) also needs to be investigated in order to determine the total effect of ARC401 on the glucose uptake pathway.

ARC401 did not show any effect on the IRS genes (one and two), or on PI3K gene expression. Since the proteins regulated by the IRS genes are themselves regulated by phosphorylation (i.e. activated upon tyrosine phosphorylation), further interrogation of the state of phosphorylation of these proteins is required. Although PI3K gene expression is not changed, its state of activity is dependent on the binding of its p85 regulatory SH2 domain subunit to tyrosine phosphorylated IRS (Sesti, 2006). Hence the real time reverse transcriptase snap-shot of PI3K expression does not necessarily discriminate between activated PI3K bound to IRS and non-activated PI3K in the cytoplasmic pool. Chakraborty (2006) described the necessity for PI3K in insulin-stimulated glucose uptake, but proposed that an additional pathway (independent of PI3K) may exist. Chakraborty proposed insulin-stimulated exocytosis of GLUT4 as mimicking that of exocytosis of synaptic vesicles. Thus soluble N-ethylmaleimide-sensitive factor attachment protein receptor (SNARE) interactions may operate parallel to PI3K initiation of GLUT4 translocation.

2. *Athrixia phylicoides* aqueous extract (ARC401) and liver cell glucose uptake and metabolism

The Chang liver cell strain was established from non-malignant human tissue of epithelial origin by R.S. Chang. Chang cells are a well established and continuously used cell line for *in vitro* glucose screening of potential drug candidates (including anti-diabetic agents) (Hwang *et al*., 2007; Van de Venter *et al*., 2008 and Adam *et al*., 2009). Chang cells were exposed to pyruvate-free 8 mM glucose media, which represents postprandial glucose concentrations. The media also contained either ARC401 extract or controls (insulin, metformin and water).

2.1. ARC401 increases glucose uptake in Chang cells acutely exposed to the extract

Sensitivity of Chang cells to stimulation of glucose uptake pathway/s was confirmed with significant increase in glucose uptake by both 1 µM insulin and 1 µM metformin positive controls. ARC401 also increased glucose uptake in the Chang cells, with a significant increase at the two higher concentrations (0.05 and 0.1 µg/µl). Insulin stimulated glucose uptake in Chang cells (although significant) was not as marked as in the C2C12 myocytes since splanchnic tissues (like liver) are known to be largely unaffected by insulin stimulation with regard to glucose uptake (DeFronzo, 2004). Similarly, the glucose uptake stimulated by ARC401 was more marked in the C2C12 myocytes than the Chang cells, further indicating insulin-mimetic properties of the extract.

2.2. ARC401 increases glucose metabolism in Chang cells acutely exposed to the extract

Chang cells were impartial to oxidisation or storage (as glycogen) of the increased amount of glucose taken up. Both oxidation of ^{14}C-glucose to $^{14}CO_2$ and glycogen storage was

significantly increased by ARC401 in the Chang cells. Chang cell oxidation of ^{14}C-glucose to $^{14}CO_2$ increased in a dose-dependent manner as concentrations of ARC401 increased. Significant increases in oxidation were observed at the two higher concentrations (0.05 and 0.1 µg/µl); interestingly, these are the same two doses that stimulated significant glucose uptake from the media in these cells. The glucose oxidation of Chang cells acutely exposed to the highest concentration of ARC401 (0.1 µg/µl) was higher than that of both insulin and metformin controls. Glycogen storage was significantly increased at all three concentrations of ARC401 tested. The glycogen content of Chang cells acutely exposed to ARC401 (at all three concentrations) was comparable with that of Chang cells acutely exposed to insulin and metformin positive controls. Both basal and insulin-stimulated glycogen synthesis ability is diminished in T2D (DeFronzo, 2004), therefore therapeutics that enhance glycogen storage in liver can aid in ameliorating the adverse effects associated with dysfunctional glucose metabolism. The ability of ARC401 to stimulate glycogen storage in Chang cells represents the ability of the extract to induce insulin-like actions in these cells, since insulin is known to increase glycogen synthase activity and subsequent glycogen storage (Cohen, 1999). The ability of Chang cells to respond to insulin-like stimulation of ARC401 in terms of glycogen storage initiates the consideration that, like insulin, ARC401 possesses the ability to decrease the hyperglycemic onslaught attributed to HGP. Overall, ARC401 enhanced metabolism of the increased glucose taken up by Chang cells.

2.3. ARC401 has no detectable effect on insulin-signalling gene expression in Chang cells acutely exposed to the extract

Gene expression analysis showed that ARC401 had no effect on insulin-signalling gene expression in Chang cells. In order to further elucidate the effect of ARC401 on the insulin signalling pathway in Chang cells, future work should include the relative expression of

GLUT1 and GLUT2, as well as the phosphorylated isoforms of IRS1/2. It would also be interesting to investigate the relative expression of the glucokinase gene in liver and liver-like cells since glucokinase plays an important role in glucose oxidation in this tissue type.

2.4. ARC401 has no cytotoxic effects on Chang cells exposed to the extract

The MTT assay is a rigorous and well described technique used to determine potential cytotoxic effects *in vitro* (Mossman, 1983). Since MTT solution (tetrazolium bromide) is reduced in active mitochondria by mitochondrial dehydrogenase to purple formazan crystals, quantification of formazan formation using this assay provides insight into the mitochondrial activity of Chang cells. ARC401 did not inhibit mitochondrial activity nor were cytotoxic effects observed in Chang cells exposed to the extract for 24 hours at increasing concentrations (0.0125 - 1 µg/µl). At all concentrations tested optical densities at 570 nm were above 60% of that of the vehicle control. At the highest concentration, ARC401 induced reduced mitochondrial activity in the Chang cells. This may be as a result of an antagonistic concentration effect (Peng *et al.*, 2005).

3. *Athrixia phylicoides* aqueous extract (ARC401) and adipocyte glucose uptake and metabolism

3T3-L1 pre-adipocytes were morphologically differentiated from fibroblastic, progenitor mesenchymal cells to rounded, fully functional, fat-producing adipocytes. Insulin, dexamethasone and isobutylmethylxanthine were added to the culture media in order to induce this differentiation since these agents are known to promote adipocyte differentiation by activating PI3K and protein kinase B (PKB, aka Akt) (Jain and Yadav, 2009). These agents also facilitate the expression of peroxisome proliferator-activated receptor gamma (PPARγ) and cytidine-cytidine-adenosine-adenosine-thymidine-enhancer-binding protein alpha, which are considered master regulators of adipogenisis (Farmer,

2006). The differentiated 3T3-L1 adipocytes and were exposed to pyruvate-free 8 mM glucose media, which physiologically represents postprandial glucose concentrations. The media also contained either ARC401 extract or controls (insulin, metformin and water).

3.1. ARC401 increases glucose uptake in differentiated 3T3-L1 adipoycytes acutely exposed to the extract

Stimulated glucose uptake via GLUT1 and GLUT4 has been demonstrated in 3T3-L1 adipocytes (Kotani *et* al., 1998 and Bosch *et al*., 2004). The differentiated adipocytes used in this study demonstrated significantly increased glucose uptake when stimulated with insulin positive control and thus mimic the physiological process of glucose uptake in normal adipose tissue. Rat adipocytes, *in vitro,* demonstrate the ability to increase translocation of GLUT4 to the plasma membrane in response to metformin, thus facilitating increased glucose uptake (Matthaei *et* al., 1991 and Kozka and Holman, 1993). In this study metformin significantly increased glucose uptake in the 3T3-L1 adipocytes following acute exposure. Acute exposure of the 3T3-L1 adipocytes to ARC401 extract increased stimulation of glucose uptake. Maximal stimulation of glucose uptake was achieved at the 0.025 and 0.05 µg/µl concentrations. Attenuation of the stimulatory glucose uptake effect of ARC401 was observed at the high concentration (0.1 µg/µl), albeit that the percentage of glucose taken up was still higher than that of the vehicle control. The attenuated glucose uptake activity at the 0.1 µg/µl concentration could be related to saturation of or changes to the stimulatory pathway.

3.2. ARC401 has no measurable effect on glucose metabolism in differentiated 3T3-L1 adipoycytes acutely exposed to the extract

ARC401 did not increase ^{14}C-glucose oxidation to $^{14}CO_2$ in the 3T3-L1 adipocytes; albeit, neither did insulin and metformin positive controls. A trend toward decreasing ^{14}C-glucose

oxidation with increasing ARC401 concentrations was seen, which may infer that ARC401 reduces glucose oxidation, and potentially favours the storage of increased glucose taken up as lipid/fat. Further experimental assay/s should be performed in order to determine the effect of ARC401 on adipogenesis in the 3T3-L1 adipocytes. The glycogen content of 3T3-L1 adipocytes was not detectable by the assay used in this study – values obtained were less than the minimum value in the standard curve (i.e. 0.04 µg/well) since adipocytes store less glycogen compared to myo- and hepato- cytes. Cells used in the glycogen content assays were lysed and homogenized to release the intracellular glycogen (see section **2.6.2** in chapter two). This method of glycogen extraction also releases cellular lipid, which may in fact compromise the glycogen determination assay by non-specifically interacting with the BioVision glycogen content kit components.

3.3. ARC401 effect on insulin-signalling gene expression in differentiated 3T3-L1 adipoycytes acutely exposed to the extract

Insulin-signalling gene expression in differentiated 3T3-L1 adipoycytes acutely exposed to ARC401 was inconclusive as the probes purchased to perform the analysis failed to bind to the cDNA synthesized from these cells. As with the undetectable glycogen content seen in these adipocytes, failure of primers binding to their target sequences on the cDNA could possibly be as a result of lipid contamination interactions. In order to further elucidate the effect of ARC401 on the insulin signalling pathway in 3T3-L1 adipocytes, future work should include analysis of insulin-signalling protein expression as well as gene expression analysis using new probes or alternatively, designing new primers.

4. Glucose stimulated insulin response and antioxidant effect of *Athrixia phylicoides* aqueous extract (ARC401) in pancreatic β-cells

Pancreatic β-cells obtained from adult, male Wistar rats were pre-exposed to ARC401

extract (0.05 µg/µl) for 24 hours and then cultured in increasing concentrations of glucose. The 2.8 mM concentration represented normal physiological glucose concentrations *in vivo*. The 17 and 35 mM glucose concentrations represented stimulated and hyper-stimulated glucose concentrations. Hyperglycaemia is a known stimulus of β-cell oxidative stress, either due to the higher demand for insulin synthesis and secretion, or as a result of glucotoxicity (Bonora, 2008). Only one experimental repeat was performed in these assays, however, the important process of establishing a viable protocol was achieved.

4.1. The effect of ARC401 on insulin secretion in response to glucose stimulation

ARC401 pre-exposed pancreatic islets showed slightly reduced first and second phase insulin response at low glucose (2.8 mM) concentrations. At higher glucose concentrations (both 17 mM and 35 mM glucose), ARC401 increased the first phase insulin response and decreased second phase insulin without neural modulation that occurs in the intact pancreas. At hyperstimulatory glucose concentrations (e.g. 35 mM), an increase in first phase insulin response would release most, if not all, insulin granules in the cytoplasm of the islets. The reduction in second phase insulin secretion (i.e. secretion of newly synthesized insulin) would be as a result of increased first phase insulin secretion. Interestingly, high glucose stimulation (at both 17 mM and 35 mM glucose) did not induce a significant increase in first or second phase insulin secretion. This assay was performed with only one repeat due to limited resource and time; however further repetition using a larger number of islets will provide significant insights into β-cell glucose response and the effect of ARC401 in this response. Several studies have reported that exposure of pancreatic islets to gluco- (or lipo-) toxic conditions activates inducible nitric oxide synthase with a concomitant reduction in insulin response to glucose stimulation (Henningsson *et al*., 2002; Salehi *et al*., 2003 and Jimenez-Felstrom *et al*., 2005). This correlates with the glucose stimulated insulin response data in this study, where high

glucose (17 mM and 35 mM) failed to significantly increase insulin secretion (and synthesis) in isolated pancreatic islets of Langerhans. Salehi *et al.* (2003) proposed that NO derived from neuronal constitutive nitric oxide synthase (ncNOS) might serve as a negative feedback inhibitor of acute glucose stimulated insulin release. Future studies should include not only quantification of NO produced by pancreatic β-cells, but also via which synthesis enzyme it was derived (i.e. be it from ncNOS, or endothelial NOS, or inducible NOS, etc.).

4.2. The antioxidant effect of ARC401 in pancreatic β-cells

β-cells used for this component of the study were only exposed to two glucose concentrations (i.e. 2.8 and 35 mM glucose). A control sample of β-cells were gated based on their higher granularity and/or larger size. Cellular debris, miscellaneous endothelial cells and other islet cells, such as α-cells and δ-cells were subsequently excluded from the analysis by this gate. The decrease in DAF-2T fluorescence indicates a decrease in NO production by β-cells pre-exposed to ARC401 at 2.8 mM glucose. This decrease in NO correlates with the slightly reduced insulin secretion by β-cells pre-exposed to ARC401 at 2.8 mM glucose. The correlation is due to NO being a key regulator of insulin secretion in β-cells (Campbell *et al.*, 2007). Although NO is an important part of insulin secretion, at increased levels it is known to provoke increased β-cell oxidative stress (Campbell *et al.*, 2007). Hyperglycaemic induction of β-cell oxidative stress and a reduced amount of anti-oxidants (e.g. glutathione) in β-cells may impair β-cell function and thus insulin secretion (Campbell *et al.*, 2007). The results in this study correlate with hyperglycaemic (35 mM glucose) induction of increased NO production by β-cells, as well as failure of the β-cells to respond to hyperglycaemia. ARC401 was unable to reduce the amount of NO produced at 35 mM glucose, which indicates that ARC401 does not have a significant effect on NO production in isolated rat pancreatic β-cells.

5. Anti-inflammatory effect of *Athrixia phylicoides* aqueous extract (ARC401) in PBMCs

PBMCs have been commonly used to demonstrate potential anti-inflammatory effects of agents. Using purified PBMCs as opposed to whole blood culture offers the advantage of not having interference from other blood cells that may act with the test compound differently and compromise the inflammatory effect in PBMCs (Crouvezier *at al*., 2001). PBMCs have also been shown to ellicit a potent inflammatory response when stimulated with LPS. In this study, LPS isolated from *E. coli* were used. These LPS significantly increased TNF-α production by PBMCs isolated from adult, male Wistar rat whole blood. ARC401 failed to decrease TNF-α in the isolated PBMCs, showing no measurable effect on induced inflammation. Although ARC401 failed to decrease TNF-α production by PBMCs stimulated by LPS, ARC401 may yet have an anti-inflammatory effect. The anti-inflammatory effect of ARC401 may be less pronounced and hence future studies should consider the use of a less potent inflammatory stimulation (e.g. the use of cytokine stimulation).

The study by Crouvezier *et al.* in 2001 demonstrated the ability of selected tea polyphenols to decrease the production of IL-1β by whole blood and purified PBMC cultures. A reduction in TNF-α was not seen in this study. Similarly, ARC401 may also ellicit an anti-inflammatory effect in PBMC's via the reduction of the pro-inflammatory cytokine IL-1β by a pathway independent of NFκB.

CHAPTER 5

CONCLUSIONS

Limitations of the study and prospective research

Despite this study showing that the aqueous extract of *A. phylicoides* increases glucose uptake and metabolism *in vitro,* the *in vivo* effects still need to be established. Absorption and metabolism of the active agents in the plant needs to be investigated. Isolating these active agents by extract fractionation will allow for synthetic mass production of an anti-diabetic drug (Haslam, 1996). Future work should involve severe hyperglycaemic conditions (e.g. above 17 mM glucose in an streptozotocin-induced diabetic rat model) since it is this severe hyperglycaemia that results in the numerous diabetic complications and also further exacerbates the deteriorating diabetic state (Johansen *et al*., 2005, and Houstis *et al*., 2006). In order to further elucidate the insulin signalling pathway, the effect of the extract on phosphorylated isoforms of key insulin signalling molecules should be investigated since these are the active forms. Since *A. phylicoides* extract may work via a pathway similar but not exclusive to insulin signalling, the effect of the extract on enzymes involved in rate limiting reactions of glucose metabolism (e.g. hexokinase, glycogen synthase) should also be investigated. New probes or primers that are specific for our 3T3-L1 cell line need to be designed and/or purchased, since the current mouse probes failed to bind to targeted sequences in the 3T3-L1 adipocytes.

The largest limitation of the *ex vivo* component of this study was the limited number of animals available for pancreatic islet isolations. Due to their relative size compared to primates or humans, adult male Wistar rats yielded an average of 200 pancreatic islets per animal; in future larger number of animals should be used. Alternatively *in vitro* β-cell lines (e.g. INS1 and MIN6 cell lines) can be used to compliment the *ex vivo* data generated. Along with repeated experimental data on insulin secretion and NO production, the effect of *A. phylicoides* extract on the total anti-oxidant status of pancreatic β-cells should be fully elucidated; i.e. total ROS versus total anti-oxidants (e.g. catalase, super oxide dismutase,

glutathione). The insulin-sparing effect of the extract should be considered in future work; i.e. the ability of the extract to sensitise tissues such that less insulin is required to maintain normoglycemia, thus reducing the stress on β-cells.

Included in future studies should also be the effect of *A. phylicoides* aqueous extract on the production of IL-6 since this pro-inflammatory cytokine is also regulated by the same NFκB as TNF-α and IL-1β. In order to determine the complete effect of ARC401 on inflammation, the effect of the extract on anti-inflammatory cytokines (e.g. interleukin 10) should be investigated. The extract may also ellicit anti-inflammatory effects attributed to plant polyphenols by suppressing the infiltration of leukocytes into target organs as demonstrated by Katiyar and colleagues in 1999. Future studies should also consider the use of less potent inflammatory stimulation (e.g. the use of cytokine stimulation).

Concluding remarks

With changes in the socio-economic climate and a new trend in merging Western lifestyle with traditional practices, new interest has been shown in herbal/natural remedies (van Wyk and Gericke, 2000, and Rampedi and Olivier, 2005*)*. Scientific verification of potential health benefits of plant therapeutics is necessary for universal acceptance.

This study demonstrates that *Athrixia phylicoides* aqueous extract not only increases the amount of glucose taken up in peripheral tissues (i.e. muscle and adipose), but also shows enhanced glucose uptake in liver *in vitro.* The extract also increased the *in vitro* ability of muscle and liver cells to metabolise glucose in an insulin-mimetic manner. *Athrixia phylicoides* extract had no measurable effect *ex vivo* on anti-oxidative and anti-inflammatory statuses of pancreatic β-cells and peripheral mononuclear cells respectively. First phase insulin secretion of pancreatic β-cells was enhanced by the extract.

The effects of *Athrixia phylicoides* aqueous extract on *in vitro* glucose metabolism suggest that this extract could potentially be beneficial to type II diabetics as an adjunct therapy.

REFERENCES

- Abdollahi M., Ranjbar A., Shadnia S., Shekoufeh N. and Rezaie A., Pesticide and oxidative stress: a review. Medical Science Monitor 2004; 10: RA141-147.

- Adam Z., Hamid M., Ismail I. and Khamis S., Effect of Ficus deltoidea extracts on hepatic basal and insulin-stimulated glucose uptake. Journal of Biological Sciences 2009; 9(8): 796-803.

- Ariga M., Nedachi T., Katagiri H., Kanzaki M., Functional role of sortilin in myogenesis and development of insulin-responsive glucose transport system in C2C12 myocytes. Journal of Biological Chemistry 2008; 283: 10208-10220.

- Arts I. and Hollman P., Polyphenols and disease risk in epidemiological studies. American Journal of Clinical Nutrition 2005; 81: 317S-325S.

- Azar M. and Lyons T.J., Diabetes, insulin treatment, and cancer risk: what is the evidence? F1000 Medical Report 2010; 18(2): 4.

- Bastard J.P., Maachi M., Lagathu C., Kim M.J., Caron M., Vidal H., Capeau J. and Feve B., Recent advances in the relationship between obesity, inflammation and insulin resistance. European Cytokine Network 2006; 17: 4-12.

- Bays H.E., Current and investigational antiobesity agents and obesity therapeutic treatment targets. Obesity Research 2004; 12(8): 1197-12211.

- Beart J.E., Lilley T.H. and Haslam E., Plant polyphenols - secondary metabolism and

chemical defense: some observations. Phytochemistry 1985; 24:33-38.

- Boden G., Role of fatty acids in the pathogenesis of insulin resistance and NIDDM. Diabetes 1997; 46: 3-10.

- Bonora E., Protection of pancreatic beta-cells: is it feasible? Nutrition, Metabolism and Cardiovascular Diseases 2008; 18(1): 74-83.

- Bosch R.R., Bazuine M., Span P.N., Willems P.H.G.M., Olthaar A.J., Van Rennes H., Maasen J.A., Tack C.J., Hermus A.R.M.M. and Sweep C.G.J., Regulation of GLUT1-mediated glucose uptake by PKCλ-PKCβII interactions in 3T3-L1 adipocytes. Biochemistry Journal 2004; 384: 349-355.

- Boynes J.W., Role of oxidative stress in development of complication in diabetes. Diabetes 1991; 40: 405-411.

- Bradford M.M., Rapid and sensitive method for the quantitation of microgram quantities of protein utilizing the principle of protein-dye binding, Analytical Biochemistry 1976; 72: 248-254.

- Brash A.R., Lipoxygenases: Occurrence, functions, catalysis and acquisition of substrate. Journal of Biological Chemistry 1999; 274: 23679-23682.

- Brownlee M., A radical explanation for glucose-induced beta cell dysfunction. Journal of Clinical Investigation 2003; 112(12): 1788-1790.

- Brunetti A., Maddux B.A., Wong K.Y. and Goldfine I.D., Muscle cell differentiation is associated with increased insulin receptor biosynthesis and messenger RNA levels. Journal of Clinical Investigation 1989; 83(1): 192-198.

- Bryant N.J., Govers R. and James D.E., Regulated transport of the glucose transporter GLUT4. Nature Reviews: Molecular and Cell Biology 2002; 3: 267-277.

- Butler A.E., Janson J., Bonner-Weir S., Ritzel R., Rizza R.A. and Butler P.C., Beta-cell deficit and increased beta-cell apoptosis in humans with type 2 diabetes. Diabetes 2003; 52: 102-110.

- Butler R., Morris A.D., Belch J.J.F., Hill A. and Struthers A.D., Allopurinol normalizes endothelial dysfunction in type 2 diabetics with mild hypertension. Hypertension 2000; 35:746-751.

- Campbell S.C., Richardson H., Ferris W.F., Butler C.S. and Macfarlane W.M., Nitric oxide stimulates insulin gene transcription in pancreatic β-cells. Biochemical and Biophysicla Research Communications 2007; 353: 1011-1016.

- Cao H., Hininger-Favier I., Kelly M.A., Benaraba R., Dawson H.D., Coves S., Roussel A.M. and Anderson R.A., Green tea polyphenol extract regulates the expression of genes involved in glucose uptake and insulin signalling in rats fed a high fructose diet. Journal of Agriculture and Food Chemistry 2007; 55(15): 6372-6378.

- Cartailler J.-P., Insulin – from secretion to action. Beta Cell Biology Consortium 2001; 1-4.

- Chakraborty C., Biochemical and molecular basis of insulin resistance. Current Protien and Peptide Science 2006; 7: 113-121.

- Chellan N., De Beer D., Muller C., Joubert E., Louw J., A toxicological assessment of *Athrixia phylicoides* aqueous extract following sub-chronic ingestion in a rat model. Human and Experimental Toxicology 2008; 27: 819-825.

- Chromczynski P. and Sacchi N., Single-step method of RNA isolation by acid guanidinium thiocyanate-phenol-chloroform extraction. Analytical Biochemistry 1987; 162(1): 156-159.

- Cohen P., The Croonian lecture: Identification of a protein kinase cascade of major importance in insulin signal transduction. Proceedings of the Royal Society of London, Series B, Papers of a Biological Character 1999; 354: 485-495.

- Crouvezier S., Powell B., Keir D. and Yaqoob P., The effects of phenolic components of tea on the production of pro- and anti-inflammatory cytokines by human leukocytes in vitro. Cytokine 2001; 13(5): 280-286.

- Cusi K., Maezono K., Osman A., Pendergrass M., Patti M.E., Pratipanawatr T., DeFronzo R.A., Kahn C.R. and Mandarino L.J., Insulin resistance differentially affects the PI 3-kinase- and MAP kinase-mediated signalling in human muscle. Journal of Clinical Investigation 2000; 105(3): 311-320.

- DeFronzo R.A., Overview of newer agents: Where treatment is going. The American Journal of Medicine 2010; 123: S38-48.

- DeFronzo R.A., Pathogenesis of type 2 diabetes mellitus. Medical Clinics of North America 2004; 88: 787-835.

- Dent P., Lavoinne A., Nakielny S., Claudwell F.B., Watt P. and Cohen F., The molecular mechanisms by which insulin stimulates glycogen synthesis in mammalian skeletal muscle. Nature 1990; 348: 302-307.

- Diabetes Discovery Platform, Photograph and image archives 2010.

- Duckworth W.C., Hyperglycaemia and cardiovascular disease. Current Artherosclerosis reports 2001; 3(5): 383-391.

- Erasto P., van de Venter M., Roux S., Grierson D.S. and Afolayan A.J., Effect of leaf extracts of Vernonia amygdalina on glucose utilization in chang-liver, C2C12 muscle and 3T3-L1 cells. Pharmaceutical Biology 2009; 47(2): 175-181.

- Estrada D.E., Ewart H.S., Tsakiridis T., Volchuk A., Ramalal T., Tritschler H. and Klip A., Stimulation of glucose uptake by the natural coenzyme alpha-lipoic acid/thiotic acid: participation of elements of the insulin signalling pathway. Diabetes 1996; 45 (12): 1798-1804.

- Farmer S.R., Transcriptional control of adipocyte formation. Cell Metabolism 2006; 4(4): 263-273.

- Fox F.W. and Young M.E.N., Food from the veld. Edible Wild Plants of Southern Africa. Delta Books (Pty) Ltd. 1982; Johannesburg, South Africa: 119-120.

- Freudenrich C., How diabetes works. HowStuffWorks.com 22 June 2001. http://health.howstuffworks.com/diseases-conditions/diabetes/diabetes.htm. Downloaded 16 October 2010.

- Ganong W.F., Review of medical physiology, 14th Edition. Prentice Hall 1989; 280-298.

- Gotoh M., Maki T., Satomi S., Porter J., Bonner-Weir S., O'Hara C.J., Monaco A.P., Reproducible high yield of rat islets by stationary in vitro digestion following pancreatic ductal or portal venous collagenase injection. Transplantation 1987; 43(5): 725-730.

- Gram J., Henriksen J.E., Grodum E., Juhl H., Hansen T.B., Christiansen C., Yderstræde K., Gjessing H., Hansen H.M., Vestergaard V. and Beck-Nielsen H., Pharmacological treatment of the pathogenetic defects in Type 2 Diabetes: The randomized multi-centre South Danish Diabetes study (SDDS). Diabetes Care 2010; ePublication ahead of print.

- Gray A.M. and Flatt P.R., Insulin-releasing and insulin-like activity of *Agaricus campestris* (mushroom). Journal of Endocrinology 1998; 157, 259–266.

- Grill V. and Bjorklund A., Overstimulation and β cell function. Diabetes 2001; 50(1): S122-S124.

- Guidelines on ethics for medical research: use of animals in research and training. South African Medical Research Council (MRC) 2004.

- Gurgul E., Lortz S., Tiedge M., Jorns A. and Lenzen S., Mitochondrail catalase over-expression protects insulin-producing cells against toxixity of reactive oxygen species and proinflammatory cytokines. Diabetes 2004; 53:2271-2280.

- Hashimoto R., Yaita M., Tanaka K., Hara Y. and Kojo S., Inhibition of radical reaction of apolipoprotein B-100 and alpha-tocopherol in human plasma by green tea catechins. Journal of Agricultural and Food Chemistry 2000; 48(12): 6380-6383.

- Haslam E., Natural polyphenols (vegetable tannins) as drugs: Possible modes of action. Journal of Natural Products 1996; 59: 205-215.

- Henningsson R., Salehi A. and Lundquist I., Role of nitric oxide synthase isoforms in glucose-stimulated insulin release. American Journal of Physiology: Cell Physiology 2002; 283: C296-304.

- Hink U., Li H.G., Mollnau H., Oelze., Matheis E., Hartmann M., Skatchkov M., Thaiss F., Stahl R.A.K., Warnholtz A., Meinertz T., Griendling K., Harrison D.G., Forstermann U., Munzel T., Mechanisms underlying endothelial dysfunction in diabetes mellitus. Circulation Research 2001; 88:E14-E22.

- Hirasawa M., Takada K., Makimura M. and Otake S., Improvement of periodontal status by green tea catechin using a local delivery system: a clinical pilot study. Journal of Periodontal Research 2002; 37(6): 433-438.

- Hoehn K.L., Hohnen-Behrens C., Cederberg A., Wu L.E., Turner N., Yuasa T., Ebina Y., James D.E., IRS1-independent defects define major nodes of insulin resistance. Cell Metabolism 2008; 7:421-433.

- Hotamisligil G.S., Inflammatory pathways and insulin action. International Journal of Obesity and Related Metabolic Disorders 2003; 27(3): S53-55.

- Houstis N., Rosen D.E. and Lander E.S., Reactive oxygen species have a causal role in multiple forms of insulin resistance. Nature 2006; 440: 944-948.

- Hutchings A., Scott A.H., Lewis G. and Cunningham A., Zulu medicinal plants: an inventory. University of Natal Press, Pietermaritzburg, South Africa 1996.

- Hwang H-J., Kwon M-J. and Nam T-J., Chemoprotective effect of insulin-like growth factor I against acetaminophen-induced cell death in Chang liver cells via ERK1/2 activiation. Toxicology 2007; 230: 76-82.

- Huijing F., A rapid enzymic method for glycogen estimation in very small tissue samples. International Journal of Clinical Chemistry 1970; 30(3): 567-572.

- Jain S. and Yadav H., In vitro adipocyte differentiation. Protocol Online (www.protocolonline.org) 2009.

- Jeppesen P.B., Gregersen S., Poulsen C.R. and Hermansen K., Stevioside acts directly on pancreatic beta cells to secrete insulin: actions independent of cyclic adenosine monophosphate and adenosine triphosphate-sensitive K+-channel activity. Metabolism 2000; 49(2): 208-214.

- Jia W., Gao W. and Tang L., Antidiabetic herbal drugs officially approved in China. Phytotherapy Research 2003; 17(10): 1127-1134.

- Jimenez-Felstrom J., Lundquist I. and Salehi A., Glucose stimulates the expression and activities of nitric oxide synthases in incubated rat islets: an effect counteracted by GLP-1 through the cyclic AMP/PKA pathway. Cell Tissue Research 2005; 319: 221-230.

- Johansen J.S., Harris A.K., Rychky D.J. and Erul A., Oxidative stress and the use of antioxidants in diabetes: Linking basic science to clinical practice. Cardiovascular Diabetology 2005; 4 (1): 5-16.

- Jung M., Park M., Lee H.C., Kang Y-H., Kang E. S. and Kim S.K., Antidiabetic agents from medicinal plants. Current Medicinal Chemistry 2006; 13: 1203-1218.

- Kaddai V., Jager J., Gonzalez T., Najem-Lendom R., Bonnafous S., Tran A., Le Marchand-Brustel Y., Gaul P., Tanti J.-F. and Cormont M., Involvement of TNF-ά in abnormal adipocyte and muscle sortilin expression in obese mice and humans. Diabetologia 2009; 52:932-940.

- Kahler W., Kuklinski B. and Plotz C., Diabetes mellitus – a free radical-associated disease. Results of adjuvant antioxidant supplementation. Zeitschrift für die gesamte innere Medizin und ihre Grenzgebiete 1993; 48 (5): 223-232.

- Kanitkar M., Gokhale K., Galande S. and Bhonde R.R., Novel role of curcumin in the prevention of cytokine-induced islet death *in vitro* and diabetogenesis *in vivo*. British Journal of Pharmacology 2008; 155: 702-713.

- Katiyar S.K., Matsui M.S., Elmets C.A and Mukhtar H., Polyphenolic antioxidant epigallocatechin-3-gallate from green tea reduced UVB-induced inflammatory responses and infiltration of leukocytes in human skin. Photochemical Photobiology 1999; 69: 148-153.

- Kim H.K., Cheon B.S., Kim Y.H. and Kim H.P., Effects of naturally occurring flavonoids on nitric oxide production in the macrophage cell line RAW 264.7 and their structure-activity relationships. Biochemical Pharmacology 1999; 58: 759-765.

- Kotani K., Ogawa W., Matsumoto M., Kitamura T., Sakaue H., Hino Y., Miyake K., Sano W., Akimoto K., Ohno S., and Kasuga M., Requirement of atypical protein kinase C for insulin stimulation of glucose uptake but not for Akt activation in 3T3-L1 adipocytes. Molecular and Cellular Biology 1998; 18(12): 6971-6982.

- Kozka I.J. and Holman G.D., Metformin blocks downregulation of cell surface GLUT4 caused by chronic insulin treatment of rat adipocytes. Diabetes 1993; 42: 1159-1165.

- Krauss S., Zhang C.Y., Scorrano L., Dalgaard L.T., St-Pierre J., Grey S.T. and Lowell B.B., Superoxide-mediated activation of uncoupling protein 2 causes pancreatic beta cell dysfunction. Journal Clinical Investigation 2003; 112(12): 1831-1842.

- Leistner O.A., Seed Plants of Southern Africa: Families and Genera, Strelitzia Volume 10. National Botanical Institute, Pretoria, South Africa 2000; 125.

- Leopoldini M., Marino T., Russo N. and Toscano M., Antioxidant properties of phenolic compounds: H-atom versus electron transfer mechanism. The Journal of Physical Chemistry A 2004; 108: 4916-4922.

- Li J.M. and Shah A.M., ROS generation by nonphagocytic NADPH oxidase: Potential relevance in diabetic nephropathy. Journal of the American Society of Nephrology 2003; 14: S221-S226.

- Li W.L., Zheng H.C., Bukuru J. and Kimpe N.D., Natural medicines used in the traditional chinese medical system for therapy of diabetes mellitus. Journal of Ethnopharmacology 2004; 92(1): 1-21.

- Ling X., Nagai R., Sakashita N., Takeya M., Horiuchi S. and Takahashi K., Immunohistochemical distribution and quantitative biochemical detection of advanced glycation end products in fetal to adult rats in rats with streptozotocin-induced diabetes. Laboratory Investigations 2001; 81:845-861.

- Logani M.K. and Davies R.E., Lipid oxidation: biologic effects and antioxidants - a review. Lipids 1980; 15(6): 485-495.

- Mander M., Medicinal plant marketing and strategies for sustaining the plant supply in the Bushbuckridge area and Mpumalanga Province. Institute for Natural Resources, University of Natal 1997; Pietermaritzburg, South Africa.

- Marchetti P., Prato S.D., Lupi R. and Guerra S.D., The pancreatic beta-cell in human type 2 diabtes. Nutrition, Metabolism and Cardiovavscular Diseases 2006; 16: 3-6.

- Mashimbye M.J., Mudau F.N., Soundy P. and Van Ree T., A new flavonol from *Athrixia phylicoides* (bush tea). South African Journal of Chemistry 2009; 59**:** 1–2.

- Mathews C.K., Van Holde K.E. and Ahern K.G., Biochemistry, third edition. Addidon Wesley Longman 2000; 831-840.

- Matthaei S., Hamann A., Klein H.H., Benecke H., Kreymann G., Flier J.S. and Greten H., Association of metformin's effect to increase insulin-stimulated glucose transport with potentiation of insulin-induced translocation of glucose transporters from intracellular pool to plasma membrane in rat adipocytes. Diabetes 1991; 40: 850-857.

- McGaw L.J., Steenkamp V. and Eloff J.N., Evaluation of Athrixia bush tea for cytotoxicity, antioxidant activity, caffeine content and presence of pyrrolizidine alkaloids. Journal of Ethnopharmacology 2007; 110(1): 16-22.

- Mohan C., Signal transduction: A short overview of its role in health and disease, second edition. MERCK/EMD Biosciences 2010; 157-162.

- Mossman, H.M.T., Rapid colorimetric assay for cellular growth and survival: application to proliferation and cytotoxic assays. Journal of Immunological Methods 1983; 65, 55–63.

- Nedachi T. and Kanzaki M., Regulation of glucose transporters by insulin and extracellular glucose in C2C12 myotubes. American Journal of Physiology and Endocrinology Metabolism 2006; 291: E817–E828.

- Nielsen M.S., Jacobsen C., Olivecrona G. Gliemann J. and Petersen C.M., Sortilin/neurotensin receptor-3 binds and mediates degradation of lipoprotein lipase. Journal of Biological Chemistry 1999; 274: 8832-8836.

- Nijveldt R.J., van Nood E., Van Hoorn D.E., Boelens P.G., Van Norren K. and Van Leeuwen P.A., Flavonoids: a review of probable mechanisms of action and potential applications. American Journal of Clinical Nutrition 2001; 74(4): 418-425.

- Niwa Y. and Miyachie Y., Antioxidant action of natural health products and Chinese herbs. Inflammation 1986; 10: 79-91.

- Nunemaker C.S. and Satin L.S., A tale of two rhythms: a comparative review of the pulsatile endocrine systems regulating insulin and GnRH secretion. Cell Science Reviews 2005; 2(1): ePublication ahead of print.

- Ojeda M.O., Silva C.V., de J. Arana Rosainz M. and Fernandez-Ortega C., TNFα production in whole blood cultures from healthy individuals. Biochemical and

Biophysical Research Communications 2002; 292: 538-541.

- Parthasarathy C., Renuka V.N. and Balasubramanian K., Sex steroids enhance insulin receptors and glucose oxidation in Chang liver cells. Clinica Chimica Acta 2009; 399: 49-53.

- Paquay J.B., Haenen G.R., Stender G., Wiseman S.A., Tijburg L.B. and Bast A., Protection against nitric oxide toxicity by tea. Journal of Agriculture and Food Chemistry 2000; 48(11): 5768-5872.

- Pearson E.R., Pharmacogenetics in diabetes. Current Diabetes Reports 2009; 9: 172-181.

- Peng L., Wang B. and Ren P., Reduction of MTT by flavonoids in the absence of cells. Colloids and Surfaces Biointerfaces 2005; 45: 108–111.

- Perriello G., Misericordia P., Volpi E., Santucci A., Santucci C., Ferrannini E., Ventura M.M., Santeusanio F., Brunetti P. and Bolli G.B., Acute antihyperglycemic mechanisms of metformin in NIDDM. Evidence for suppression of lipid oxidation and hepatic glucose production. Diabetes 1994; 43(7): 920-928.

- PK Group standard protocol, Haemocytometer counting. Cardiff University 2004. http://www.cardiff.ac.uk/biosi/staffinfo/kille/Methods/Cellculture/HAEMO.html. Downloaded on 31 October 2010.

- Pooley E., A field guide to the wild flowers of KwaZulu-Natal and the eastern region. Natal Flora Publications Trust, Durban 1998; 442.

- Porte D. Jr., Banting lecture 1990. Beta-cells in type II diabetes mellitus. Diabetes 1991 40(2): 166-180.

- Radziuk J., Bailey C.J., Wiernsperger N.F. and Yudkin J.S., Metformin and its liver targets in the treatment of type 2 diabetes. Current Drug Targets – Immune, Endocrine and Metabolic Disorders 2003; 3: 151-169.

- Rahimi R., Nikfar S., Larijani B. and Abdollahi M., A review on the role of antioxidants in the management of diabetes and its complications. Biomedicine and Pharmacotherapy 2005; 59: 365-373.

- Rampedi I. and Olivier J., The use and potential commercial development of Athrixia Phylicoides. Acta clínica odontológica 2005; 37: 165-183.

- Randle P.J., Garland P.B., Hales C.N. and Newsholme E.A., The glucose fatty-acid cycle. Its role in insulin sensitivity and the metabolic disturbances of diabetes mellitus. Lancet 1963; 1(7285): 785–789.

- Reaven G.M. Banting lecture 1988. Role of insulin resistance in human disease. Diabetes 1988; 37 (12): 1595-1607.

- Rengarajan S., Parthasarathy C., Anitha M. and Balasubramanian K., Diethylhexyl phthalate impairs insulin binding and glucose oxidation in Chang liver cells. Toxicology

in Vitro 2007; 21; 99-102.

- Robertson R.P., Harmon J., Tran P.O., Tanaka Y., Takahashi H. (2003) Glucose toxicity in beta-cells: Type 2 diabetes, good radicals gone bad, and the glutathione connection. Diabetes 52:581-587.

- Rotter V., Nagaev I. and Smith U., Interleukin-6 (IL-6) induces insulin resistance in 3T3-L1 adipocytes and is, like IL-8 and tumor necrosis factor-ά, overexpressed in human fat cells from insulin-resistant subjects. Journal of Biological Chemistry 2003; 278:45777-45784.

- Salehi A., ekelund M. and Lundquist I., Total parental nutrition modulates hormone release by stimulating expression and activity of inducible nitric oxide synthase in rat pancreatic islets. Hormone Metabolism Research 2003; 35: 48-54.

- Sang S., Tian S., Stark R.E., Yang C.S. and Ho C.T., New dibenzotropolone derivatives characterized from black tea using LC/MS/MS. Bioorganic and Medicinal Chemistry 2004; 12(11): 3009-3017.

- Sesti G., Pathophysiology of insulin resistance. Best Practice and Research Clinicla Endocrinology and Metabolism 2006; 20(4): 665-679.

- Shepherd P.R. and Kahn B.B., Glucose transporters and insulin action. The New England Journal of Medicine 1999; 341: 248-257.

- Schewe T. and Sies H., Myeloperoxidase-induced lipid peroxidation of LDL in the presence of nitrite. Protection by cocoa flavanols. Biofactors 2005; 24(1-4): 49-58.

- Shulman G.I., Cellular mechanisms of insulin resistance. The Journal of Clinical Investigation 2000; 106: 171-176.

- Smith L.W. and Culvenor C.C.J., Plant sources of hepatotoxic pyrrolizidine alkaloids. Journal of Natural Products 1981; 44: 129-152.

- Stevens A. and Lowe J., Human histology, third edition. Elsevier Mosby 2005; 285-287.

- Strijdom H., Muller C. and Lochner A., Direct intracellular nitric oxide detection in isolated adult cardiomyocytes: flow cytometric analysis using the fluorescent probe, diaminofluorescein. Hournal of Molecular and Cellular Cardiology 2004; 37: 897-902.

- Tanaka Y., Gleason C.E., Tran P.O., Harmon J.S. and Robertson R.P., Prevention of glucose toxicity in HIT-T15 cells and Zucker diabetic fatty rats by antioxidants. Proceedings of the National Academy of Sciences of the United States of America 1999; 96: 10857-10862.

- Tsai J-T., Liu H-C. and Chen Y-H., Suppression of inflammatory mediators by cruciferous vegetable-derived indole-3-carbinol and phenylethyl isothiocyanate in lipopolysaccharide-activated macrophages. Mediators of Inflammation 2010; ePublication ahead of print.

- Valko M., Leibfritz D., Moncol J., Cronin M.T.D., Mazur M. and Telser J., Free radicals and antioxidants in normal physiological functions and human disease. International Journal of Biochemistry and Cell Biology 2007; 39:44-84.

- Van de Venter, M., Roux, S., Bungu, L.C., Louw, J., Crouch, N.R., Grace, O.M., Maharaj, V., Pillay, P., Sewnarian, P., Bhagwandin, N. and Folb, P., Antidiabetic screening and scoring of 11 plants traditionally used in South Africa. Journal of Ethnopharmacology 2008; 119:81-86.

- Van Wyk B-E. and Gericke M. People's Plants. A Guide to Useful Plants of Southern Africa. Briza Publications, Pretoria, South Africa 2000, pp102-103.

- Watt J.M. and Breyer-Brandwijk M.G., The Medicinal and Poisonous Plants of Southern Africa. E & S Livingstone, Edinborough, UK 1932; 70.

- Wellen K.E. and Hotamisligil G.S., Inflammation, stress, and diabetes. The Journal of Clinical Investigation 2005; 115 (5): 1111-1119.

- Wiernsperger N.F., Membrane physiology as a basis for the cellular effects of metformin in insulin resistance and diabetes. Diabetes Metabolism 1999; 25(2): 110-127.

- Wild S, Roglic G., Green A., Sicree R. and King H., Global prevalence of diabetes: estimates for the year 2000 and projections for 2030. Diabetes Care 2004; 27 (10): 1047-1053.

- Wisman K.N., Perkins A.A., Jeffers M.D. and Hagerman A.E., Accurate assessment of the bioactivities of redox-active polyphenolics in cell culture. Journal of Agricultural Food Chemistry 2008; 56: 7831-7837.

- ZenBio Instruction Manual ZBM0009.02 3T3-L1 Cell Care Manual: Maintenance and Differentiation of 3T3-L1 Preadipocytes to Adipocytes NC, USA 2010 ZenBio Inc.

- Zhang H-Y., Chen L-L., Li X-J. and Zhang J., Evolutionary inspirations for drug discovery. Trends in Pharmacological Sciences 2010; 31(10): 443-448.

APPENDIX I – Reagent Components

1. Dulbecco's modified Eagle's medium (DMEM) (Cat No.: 12-741F)

Inorganic salts	**mg/L**
$CaCl_2$ (anhyd.)	200
$Fe(NO_3)_3 \cdot 9H_2O$	0.10
KCl	400
$MgSO_4 \cdot 7H_2O$	200
NaCl	6 400
$NaHCO_3$	3 700
$NaH_2PO_4 \cdot H_2O$	125

Amino acids	**mg/L**
L-Arginine•HCl	84
L-Cysteine	48
L-Glutamine	584
Glycine	30
L-Histidine•HCl•H_2O	42
L-Isoleucine	104.8
L-Leucine	104.8
L-Lysine•HCl	146.2
L-Methionine	30
L-Phenylalanine	66
L-Serine	42
L-Threonine	95.2

Amino acids	**mg/L**
L-Tryptophan	16
L-Tyrosine	72
L-Valine	93.6

Vitamins	**mg/L**
D-Ca Pantothenate	4
Choline chloride	4
Folic acid	4
i-Inositol	7
Nictotinamide	4
Pyridoxine•HCl	4
Riboflavin	0.4
Thiamine•HCl	4

Other components	**mg/L**
Glucose	4 500
Phenol red	15

2. Eagle's modified essential medium (EMEM) (Cat No.: 12-662F)

Inorganic salts	**mg/L**
$CaCl_2 \cdot 2H_2O$	265
KCl	400
$MgSO_4 \cdot 7H_2O$	200
NaCl	6 800
$NaHCO_3$	2 200
$NaH_2PO_4 \cdot H_2O$	140

Amino acids	**mg/L**
L-Alanine	8.9
L-Arginine•HCl	126.4
L-Asparagine	13.21
L-Aspartic acid	13.3
L-Cysteine	24
L-Glutamic acid	14.7
Glycine	7.5
L-Histidine•HCl•H_2O	42
L-Isoleucine	52.4
L-Leucine	52.4
L-Lysine•HCl	73
L-Methionine	15
L-Phenylalanine	33
L-Proline	11.5

Amino acids	**mg/L**
L-Serine	10.5
L-Threonine	47.6
L-Tryptophan	10.2
L-Tyrosine	36.2
L-Valine	46.8

Vitamins	**mg/L**
D-Ca Pantothenate	1
Choline chloride	1
Folic acid	1
i-Inositol	2
Nictotinamide	1
Pyridoxal•HCl	1
Riboflavin	0.1
Thiamine•HCl	1

Other components	**mg/L**
Glucose	1 000
Phenol red•Na	10
Sodium pyruvate	110

3. Dulbecco's modified Eagle's medium base (Cat No.: D5030)

Inorganic salts	**mg/L**
$CaCl_2$ (anhydrous)	200
$Fe(NO_3)3•9H_2O$	0.10
KCl	400
$MgSO_4$ (anhydrous)	97.67
NaCl	6 400
$NaH_2PO_4•H_2O$	109

Amino acids	**mg/L**
L-Arginine•HCl	84
L-Cysteine•2HCl	62.6
Glycine	30
L-Histidine•HCl• H_2O	42
L-Isoleucine	105
L-Leucine	105
L-Lysine•HCl	146
L-Methionine	30
L-Phenylalanine	66
L-Serine	42
L-Threonine	95
L-Tryptophan	16
L-Tyrosine•2Na•2 H_2O	103.8
L-Valine	94

Vitamins	**mg/L**
Choline Chloride	4
Folic Acid	4
Myo-Inositol	7.2
Niacinamide	4
D-Pantothenic Acid Hemicalcium	4
Pyridoxal•HCl	4
Riboflavin	0.4
Thiamine•HCl	4

4. RPMI 1640 Medium (Cat No.: 12-702F)

Inorganic salts	**mg/L**
$Ca(NO_3)_2•4H_2O$	100
KCl	400
$MgSO_4•7H_2O$	100
NaCl	6 000
$NaHCO_3$	2 000
$Na_2HPO_4•7H_2O$	1 512

Amino acids	**mg/L**
L-Arginine	200
L-Asparagine•H_2O	50
L-Aspartic acid	20
L-Cysteine	50
L-Glutamic acid	20
L-Alanyl-L-Glutamine (UltraGlutamine 1)	446
Glycine	10
L-Histidine	15
Hydroxy L•Proline	20
L-Isoleucine	50
L-Leucine	50
L-Lysine•HCl	40
L-Methionine	15
L-Phenylalanine	15

Amino acids	**mg/L**
L-Proline	20
L-Serine	30
L-Threonine	20
L-Tryptophan	5
L-Tyrosine	20
L-Valine	20

Vitamins	**mg/L**
p-Aminobenzoix Acid	1
d-Biotin	0.2
D-Ca Pantothenate	0.25
Choline chloride	3
Folic acid	1
i-Inositol	35
Nictotinamide	1
Pyridoxine•HCl	1
Riboflavin	0.2
Thiamine•HCl	1
Vitamin B12	0.005

Other components	**mg/L**
Glucose	2 000
Glutathione (reduced)	1
Phenol red•Na	5

5. Dulbecco's phosphate buffered saline (PBS) (Cat No.: 17-513)

Inorganic salts	**mg/L**
$CaCl_2•H_2O$	130
KCl	200
KH_2PO_4	200
$MgCl_2•6H_2O$	100
NaCl	8 000
$Na_2HPO_4•7H_2O$	2 160

1. Hanks Balanced Salt Solution (Cat No.: 14025)

Inorganic salts	**mg/L**
$CaCl_2•H_2O$	186
KCl	400
KH_2PO_4	60
$MgSO_4•7H_2O$	200
NaCl	8 000
$NaHCO_3$	350
$Na_2HPO_4•7H_2O$	90

Other components	**mg/L**
Glucose	1 000

6. Krebs-Ringer bicarbonate HEPES buffer

Component	**mmol/L**
NaCl	115
$NaHCO_3$	24
KCl	5
$MgCl_2$	1
$CaCl_2$	2.5

2% BSA

10 mM HEPES Buffer

7. Sorennson's Buffer pH 10.5

0.751 g glycine (0.1M) + 0.584 g NaCl (0.1M) (in 100 ml cell culture tested water).

4 g NaOH (1M) in 100 ml cell culture tested water (to equilibrate buffer to pH 10.5).

9. 0.3 M NaOH + 1% SDS

12 g NaOH (0.3M) + 100 ml 10% SDS solution (in 1 L cell culture tested water).

9. Trypsin (Cat No.: 17-161F)

0.5 g/L irradiated porcine trypsin + 0.2 g/L Versene® (EDTA)

APPENDIX II – Supplementary tables

Table 2. Abbreviated cell sample labels for C2C12 (**a**), Chang (**b**) and 3T3-L1 (**c**) cells

a.

Sample	Abbreviated Label
Insulin (1 .0 µM)	A1
Metformin (1 .0 µM)	A2
Vehicle (water)	A3
ARC401 (0.05 µg/µl)	A5
Insulin (1 .0 µM)	B1
Metformin (1 .0 µM)	B2
Vehicle (water)	B3
ARC401 (0.05 µg/µl)	B5
Insulin (1 .0 µM)	C1
Metformin (1 .0 µM)	C2
Vehicle (water)	C3
ARC401 (0.05 µg/µl)	C5

b.

Sample	Abbreviated Label
Insulin (1 .0 µM)	D1
Metformin (1 .0 µM)	D2
Vehicle (water)	D3
ARC401 (0.05 µg/µl)	D5
Insulin (1 .0 µM)	E1
Metformin (1 .0 µM)	E2
Vehicle (water)	E3
ARC401 (0.05 µg/µl)	E5
Insulin (1 .0 µM)	F1
Metformin (1 .0 µM)	F2
Vehicle (water)	F3
ARC401 (0.05 µg/µl)	F5

c.

Sample	Abbreviated Label
Insulin (1 .0 µM)	G1
Metformin (1 .0 µM)	G2
Vehicle (water)	G3
ARC401 (0.05 µg/µl)	G5
Insulin (1 .0 µM)	H1
Metformin (1 .0 µM)	H2
Vehicle (water)	H3
ARC401 (0.05 µg/µl)	H5
Insulin (1 .0 µM)	I1
Metformin (1 .0 µM)	I2
Vehicle (water)	I3
ARC401 (0.05 µg/µl)	I5

Table 3. Nanodrop quantification of RNA (ng/µl and µg/ml) and 20 µg RNA dilution in RNase-free water (µl) for C2C12 cells (**a**) Chang cells (**b**) and 3T3-L1 cells (**c**)

a.

Sample	ng/µl	20 µg RNA (µl)	Water (µl)
A1	619.02	32.31	9.69
A2	226.82	42.00	0.00
A3	222.90	42.00	0.00
A5	758.97	26.35	15.65
B1	834.35	23.97	18.03
B2	743.57	26.90	15.10
B3	559.58	35.74	6.26
B5	856.93	23.34	18.66
C1	129.50	42.00	0.00
C2	241.41	42.00	0.00
C3	380.45	42.00	0.00
C5	19.18	42.00	0.00

b.

Sample	ng/µl	20 µg RNA (µl)	Water (µl)
D1	1132.79	17.66	24.34
D2	1274.97	15.69	26.31
D3	279.76	42.00	0.00
D5	1318.56	15.17	26.83
E1	533.78	37.47	4.53
E2	1168.22	17.12	24.88
E3	1237.71	16.16	25.84
E5	513.26	38.97	3.03
F1	2885.40	6.93	35.07
F2	123.15	42.00	0.00
F3	2230.42	8.97	33.03
F5	1776.42	11.26	30.74

c.

Sample	ng/µl	20 µg RNA (µl)	Water (µl)
G1	322.03	42.00	0.00
G2	757.10	26.42	15.58
G3	686.17	29.15	12.85
G5	827.38	24.17	17.83
H1	294.55	42.00	0.00
H2	195.95	42.00	0.00
H3	267.88	42.00	0.00
H5	121.00	42.00	0.00
I1	198.76	42.00	0.00
I2	7.44	42.00	0.00
I3	292.95	42.00	0.00
I5	312.68	42.00	0.00

Table 4. Nanodrop quantification of RNA (ng/µl and µg/ml) and 1 µg RNA dilution in RNase-free water (µl) for C2C12 cells (**a**) Chang cells (**b**), 3T3-L1 cells (**c**) and positive and negative controls (**d**)

a.

Sample	ng/µl	1 µg RNA (µl)	Water (µl)
A1	338.67	2.95	7.05
A2	160.97	6.21	3.79
A3	158.54	6.31	3.69
A5	333.96	2.99	7.01
B1	332.53	3.01	6.99
B2	329.79	3.03	6.97
B3	330.26	3.03	6.97
B5	333.18	3.00	7.00
C1	63.50	10.00	0.00
C2	173.35	5.77	4.23
C3	264.18	3.79	6.21
C5	18.80	10.00	0.00

b.

Sample	ng/µl	20 µg RNA (µl)	Water (µl)
D1	343.95	2.91	7.09
D2	330.17	3.03	6.97
D3	194.80	5.13	4.87
D5	317.49	3.15	6.85
E1	370.41	2.70	7.30
E2	342.51	2.92	7.08
E3	344.22	2.91	7.09
E5	325.68	3.07	6.93
F1	239.29	4.18	5.82
F2	Insufficent sample - removed from experiment		
F3	303.77	3.29	6.71
F5	397.94	2.51	7.49

c.

Sample	ng/µl	20 µg RNA (µl)	Water (µl)
G1	230.92	4.33	5.67
G2	327.70	3.05	6.95
G3	340.46	2.94	7.06
G5	324.21	3.08	6.92
H1	212.80	4.70	5.30
H2	143.20	6.98	3.02
H3	204.68	4.89	5.11
H5	83.14	10.00	0.00
I1	148.20	6.75	3.25
I2	9.74	10.00	0.00
I3	186.10	5.37	4.63
I5	237.44	4.21	5.79

d.

Sample	ng/µl	1 µg RNA (µl)	Water (µl)
Amb Mouse +ve control	0.00	1.00	9.00
Amb Human +ve control	0.00	1.00	9.00
Water -ve control	0.00	0.00	10.00

Table 5. Sample key for cDNA PCR test plate

Abbreviated Label	Key	Abbreviated Label	Key
A1	1	E3	21
A2	2	E5	22
A3	3	F1	23
A5	4	F3	24
B1	5	F5	25
B2	6	G1	26
B3	7	G2	27
B5	8	G3	28
C1	9	G5	29
C2	10	H1	30
C3	11	H2	31
C5	12	H3	32
D1	13	H5	33
D2	14	I1	34
D3	15	I2	35
D5	16	I3	36
E1	17	I5	37
E2	18	Amb Mouse	38
Water	20	Amb Human	39